Identification of Mechanisms Behind Converter-Related Issues in Power Systems Based on an Overview of Real-Life Events

Philippe De Rua, Thomas Roose, Özgür Can Sakinci, Nathalia de Morais Dias Campos and Jef Beerten

ELECTA, KU Leuven, Belgium and EnergyVille, Genk, Belgium

INTRODUCTION

- Increasing share of power-electronic (PE) converters impacts the dynamic behavior of electrical networks.
- Classifications are regarded as essential tools for identifying converter-related instabilities and interactions.
- A bottom-up approach based on an extensive overview of problematic real-life events involving PE converters is presented for identifying the underlying mechanisms and constructing more-encompassing classifications.

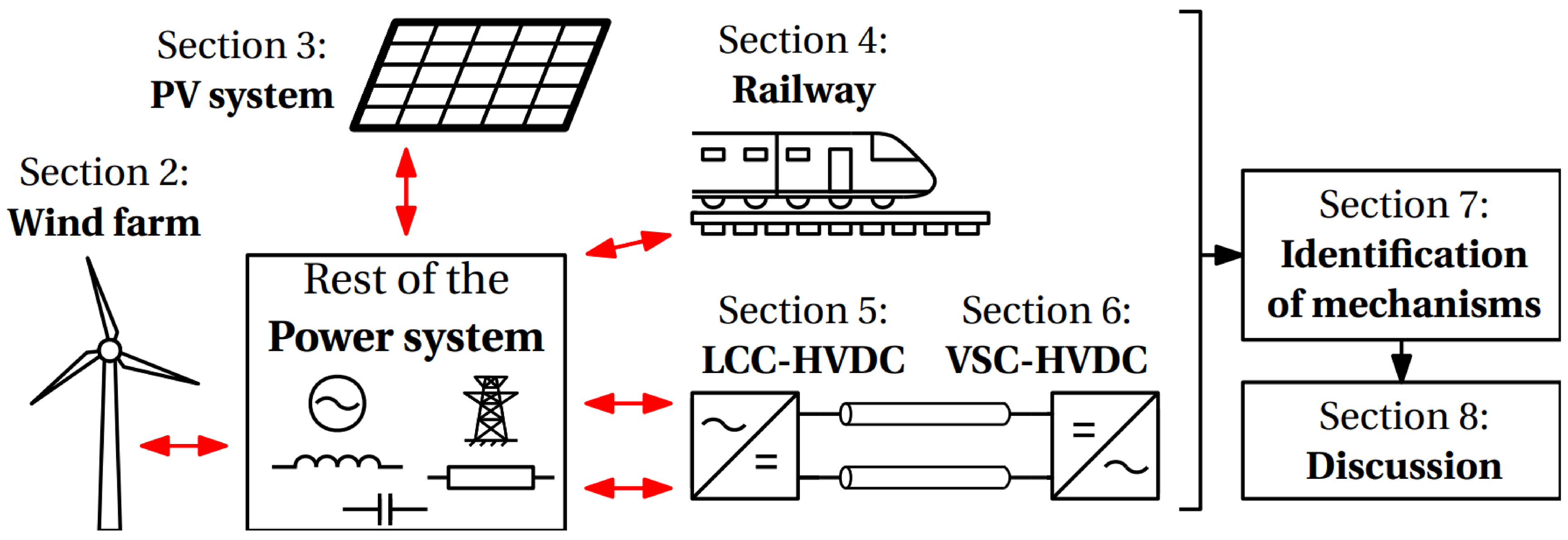

OVERVIEW OF REAL-LIFE EVENTS

- Numerous events in which converters contributed to (i) network instabilities, (ii) adverse forms of interactions, or (iii) degradation of power quality are reviewed.
- The comprehensive cross-system overview focuses on (1) WF systems, (2) PV systems, (3) electrical RW systems, (4) LCC-HVDC systems, and (5) VSC-HVDC/STATCOM systems.

Table Events involving VSC-HVDC and STATCOM systems

Context	ID	Ref.	Trigger	Outcome	$f_{osc.}$ [Hz]	f_1 [Hz]	Terminology in references
interactions with the AC grid	VSC1	[11]	increase in transmitted power	electrical SSOs	20-30	50	"subsynchronous oscillations"
	VSC2			electrical SSOs	20-30	50	
	VSC3	[69, 70]	change in AC grid topology	electr. supersynchr. osc.	451	50	"harmonic instability" "harmonic interactions"
	VSC4	[71]	fault	electr. supersynchr. osc.	830	50	"overvoltage phenomena"
	VSC5	[72]	change in AC grid topology	electr. supersynchr. osc.	≈ 1500	50	"excitation of resonance frequency"
	VSC6	[73]		electr. supersynchr. osc. converter tripping	1700	50	"control instability" "harmonic interactions"
	VSC7	[74, 75]		electr. supersynchr. osc.	1270	50	"instability phenomena" "high-frequency resonance" "harmonic resonance"
	VSC8	[11]	HVDC control mode switch	electr. supersynchr. osc.	> 1000	50	"oscillations in the range of high frequency"
	VSC9	[76]	increased time delay	electr. supersynchr. osc.	700, 1800	50	"high frequency resonances" "resonant instability"
	VSC10	[77]	STATCOMs in weak grid configuration	elec. sub. & super. osc.	2.5, 97.5	50	"sub- and super-synchronous interactions"
interactions with the DC grid	VSC11	[78, 79]	HVDC control mode switch	elec. osc.	550	0	"high frequency resonances" "resonant instability"
	VSC12	[80, 81]	increase in transmitted power	elec. osc.	23.6–25.2	0	"subsynchronous oscillations"

IDENTICATION OF UNDERLYING MECHANISMS

- From analogies between events, three types of underlying mechanisms are identified: (1) converter or control limitations, (2) power quality degradation, and (3) control interactions.
- A *mechanism* is the intermediate process between the initial trigger and the eventual outcome of the event.

<table>
<tr><th colspan="3">CONVERTER OR CONTROL LIMITATIONS</th><th>POWER QUALITY DEGRADATION</th><th>CONTROL INTERACTIONS</th></tr>
<tr><td>(A1) limited under/over-voltage ride-through capability</td><td rowspan="2">(B1) limited/inadequate voltage support</td><td rowspan="3">(C) limited synchronization capability</td><td rowspan="2">(D) nonlinear converter or control behavior</td><td>(F) electrical interactions among converter controls and/or with passive grid components</td></tr>
<tr><td>(A2) limited under/over-freq. ride-through capability</td><td>(G) electrical interactions between converter-controlled rotating machines and passive grid components</td></tr>
<tr><td>(A3) limited over-current ride-through capability</td><td>(B2) limited/inadequate frequency support</td><td>(E) amplification of converters emissions by passive grid components</td><td>(H) electromechanical interactions between converter controls and rotating machines</td></tr>
<tr><td colspan="3">fundamental frequency phenomena</td><td colspan="2">non-fundamental frequency phenomena</td></tr>
</table>

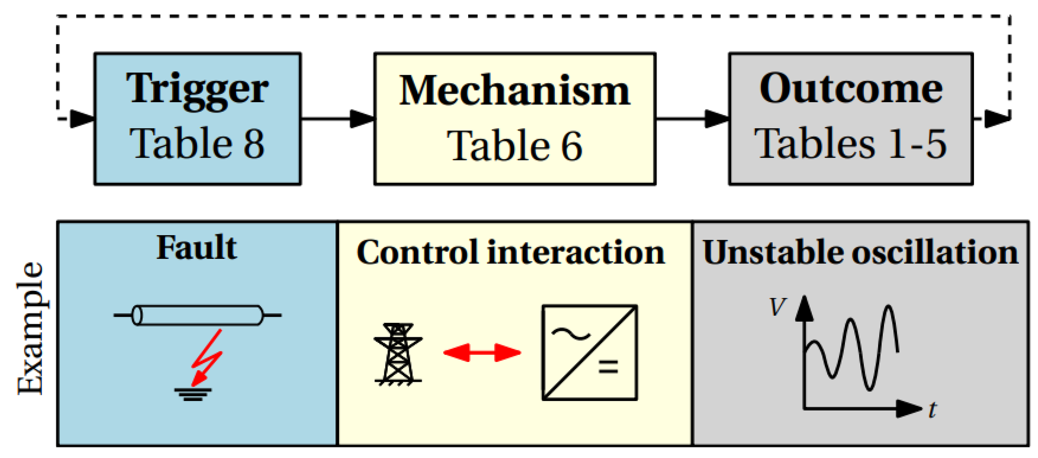

DISCUSSION

- Mechanisms can happen simultaneously as a response to the same trigger, or consecutively when the outcome of one mechanism acts as a trigger to one or several other mechanisms.

ID	Trigger	Events
T1	Faults	WF2, WF6, WF8, WF10, PV1-PV3, PV5 and VSC4
T2	Switching of lines or capacitor banks	WF1, WF3, WF7, PV6, LCC1, VSC3 and VSC5-VSC7
T3	Power variations/fluctuations	WF4, WF8-10, RW1, RW2, LCC2, LCC3, VSC1, VSC2, VSC9 and VSC12
T4	Change of control mode	LCC3, VSC8 and VSC11
T5	Non-fundamental frequency components	WF5, WF8, WF10, PV4, RW4, RW5-RW7 and LCC9
T6	Normal operation with low load, weak grid or natural grid resonance	PV7, RW9-RW19, LCC4, LCC5, LCC7, LCC8 and VSC10
T7	Not given or known	WF5, PV8-PV10, RW3, RW8 and LCC6

- Both the mechanisms and their triggers impact the choice of modeling requirements, i.e. linearized or nonlinear mathematical framework.
- Used terminology is often diverse and system-specific, relying mostly on frequency-dependent considerations.

EXAMPLE

Large offshore WF in the UK (event WF8)

1. A fault (Trigger T1) initiated an interaction between WF controls and poorly-damped grid resonance (Mechanism F), resulting in growing voltage oscillations (Outcome).
2. The oscillations (Trigger T5) set off the over-current protection control (Mechanism A3), causing converters to trip (Outcome).
3. The reduced power generation (Trigger T3) associated with limited frequency-support capabilities (Mechanism B2) resulted in a frequency collapse (Outcome).

With the support of the Energy Transition Fund

Empowered by KU Leuven, VITO, imec & UHasselt

Spatial Representation of Renewable Technologies In Generation Expansion Planning Models

K. Phillips, J. Moncada, H. Ergun, E. Delarue

INTRODUCTION

- This work analyzes how the spatial representation used to model intermittent renewable generation technologies, impacts the results of generation expansion planning models
- It is shown that the spatial resolution, and to a lesser extent the spatial aggregation method used in a planning model, have a significant influence on the obtained system cost.
- The effect is quantified in a case study of European geographical scale, by varying the spatial resolution from highly resolved (hundreds of sites) to highly aggregated (1 site).

Model Description

- A linear GEP model with a central planner perspective is used
- Objective function to be minimized consists of investment- and fuel cost of typical generating technologies
- The model is purposefully kept simple to isolate the effect of renewable representation
- Fixed storage capacity is included

METHODOLOGY

- High resolution (2700 locations) input data is aggregated into cells in different ways
- Each cell corresponds to one technology available to the GEP model for investment
- Each cell is characterized by its unique production time series
- Production time series reflect the estimated hourly per unit production of PV or wind capacity placed in the relevant cell

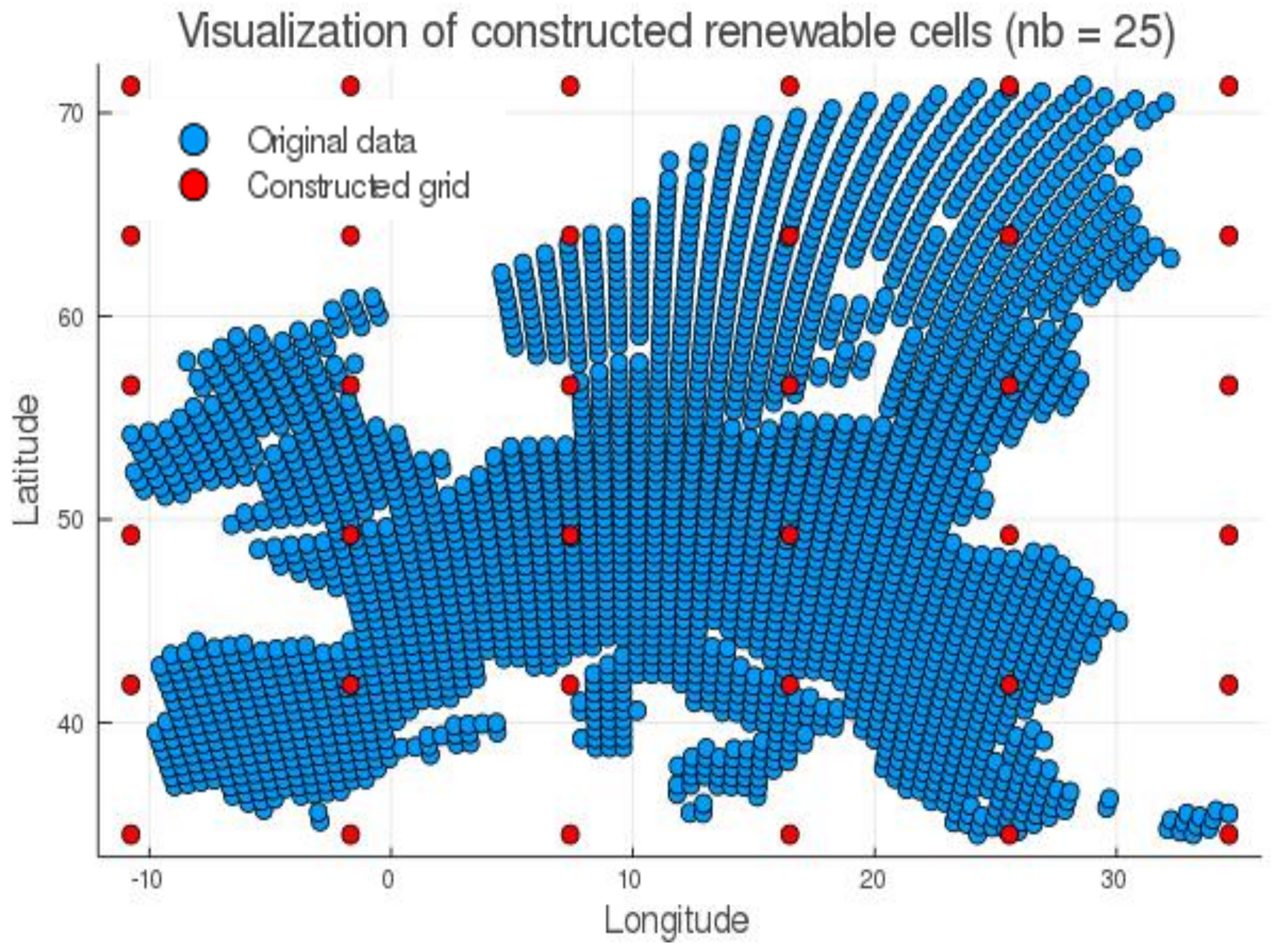

1. Variation in the spatial *resolution*

- Number of renewable cells is varied from 1 to 900
- Production time series are obtained by averaging the input data on an hourly basis

2. Variation in the spatial *aggregation*

- Different ways of aggregating the hourly data within a cell are compared
- Average, weighted average, and median time-series

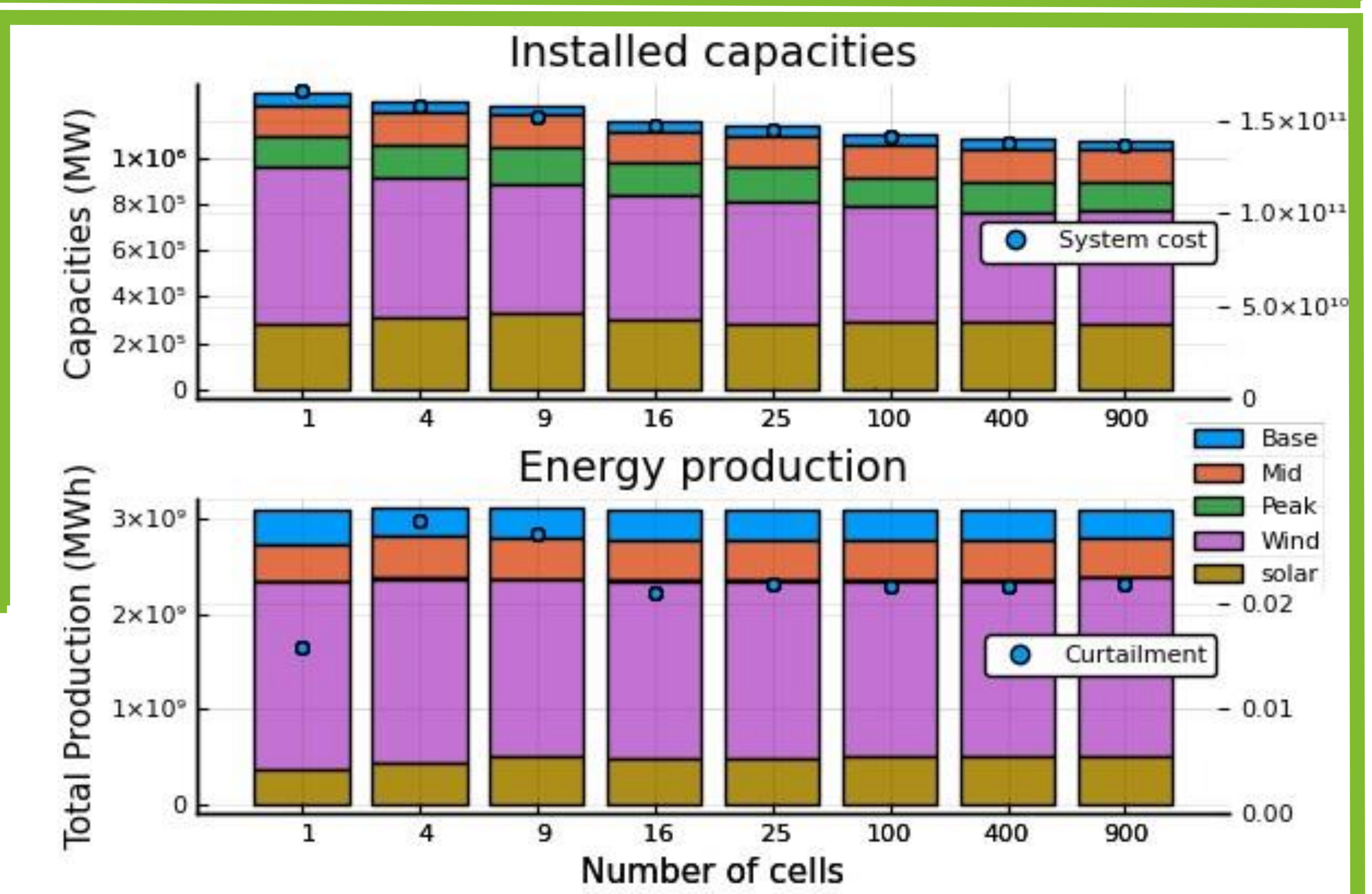

Results

1. Spatial *resolution*

- In high resolution, more interesting renewable generation sites can be identified → Strong decrease (~ 18%) in total system cost
  - Majority of cost reduction (~ 70%) achieved with 25 cells
- Opposing trend of solar and wind technologies
  - Wind: decrease in capacity (25%) for constant production
  - Solar: constant capacity for increased production (30%)

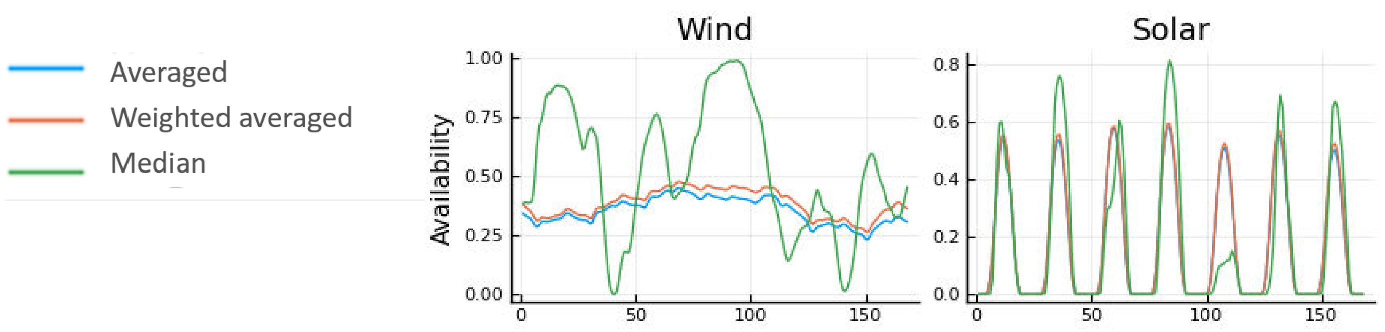

2. Spatial *aggregation*

- Model *input* strongly depends on aggregation technique
- When optimizing a single model region: model *output* depends strongly on aggregation technique
- Effect quickly diminishes with increasing number of model regions

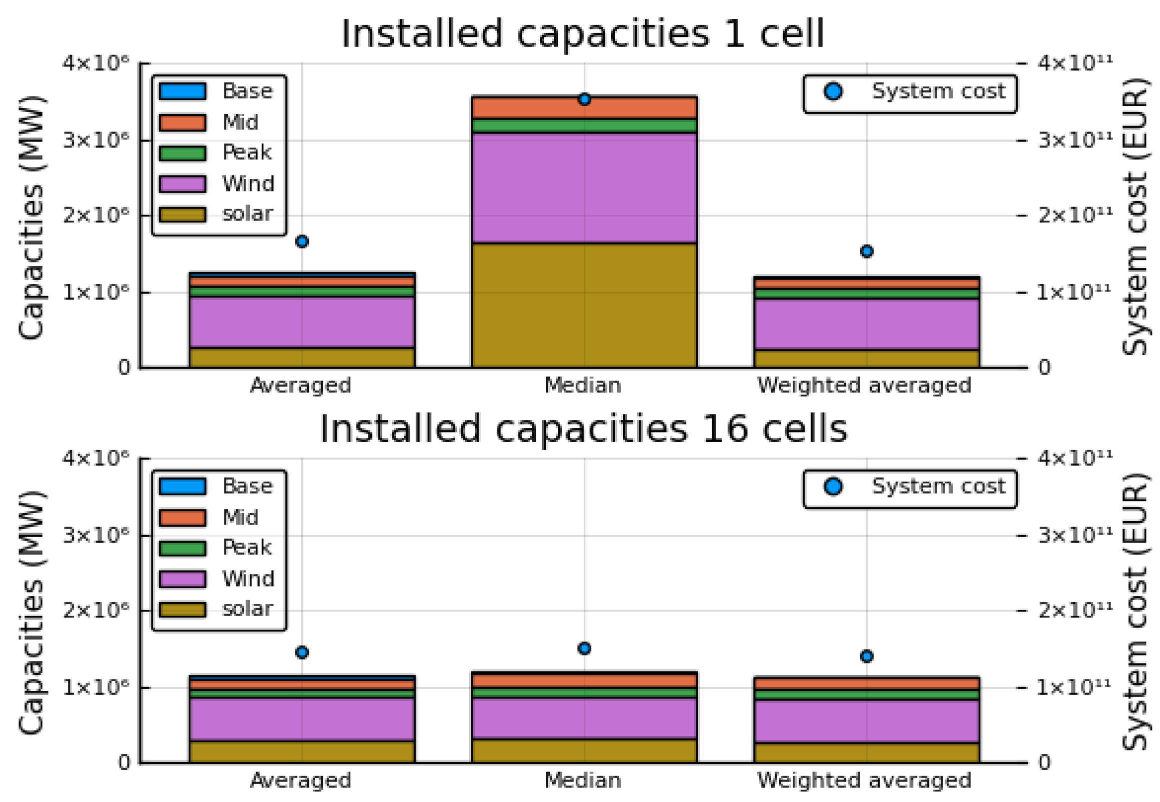

With the support of the Energy Transition Fund

Renewable-based regions in power system planning models

K. Phillips, J. Moncada, H. Ergun, E. Delarue

Energy Ville

Empowered by KU Leuven, VITO, imec & UHasselt

INTRODUCTION

- The result of generation expansion planning models depends on the spatial resolution that is used
- Resolution dependency is driven by 2 opposing factors
    1. Spatial dependence of renewable sites
    2. Identification of transmission bottlenecks

How can we approach models with high spatial resolution while using only few model regions?

PyPSA-EUR model

- Existing Open-Source tool
- Linear optimization from a central planner perspective
- Combined transmission and generation expansion
- Flexible in the desired resolution of both renewable sites and network nodes

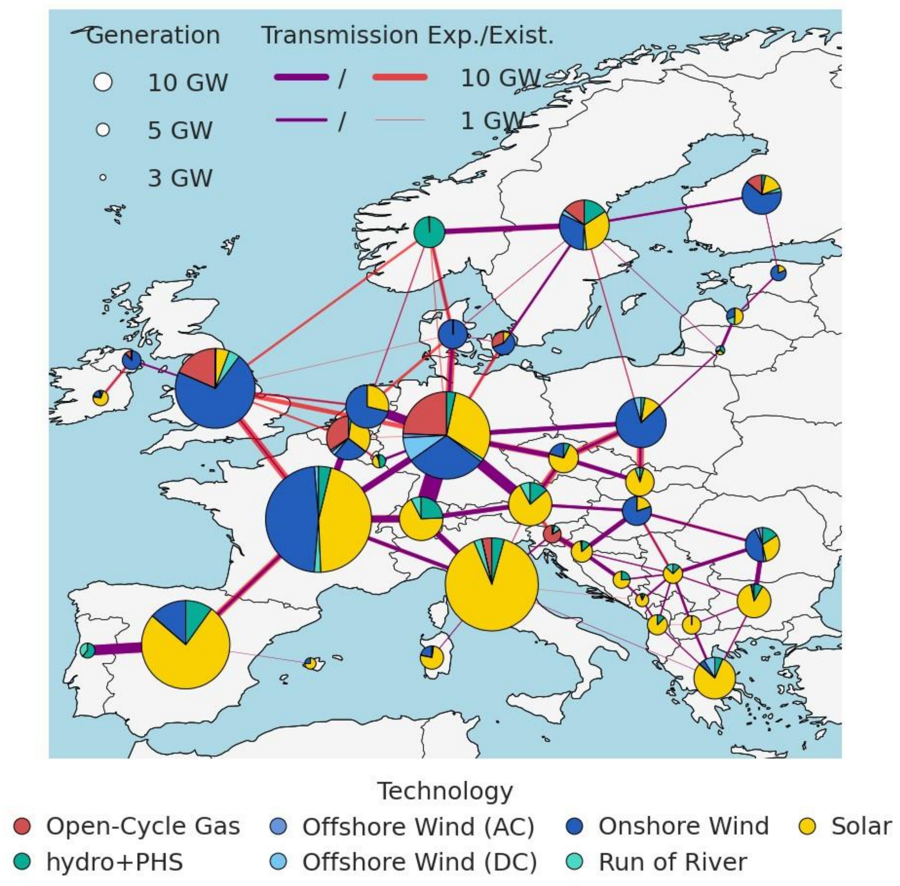

METHODOLOGY

Look at how model regions are generated

Conventional approach

- Start from countries
- Calculate properties for one or more nodes in each country
- Add connections

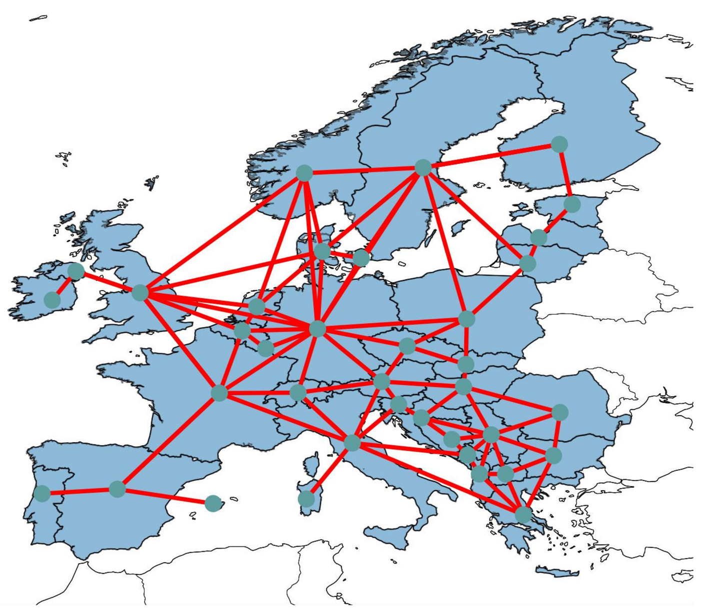

Our approach

- Start from renewable potential
- Generate regions with similarity-based clustering
- Replace countries with these regions

Research horizon

Fixed

- Full year optimization
- Stringent CO_2 limit

Varied

- Number of network nodes
- Number and origin of renewable-based regions
- Line expansion limit

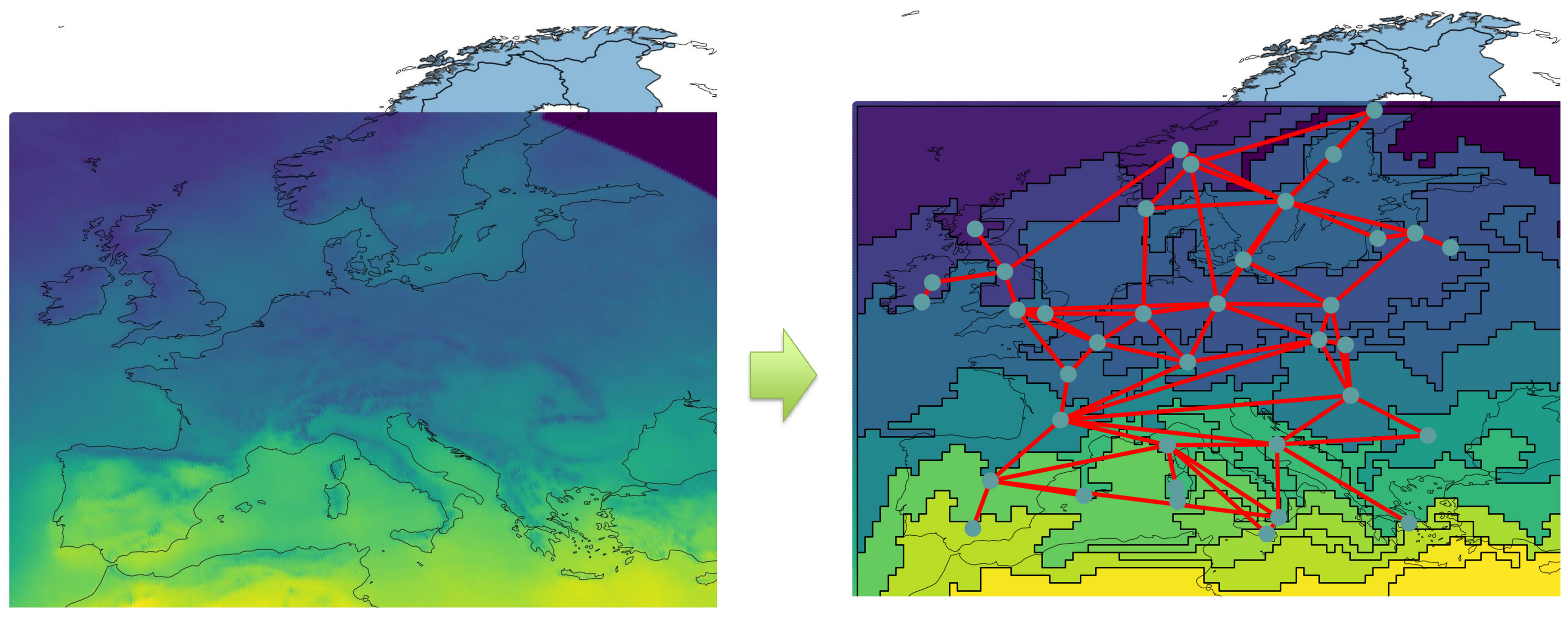

Nodal balances 37 nodes

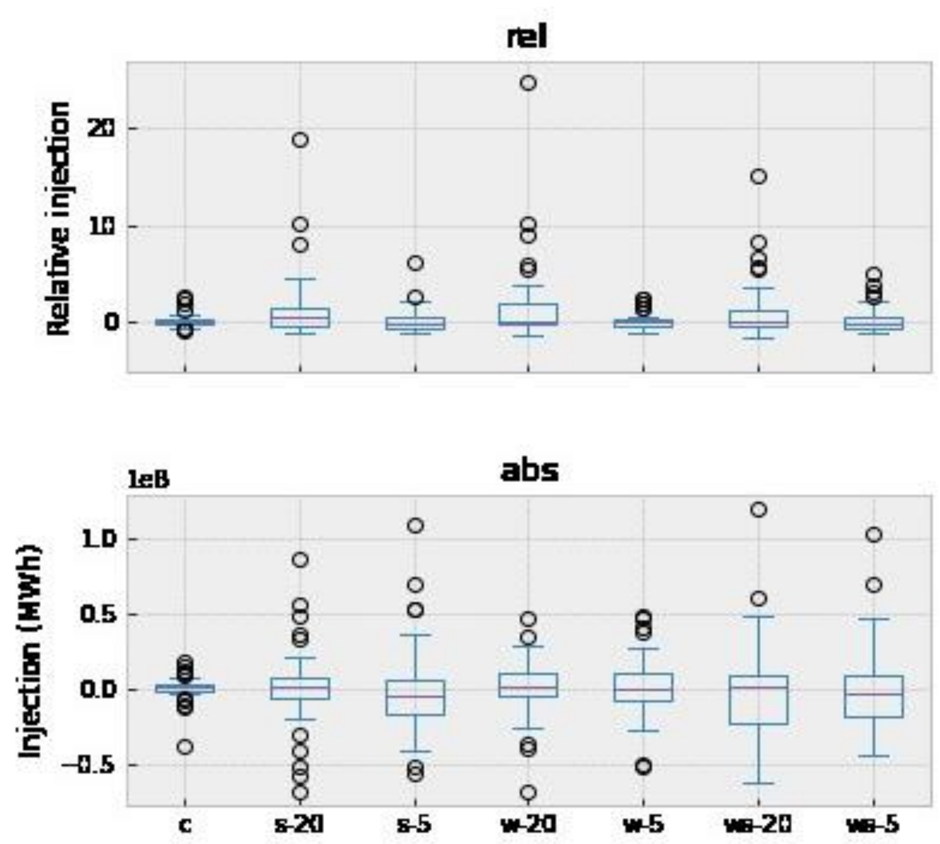

Results

- Convergence at high network resolution
- Focus on differences in low-resolution

Pre-optimization

- More transmission volume is represented in all renewable-based aggregations than in the country-based case
- Few renewable regions lead to more balanced size of nodal regions

Optimized system

- A clear distinction emerges between generating and consuming regions ↔ balanced, self-providing countries
- Identification of transmission needs that are not visible in the country-based model
- Similar total cost but shift from generation to transmission investment

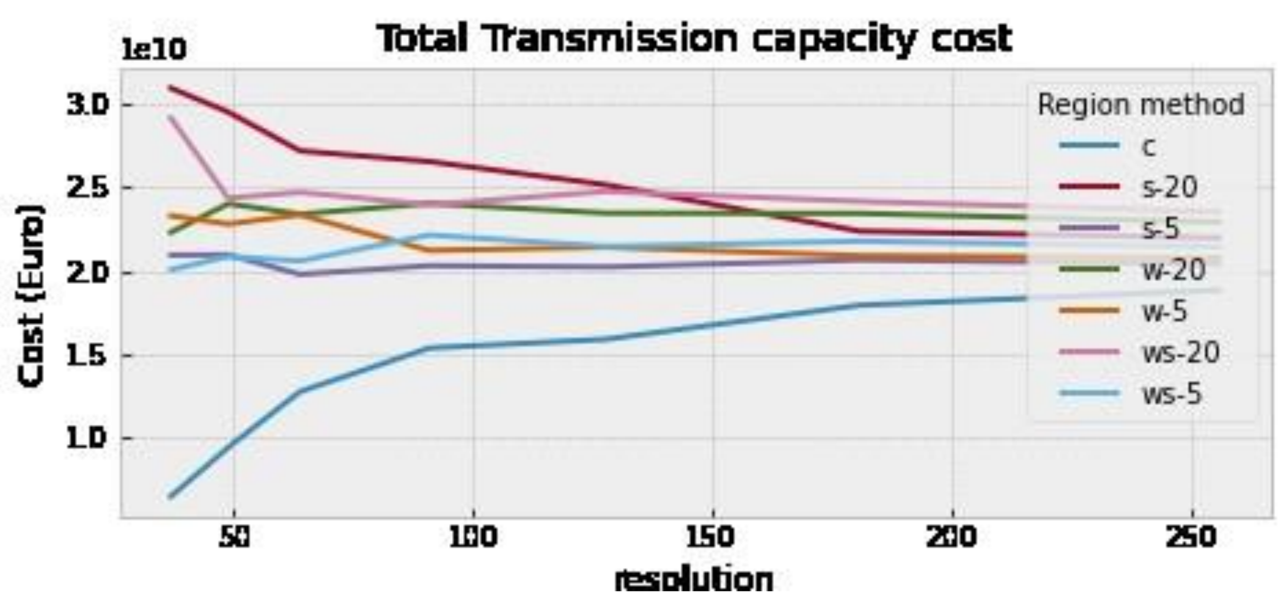

KU LEUVEN vito imec UHASSELT economie

With the support of the Energy Transition Fund

Real-time Control Hardware-In-The-Loop Setup for Two Terminal HVDC-MMC system

Jan Kircheis, Dongyeong Lee and Jef Beerten
ELECTA, KU Leuven, Belgium and EnergyVille, Genk, Belgium

INTRODUCTION

- A real-time Control Hardware-in-the-loop (CHiL) setup for two terminal HVDC-MMC studies is presented.
- Using real control hardware interfaced with a real-time simulator enables high-fidelity testing of MMC controls.
- Detailed time-domain simulations of the two terminal MMC-HVDC setup are presented.

SYSTEM UNDER STUDY

- Two terminal HVDC grid with AC grids represented by Thevenin equivalents.
- Frequency-dependent DC cable model.
- MMC submodule switching modeled in detail.
- Grid-following controls.
- Energy balancing controls modeled.

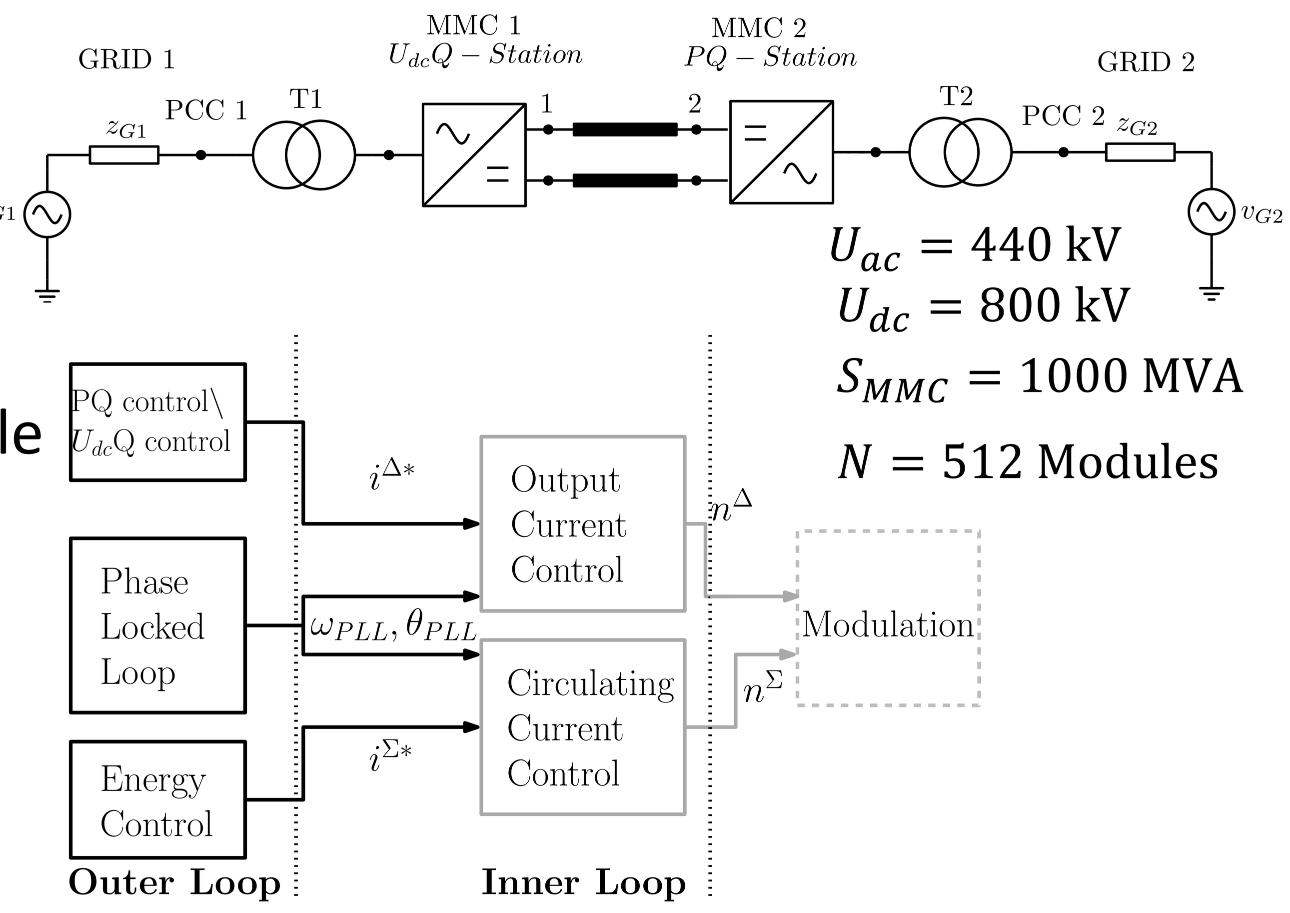

HARDWARE IMPLEMENTATION

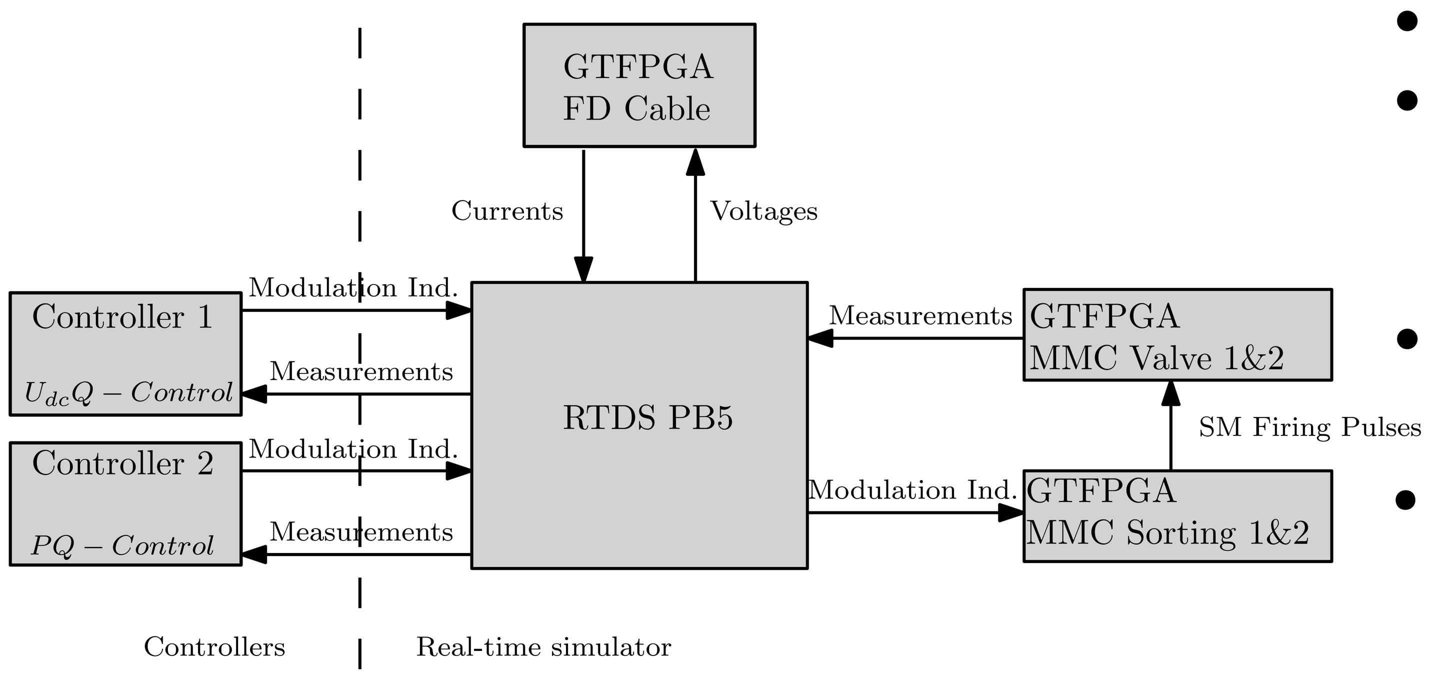

- Small simulation timestep 3µs.
- Dedicated GTFPGA unit for frequency-dependent cable simulation.
- Dedicated GTFPGA units for MMC valve & MMC firing control.
- $U_{dc}Q$-Controller and PQ-Controller connected via fiber optic cable.

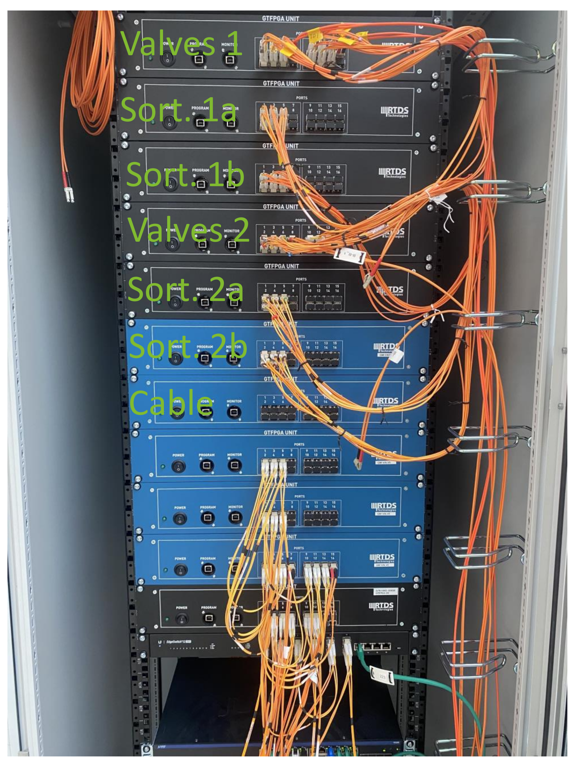

RESULTS

- Time-domain simulation of the setup with different DC control tuning

- At 4s: Connecting MMC1 to DC cable
- At 9s: Deblocking of MMC1 and starting controls
- At 11s: Connecting MMC2 to DC cable
- At 16s: Deblocking of MMC2 and starting controls (Pref=500MW)

- Case 1: Base control system tuning

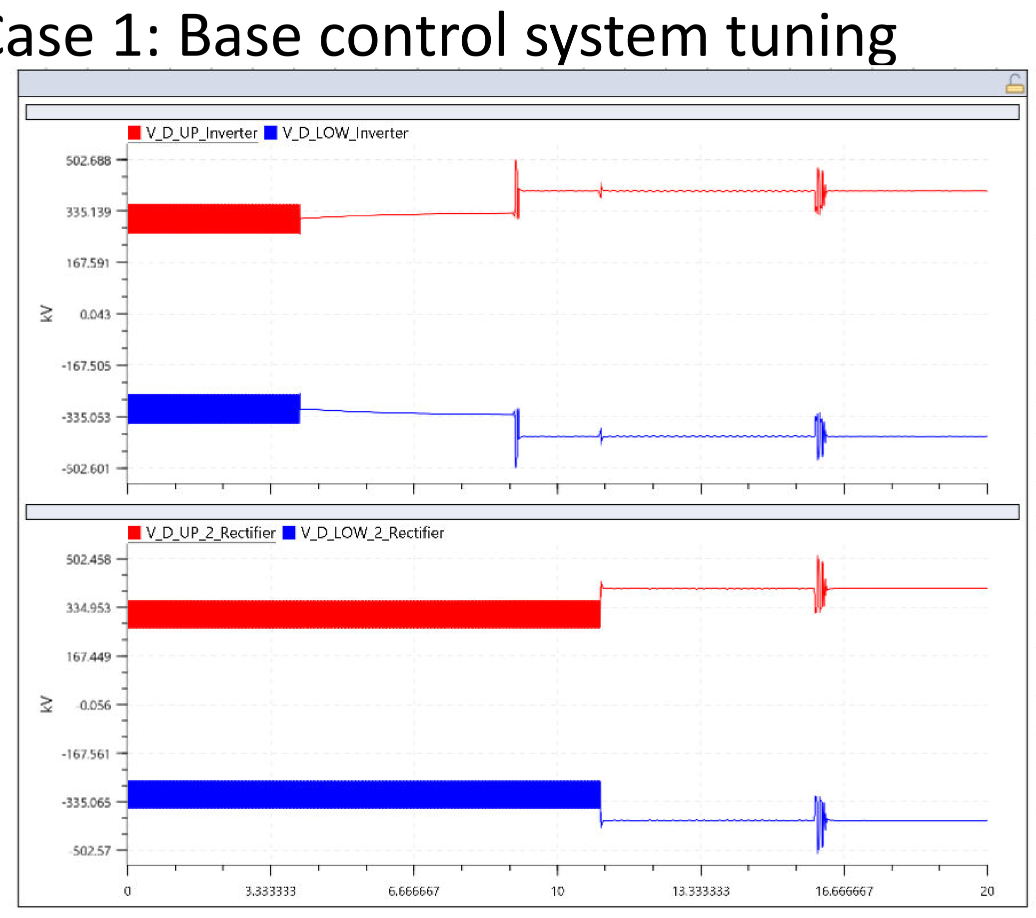

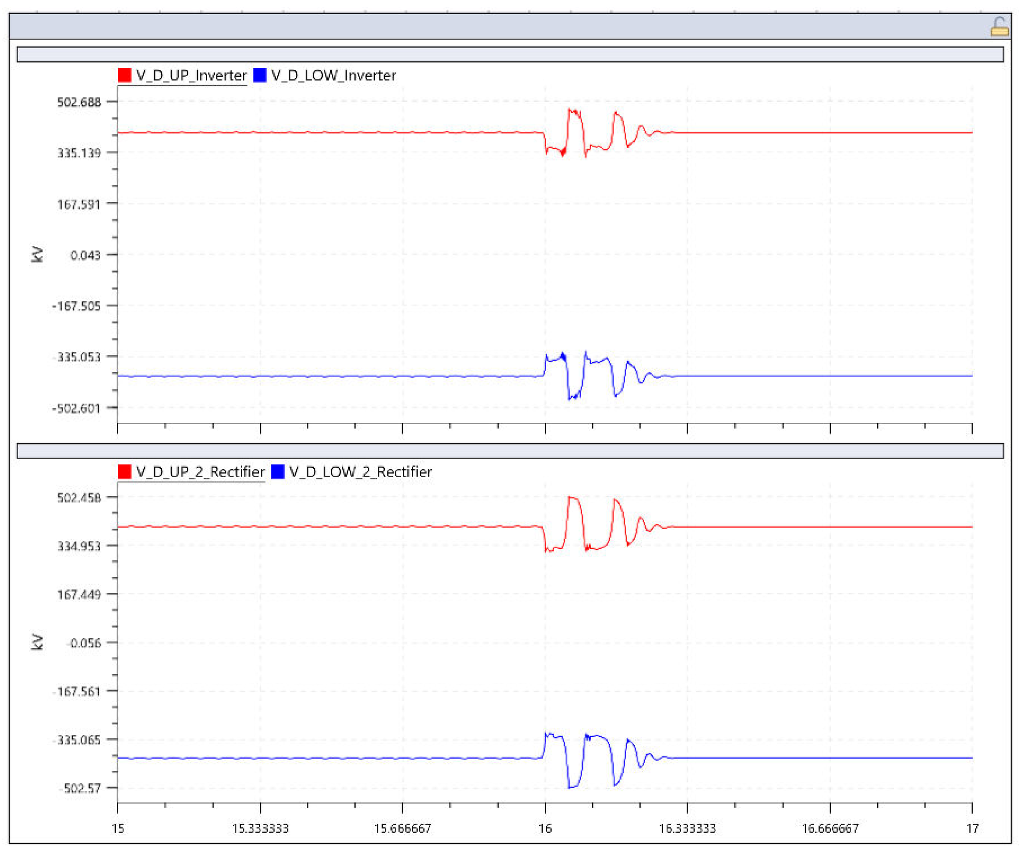

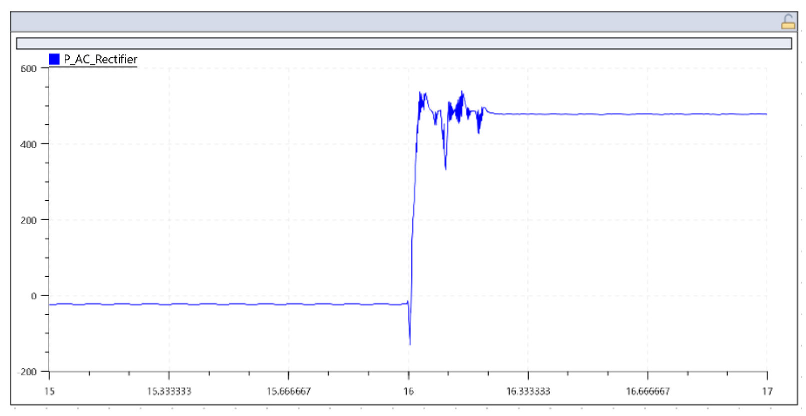

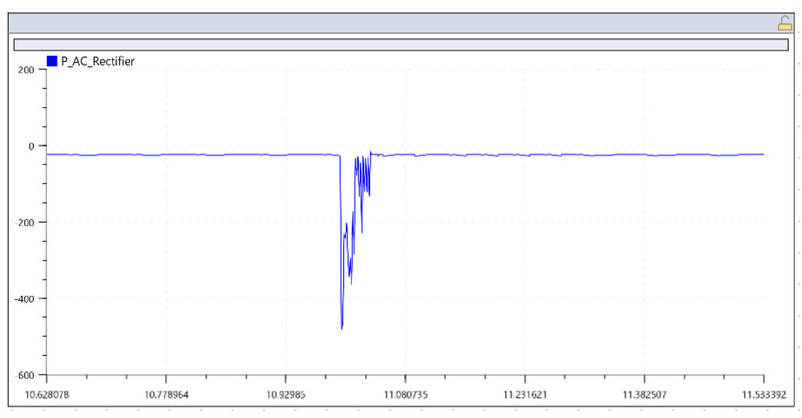

- Case 2: Slow control system tuning (1/3 slower)

❖ DC voltage response is slower and more oscillatory with slower tuning
❖ P rectifier response also affected

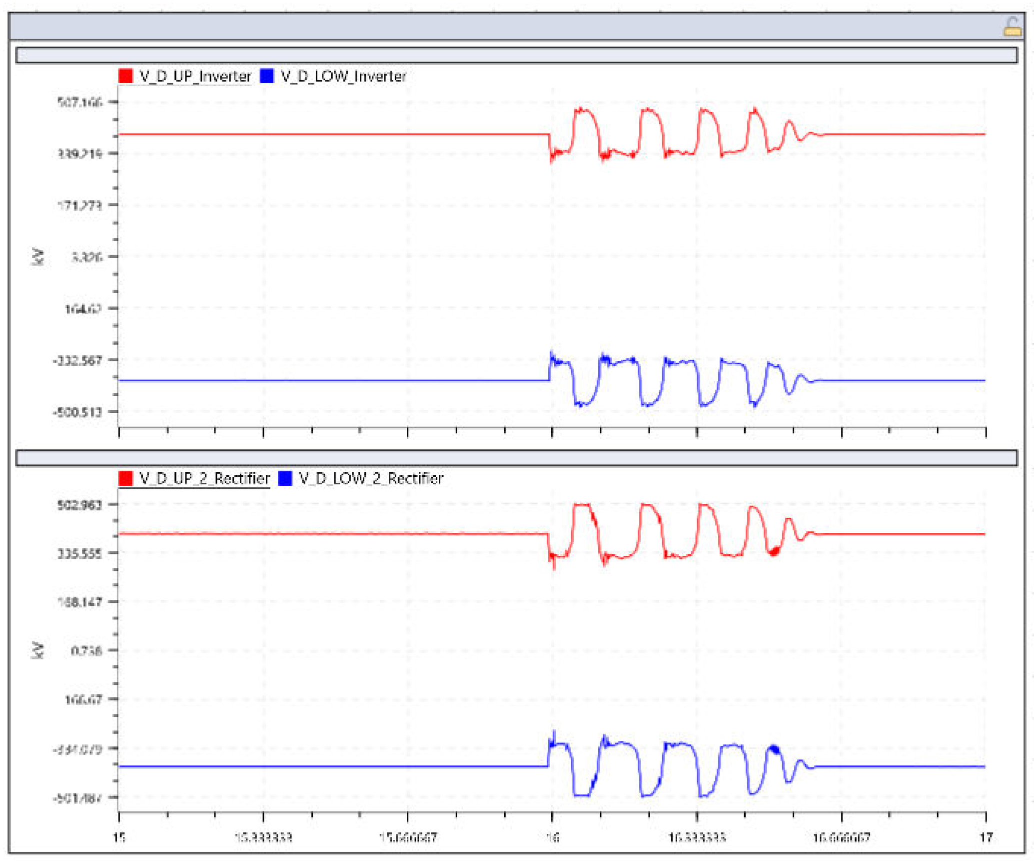

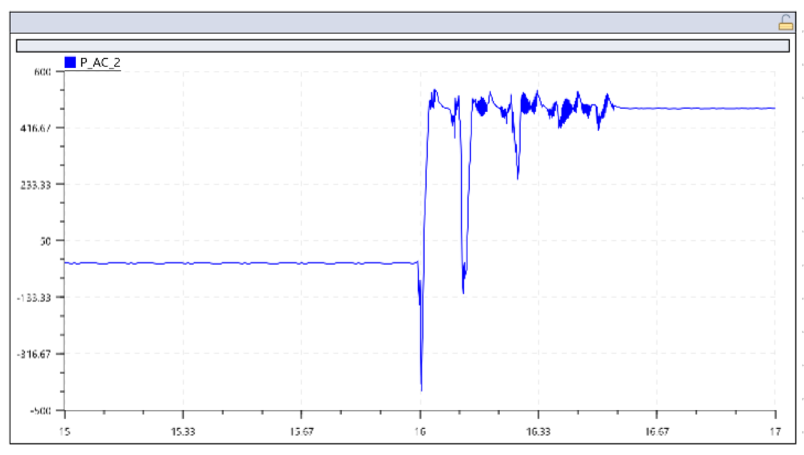

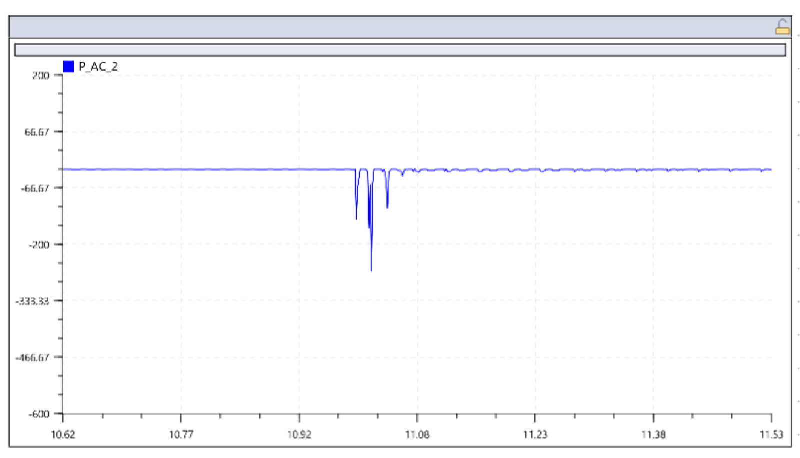

With the support of the Energy Transition Fund

Frequency-Domain Component Models for HVDC Protection Studies

Mudar Abedrabbo, Willem Leterme and Dirk Van Hertem
mudar.abedrabbo@kuleuven.be

Energy Ville
Empowered by KU Leuven, VITO, imec & UHasselt

1. Introduction & Motivation

- HVDC protection design is challenging due to the large number of parameters influencing the DC-side contingencies (e.g. DC-side faults).
- To design a fast and robust HVDC protection systems, transient studies over a wide range of parameters are required.

Transient Analysis

Time domain approach (e.g. EMT-type software)	Frequency-domain approach
Pros:	**Pros:**
❖ Straightforward modeling: ✓ Switching ✓ Non-linear components	❖ No time step selection ❖ Frequency-dependency: straightforward
Cons:	**Cons:**
❖ Time step selection ❖ Modeling frequency-dependent components is not straightforward	❖ Modeling non-linear components is not straightforward

- Frequency domain models for HVDC components (i.e. HVDC converters, HVDC circuit beakers) are still missing.
- The main contribution of this paper is to propose **frequency-domain models of HVDC converters** (half- and full-bridge MMCs) and **HVDC circuit breakers** that can be used for HVDC protection studies.

2. Half-Bridge & Full-Bridge Modular Multilevel Converter

- The converter response to the DC-side fault is divided into four stages for a half-bridge MMC and three stages for a full-bridge MMC.
- Transition instants between these stages are determined from the AC- and DC-side electrical quantities of the MMC.

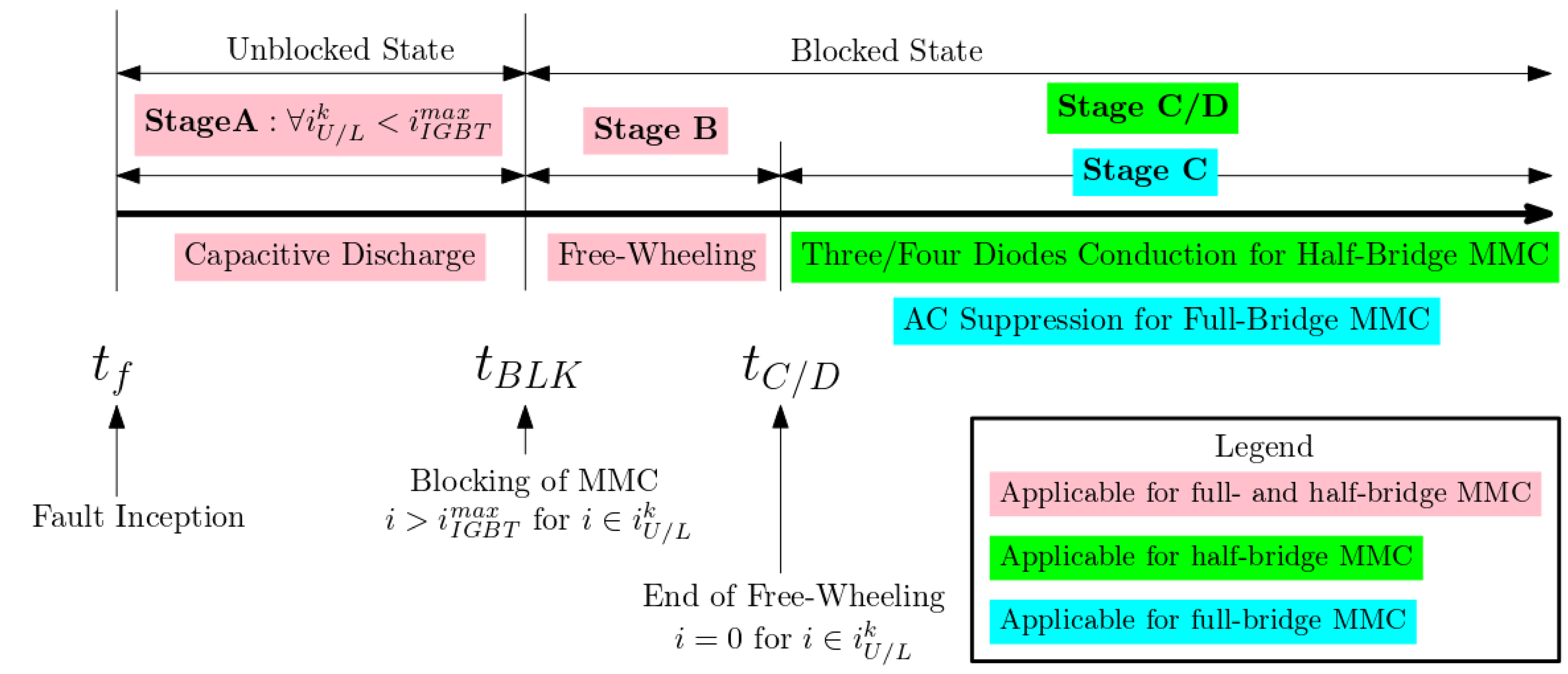

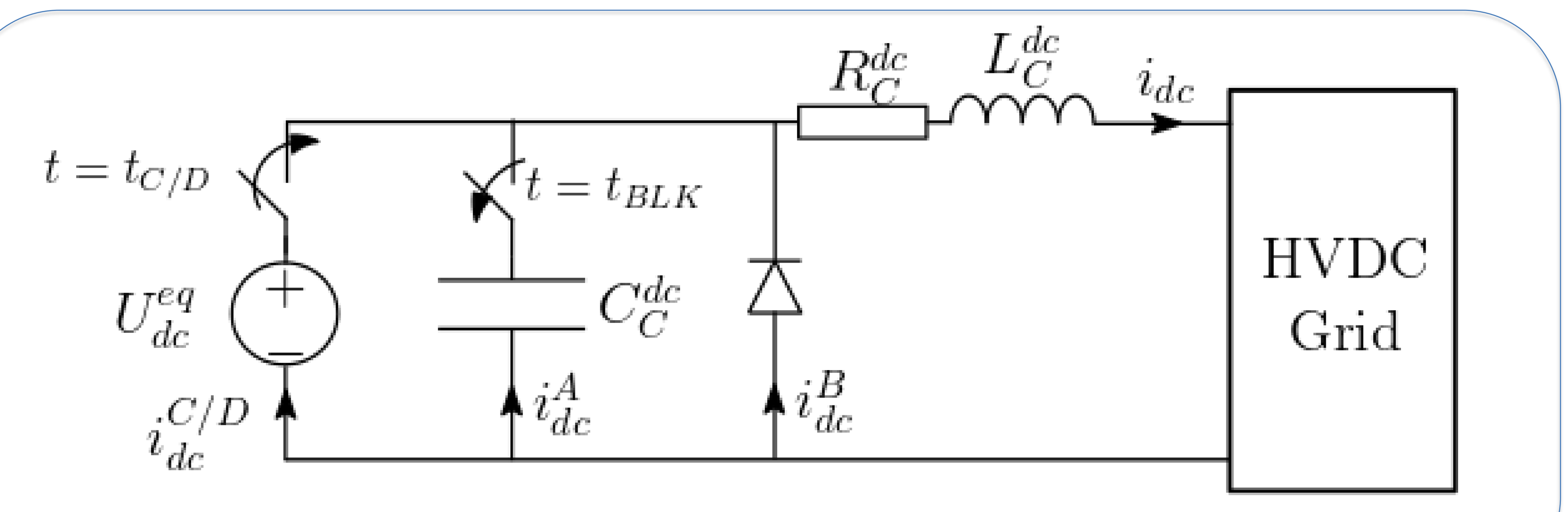

DC-side equivalent circuit of the half-bridge MMC during stages A, B, C , D

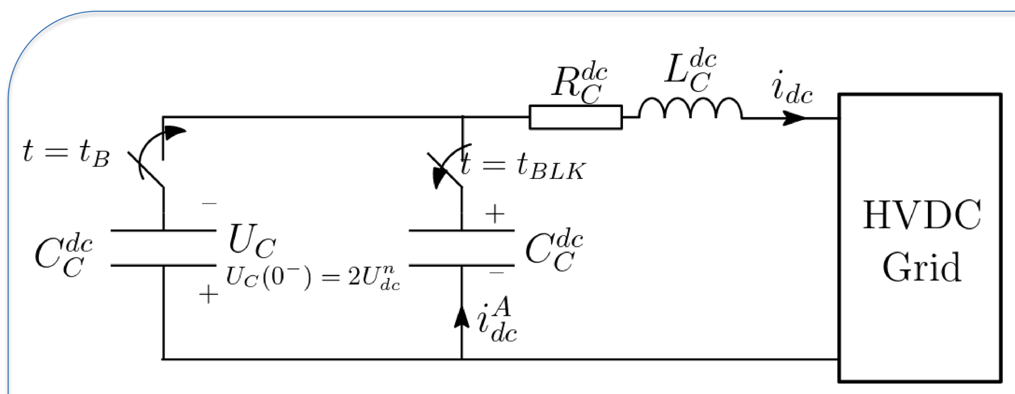

DC-side equivalent circuit during stages A & B for full-bridge MMC

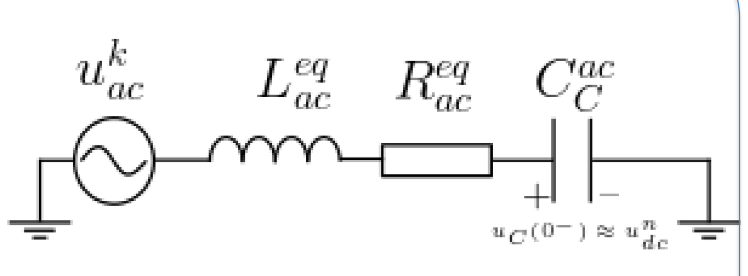

Equivalent circuit per phase during stage C for full-bridge MMC

3. HVDC Circuit Breaker (DCCB)

- For system studies, the DCCB can be modeled as a single component with two parallel branches: (1) An ideal switch, (2) single surge arrester.
- The surge arrester has a non-linear U-I characteristic ➔ This nonlinearity is approximated using the piece-wise fitting.
- Surge arrester is modeled as a component with multiple branches consisting of voltage sources, resistors and ideal switches.π

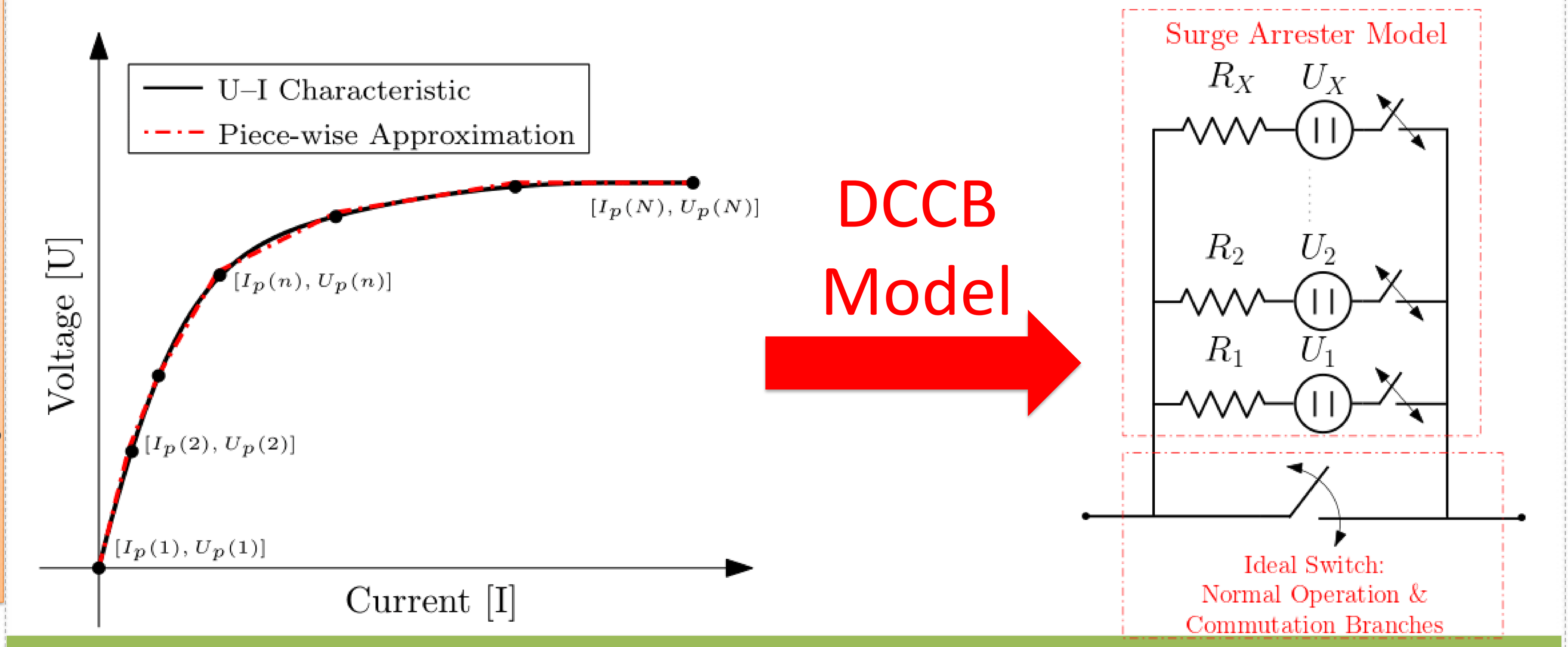

4. Validation of Frequency-Domain Models

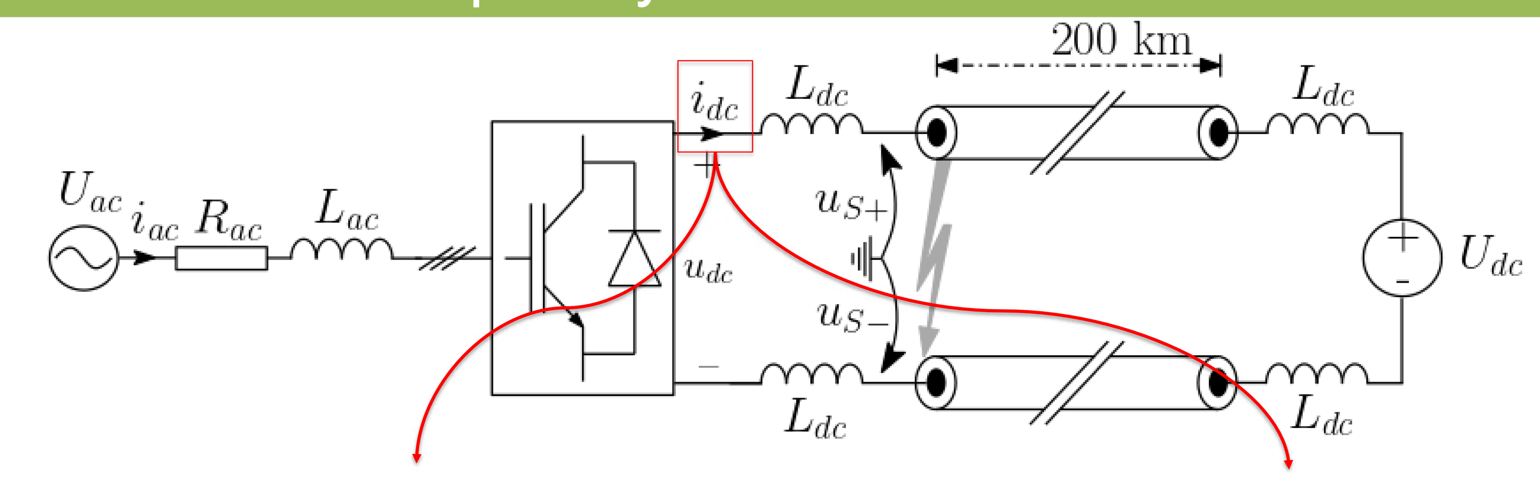

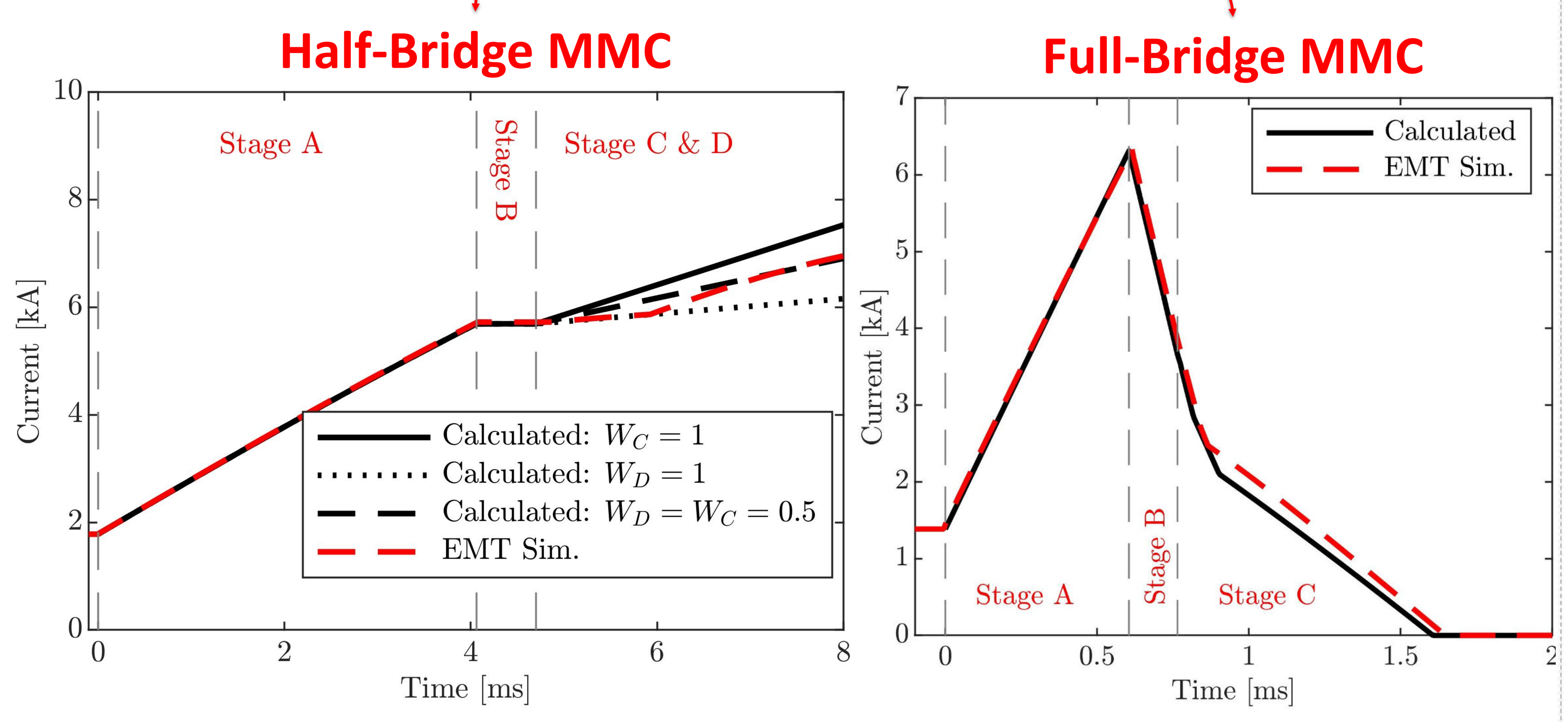

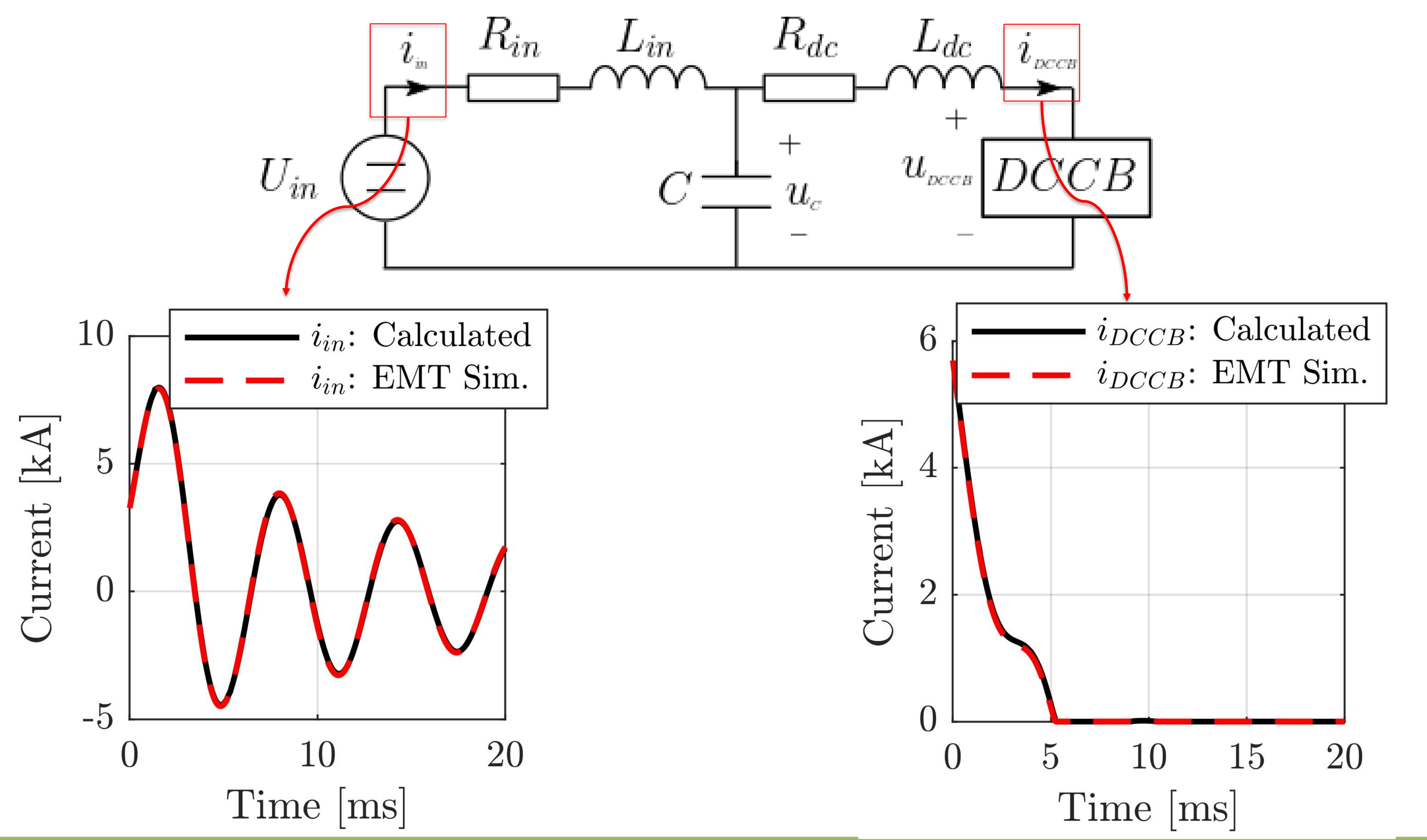

5. Conclusion

- The accuracy for the half-bridge MMC modeling in frequency-domain is given up compared with the time-domain modeling, however, a computationally efficient implementation is achieved.
- Highly accurate full-bridge MMC and DCCB models can be implemented in the frequency-domain, where the piece-wise approximation can be used for the non-linear components.

With the support of the Energy Transition Fund

Analysing the Performance of Incremental Quantity based Directional Time-Domain Protection near HVAC Cables and VSC HVDC Converters

Joachim Vermunicht, Willem Leterme, Dirk Van Hertem
Dept. Electrical Engineering, KU Leuven/EnergyVille, Leuven/Genk, Belgium

Context
New grid elements are being increasingly used in today's power grid. These new grid elements behave differently compared to synchronous machines and overhead lines during transients and faults.
An increased share of underground HVAC cables affects the system's resonance frequencies, whereas VSCs have limited fault current and introduce actively controlled current phase shifts during short-circuit faults.

Need
Legacy protection currently installed in the grid encounters problems. Conventional distance protection malfunctions near VSC, examples are: incorrect zone selection or directional decision and extended settling time.
However, few studies focus on how incremental quantity-based transmission line protection performs under changed source conditions.

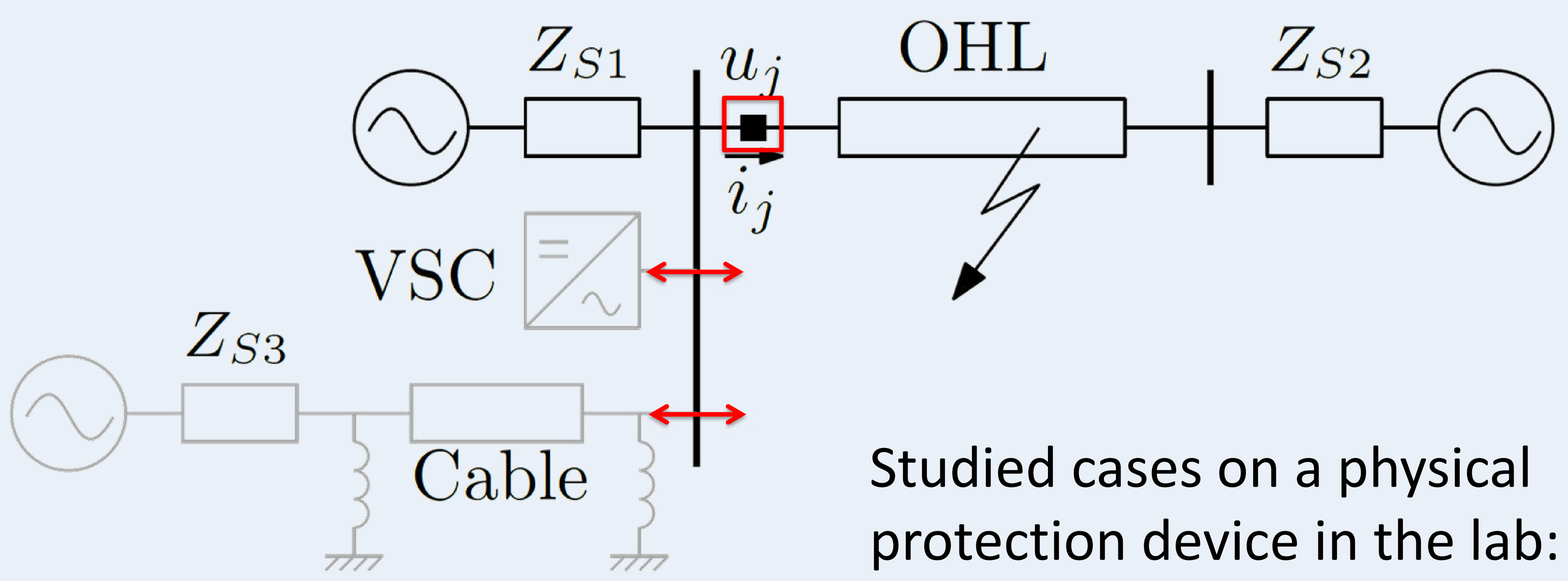

Studied cases on a physical protection device in the lab:

- Benchmark: 60
- Cable: 180
- VSC: 90

Main contributions
Analysing the impact of new grid elements on time-domain protection, namely the impact of:

1. cable resonances triggered by a fault,
2. changed current injection angles by VSC HVDC converters during fault.

Case studies leading to an incorrect assertion of the reverse detection function:

- Cable oscillations change the expected polarity relationship of incremental quantities.
- VSC fault controls cause phase shifts of the incremental current quantity.

Cable

Oscillations persist in the incremental values

Forward and subsequent reverse detection

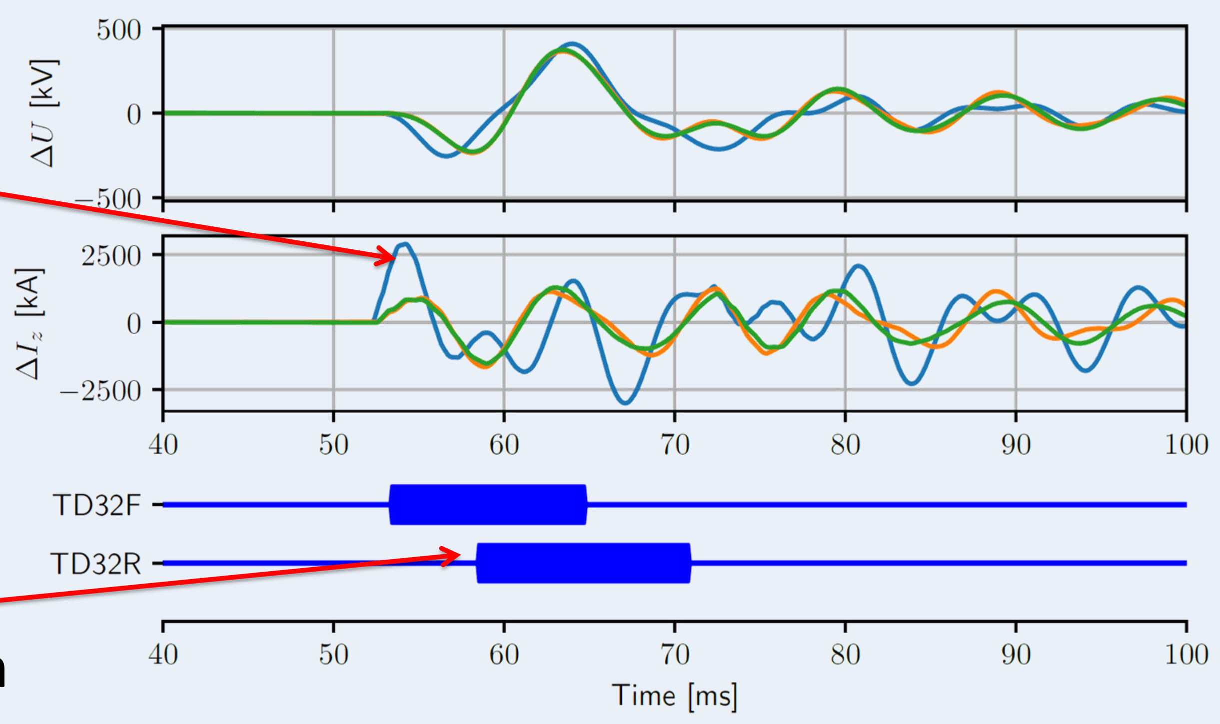

Benchmark

Expected forward detection

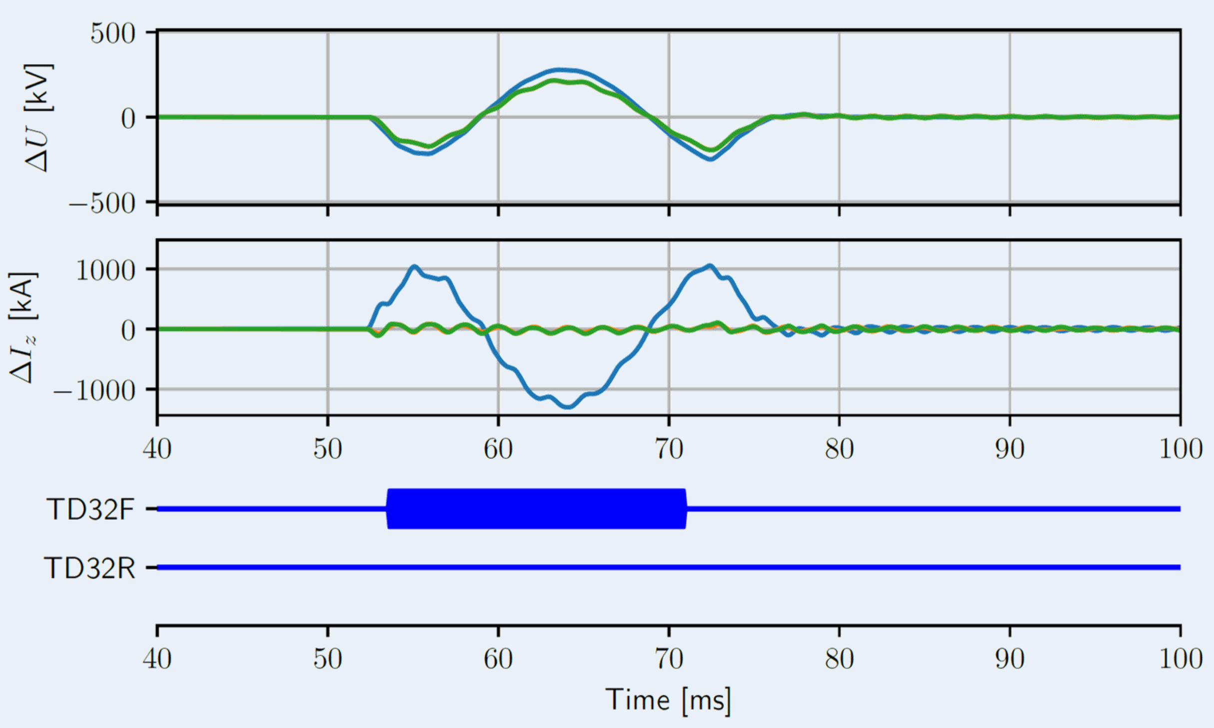

Key takeaways

- Cable resonances change the polarity of incremental quantities, resulting in a decrease of dependability margin and potential security issues.
- Fast reactive current injection by a VSC can cause protection malfunction of IQ protection.
- Unconventional fault behaviour, that deviates from resistive-inductive behaviour, is not filtered out by the input filters of this time-domain protection.

Case study with VSC

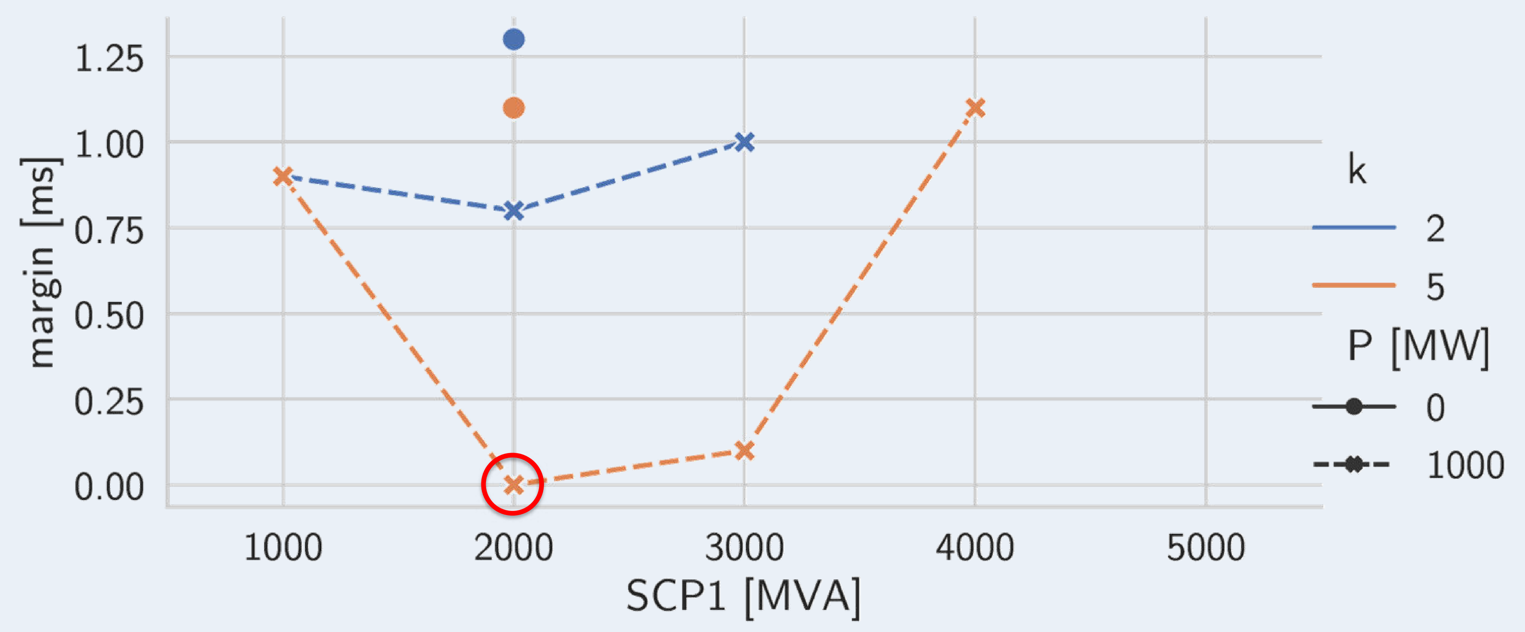

The smallest time margin between forward and (incorrect) reverse detection functions occurs for: a weak local bus and fast fault current injection with a large injection factor.

With the support of the Energy Transition Fund

Evaluation of AC protection near HVDC convertors

Joachim Vermunicht, Rick Loenders, Sadegh Mousavi
Shoushtari, Geraint Chaffey, Gert Verbeek, Willem Leterme, Dirk Van Hertem
Dept. Electrical Engineering, KU Leuven/EnergyVille, Leuven/Genk, Belgium

Energy Ville
Empowered by KU Leuven, VITO, imec & UHasselt

Context
Converter-interfaced renewable energy sources, and voltage source converter (VSC) HVDC links are being used more and more, whereas synchronous generation is gradually phased out.

These converter interfaced elements lead to a huge change in the way the system responds to faults: first, converters can only supply a limited amount of fault current, and second, their control loops, control the fault current to have different characteristics compared to that delivered by synchronous generation.

Main contributions
Study on converter effects on the apparent impedance measured by distance relays:
- Systematic analysis on the parameters within the faulted network that impact the impedance locus of distance protection.
- Development of an automation framework for protection studies with accurate equivalent models for VSC converters and Hardware-in-the-Loop (HiL).

Case studies
Steady-state assessment of apparent impedance. Effect of VSC on apparent impedance by variation of relative grid strength SCPgrid 1 ↘ .

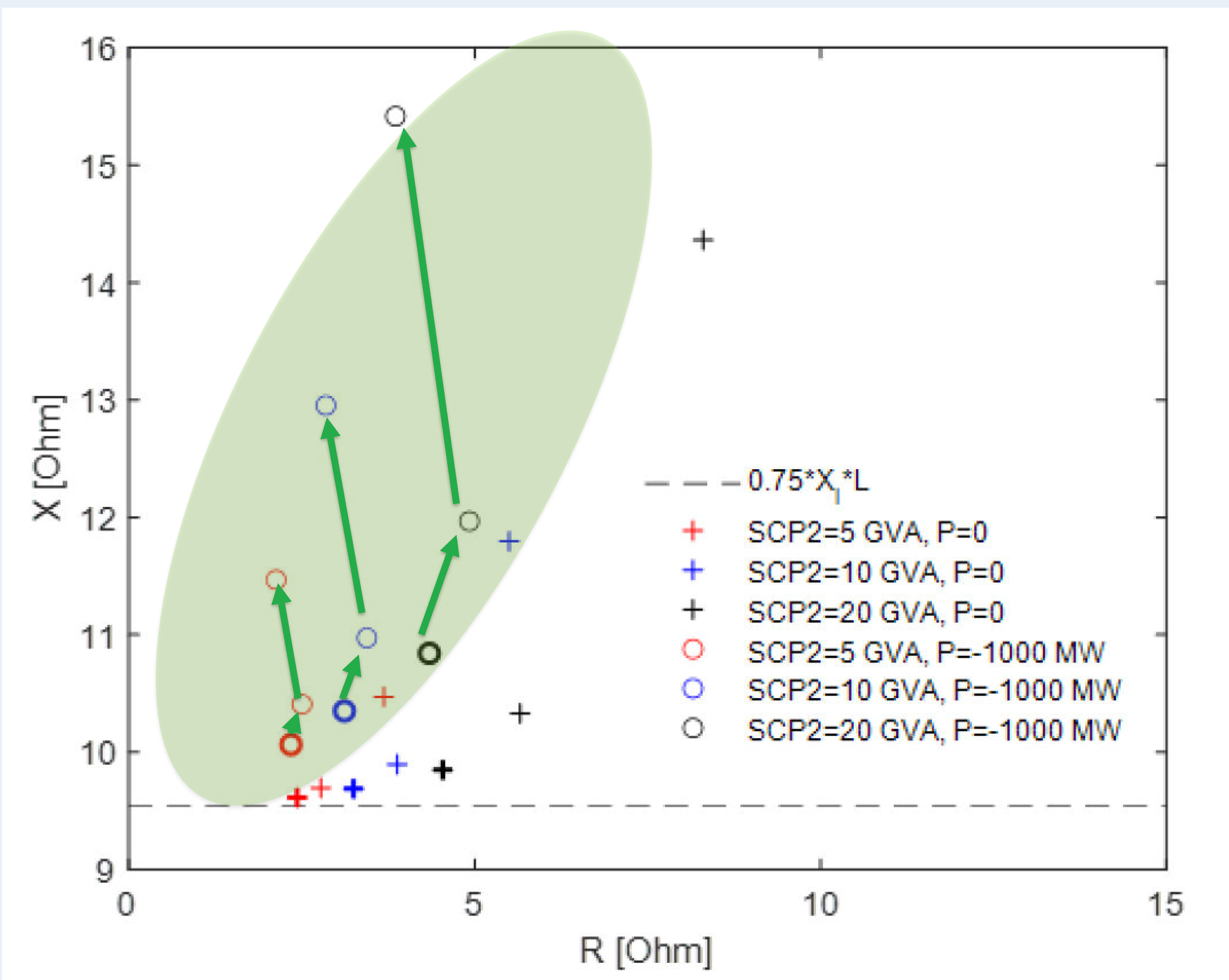

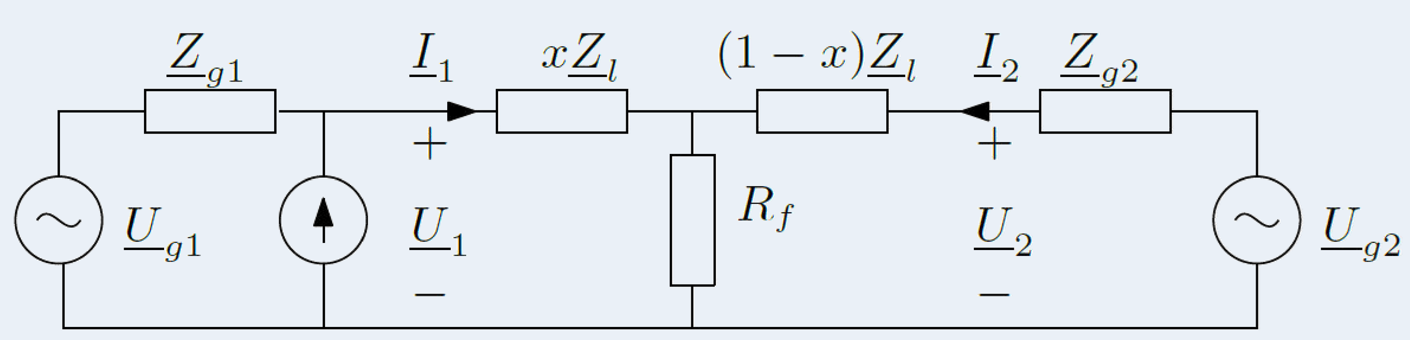

Published in:
Leterme, Willem, et al. "Systematic study of impedance locus of distance protection in the vicinity of VSC HVDC converters." 16th International Conference on Developments in Power System Protection (DPSP 2022). Vol. 2022. IET, 2022.

Need
Current legacy protection devices in the grid encounter problems due to fundamentally changes to short-circuit characteristics.

Digital Grid Emulation Lab

Automation framework for protection studies

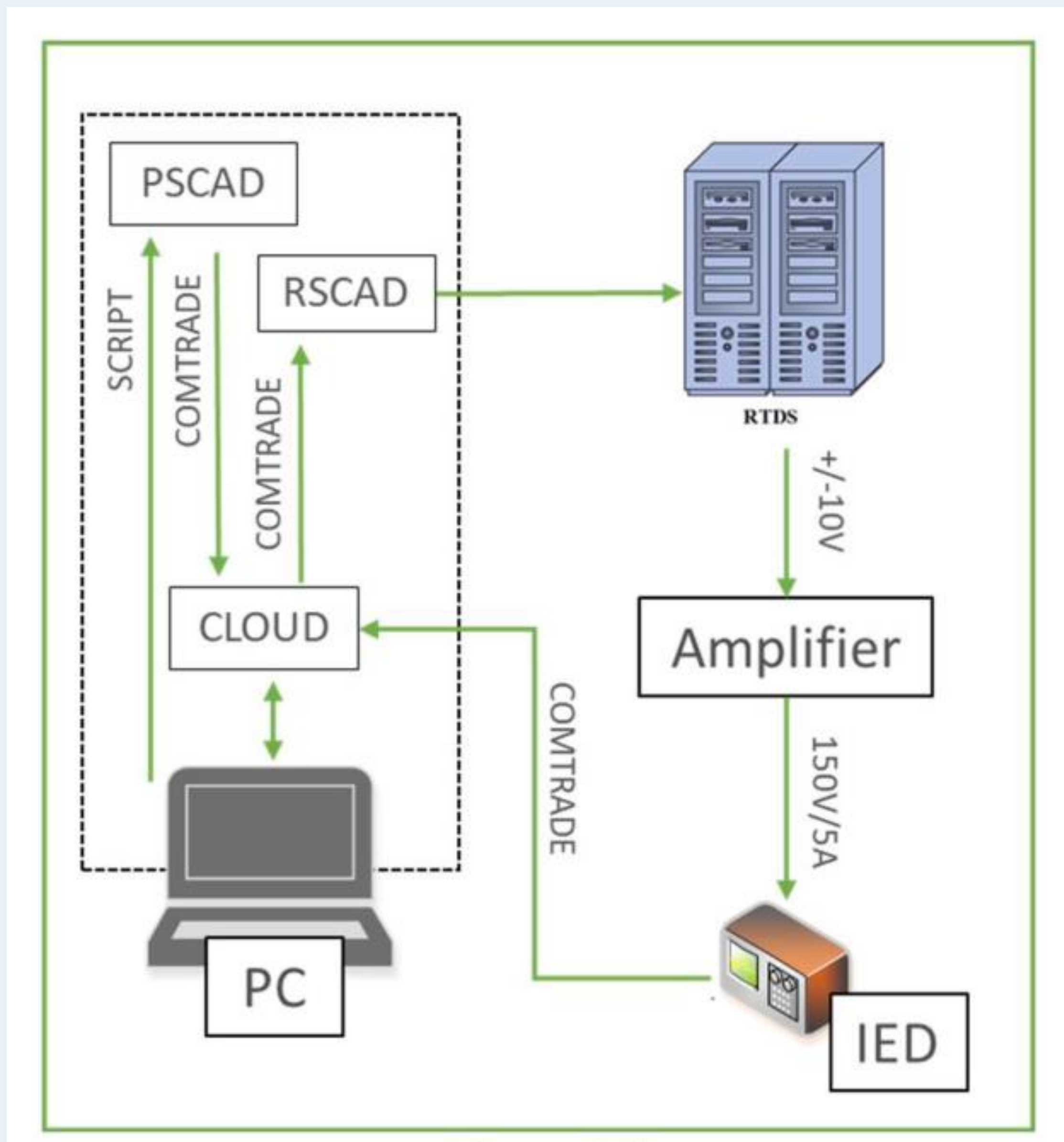

Key takeaways
- Most problems arise in situations where the converter dominates the local short-circuit current and with a large remote short-circuit current contribution.
- Steady-state methods allow for an efficient pre-selection of protection tests towards post-transient analysis.

KU LEUVEN vito imec UHASSELT economie

With the support of the Energy Transition Fund

Financial Viability of a Full-Scale Meshed HVDC Grid and Hybrid Offshore Assets in the North Sea

C.K. Jat, J. Dave, S. Hardy, H. Ergun, D. Van Hertem

Energy Ville

Empowered by KU Leuven, VITO, imec & UHasselt

Neptune

Financial schematic for decision making under uncertainty:

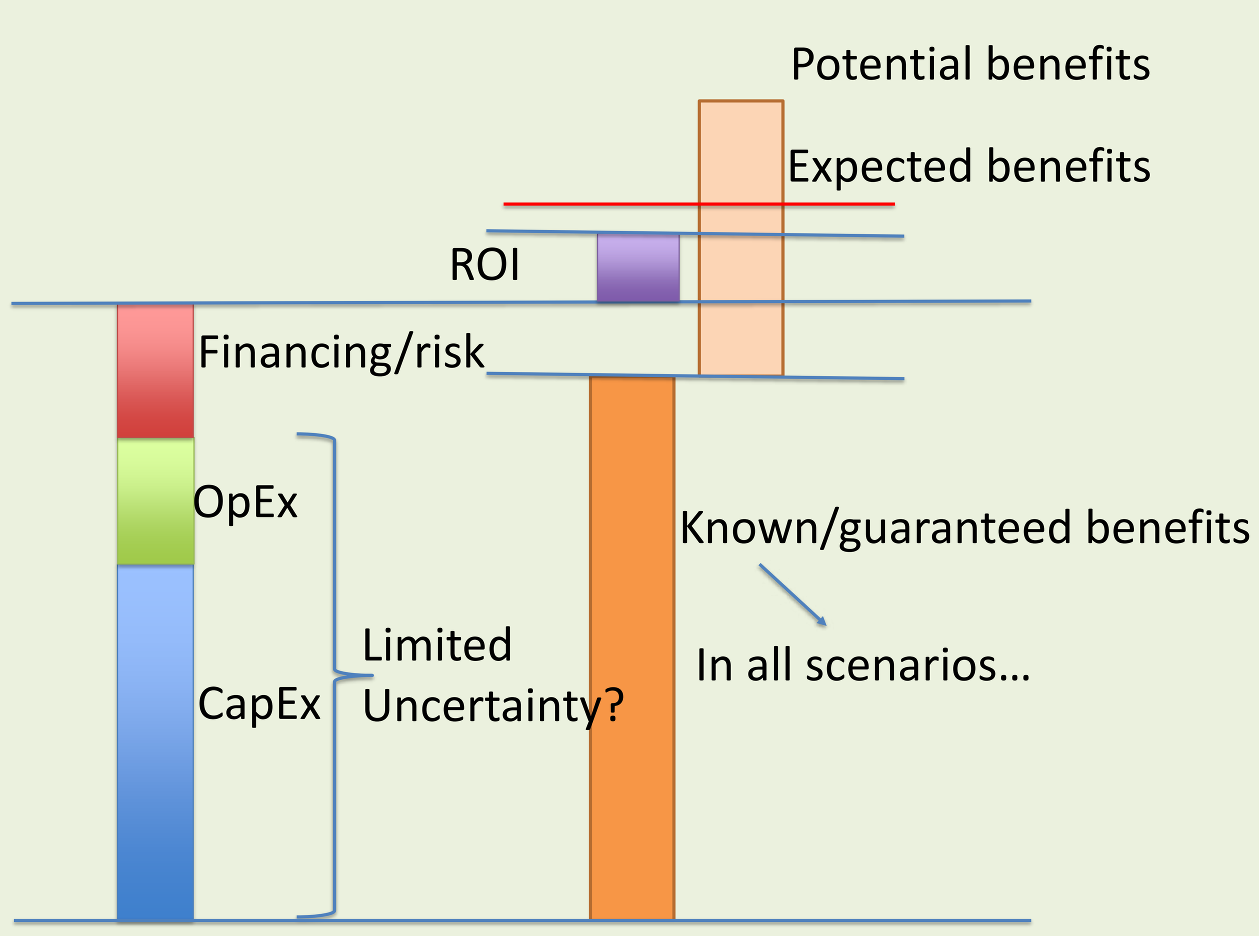

Annual profit of a line connecting different price zones can approximately be calculated as:

$$Annual\ Prices\ differece = \sum_{i=1}^{8760} |p_{Ai} - p_{Bi}| \ \left[\frac{€}{\frac{MW}{year}}\right]$$

ENTSO scenarios considered for the analysis:

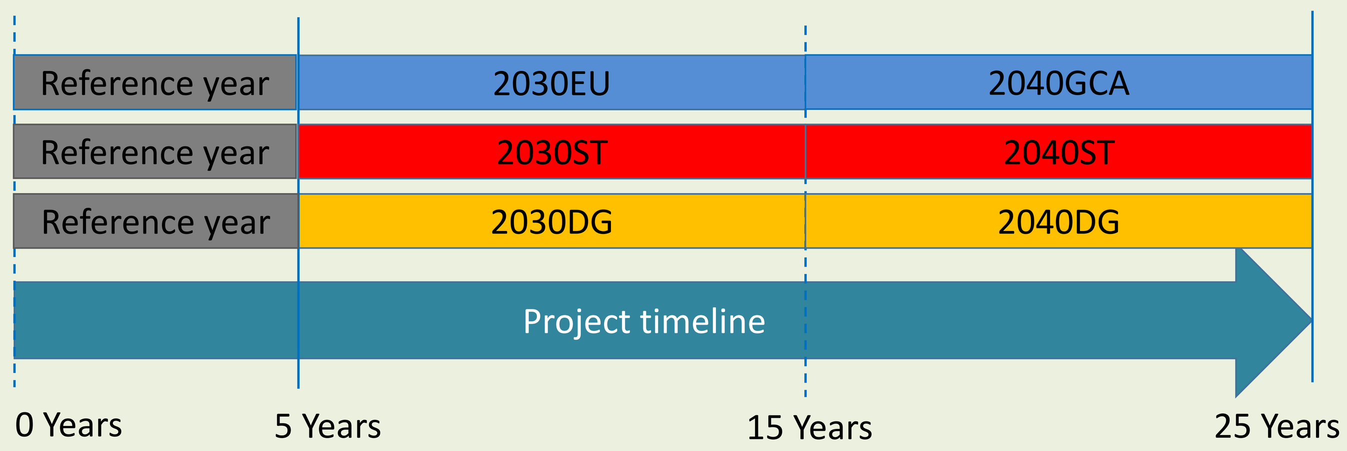

HVDC demonstration grid:

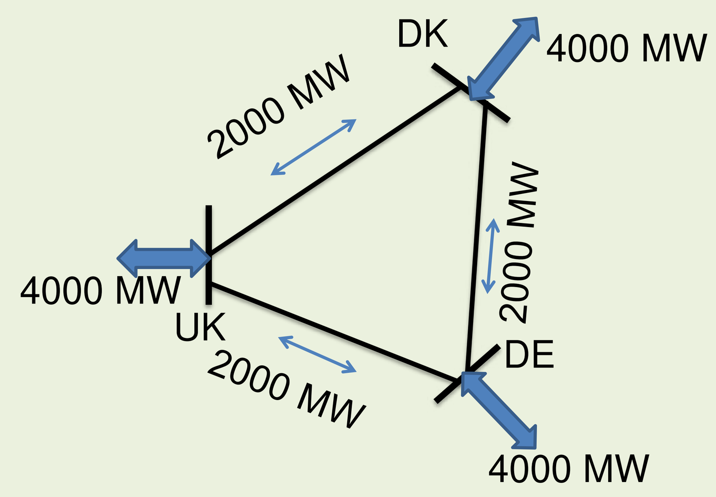

Lifetime benefits under different scenarios and interest rates:

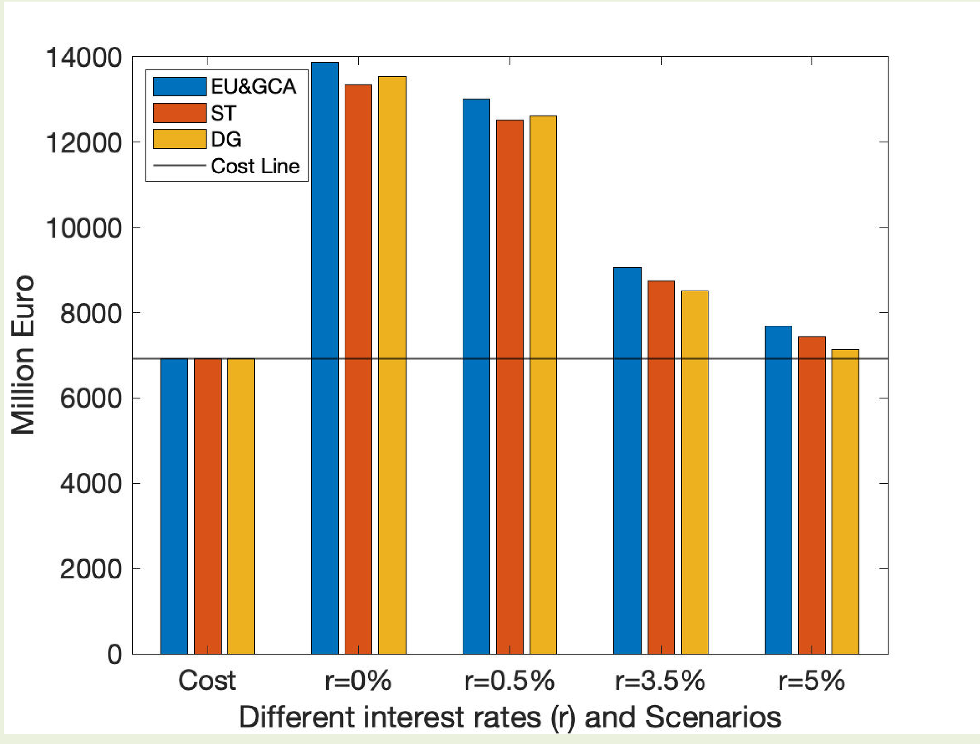

Payback time under different scenarios and interest rates:

Scenario	Payback Period (Yrs) with interest rate of			
	5%	3.5%	0. 5%	0%
2030EU 2040GCA	17.71	13.56	10.37	9.99
2030ST 2040ST	19.61	14.09	10.66	10.26
2030DG 2040DG	23.45	17.94	12.62	12.04

Payback period (years) sensitivity w.r.t. 'UK-DE' link:

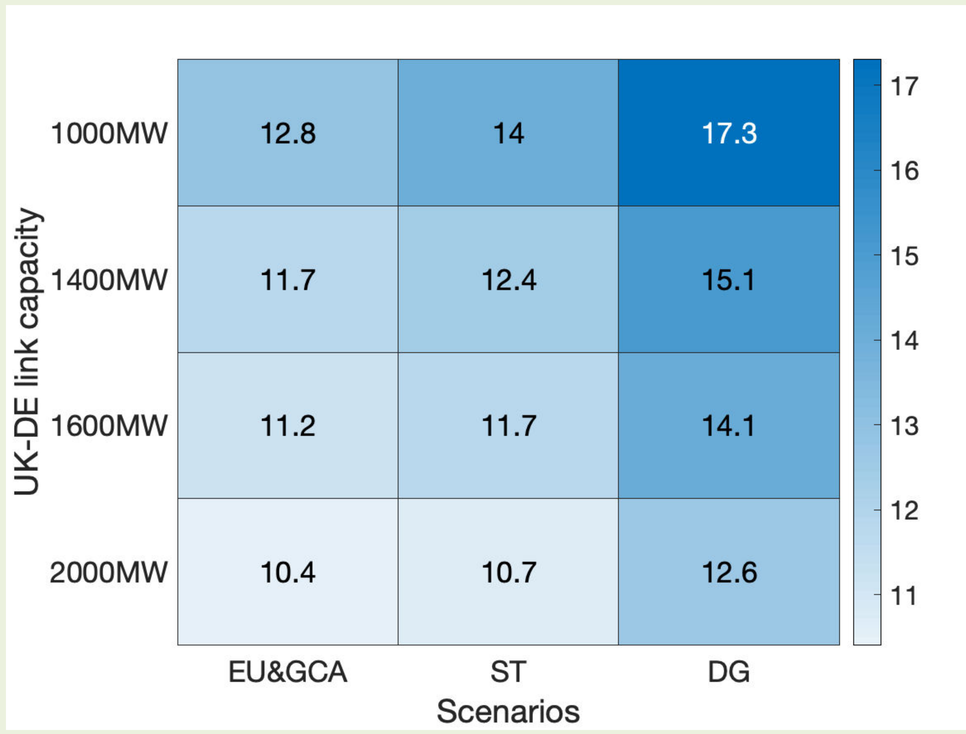

Conclusions:

1. Demonstrator pays back its investment even for the worst-case scenarios while having potential to provide high returns in favorable scenarios.
2. The payback period is sensitive to the HVDC line capacities; therefore, it can further be optimized by formulating an optimization model with various line and converter capacities.

A transmission netwrok expansion plannig problem as an optmization model considering:

- Two different connection schemes for offshore wind farms.
  1. Business as usual: Radial connection to the home market.
  2. Hybrid offshore assets: Offshore wind farm as a separate marke zone, developed along with other offshore transmission assets (HOA).
- Various transmission capacities for the HVDC line and converter capacities:
  1. 2 GW and 4 GW limits for the transmission lines
  2. 0 to 4 GW range for the converter capacity selection
- All the Entso-e scenarios are considered along with four distict reference years
  - Thus optimized for the expectd (average) value for the 3*4=12 scenarios

Conclusions:

1. Economic feasibility of the HVDC demonstration grid is analysed using the payback period, lifetime benefits, and wind curtailment as performance metrics. The analysis leverages the arbitrage opportunities created by the price differences among the connected countries. A scenario-based stochastic optimization approach is adopted to deal with the uncertainty of long-term planning. The grid is found to be financially viable, however, the total benefits of the grid and exact topology depends on the choice of capacity.
2. The "business as usual" radial connection design for OWPPs is compared to one considering the possibility of HOAs. It is observed that an HOA based design has significantly higher profit and less wind curtailment compared to the radial, home market design.
3. Optimal topology for 2GW connection capacity requires more transmission paths.

Candidate HVDC lines:

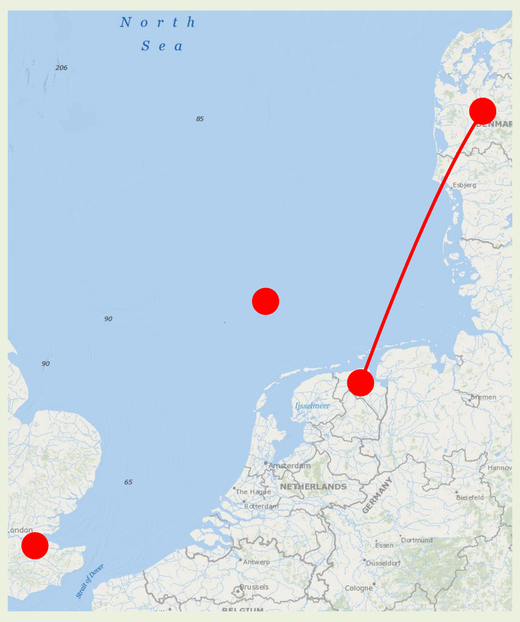

Optimal topology for the radial connection design

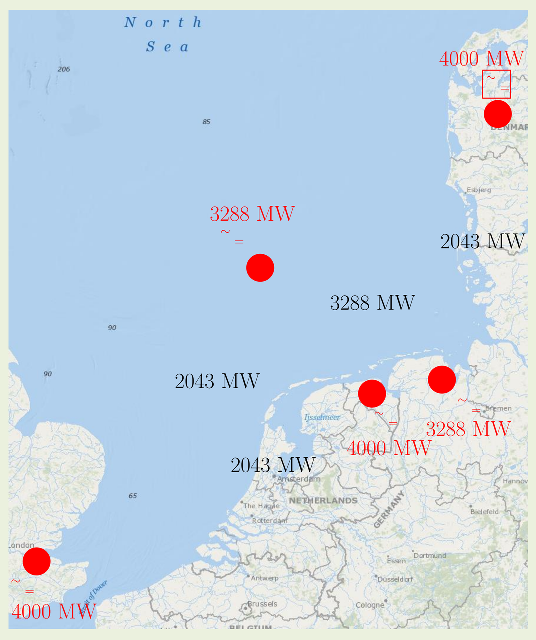

Optimal topology for HOA design with 2 GW line limits

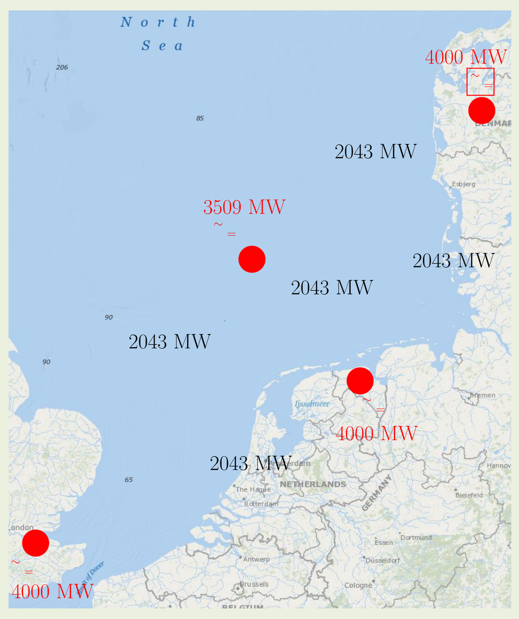

Optimal topology for HOA design with 4 GW line limits

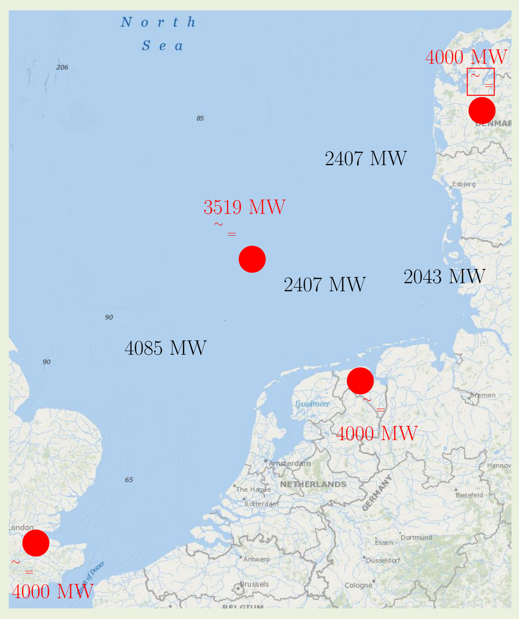

References:

1. C. K. Jat, J. Dave, H. Ergun, D. Van Hertem, A multi-terminal hvdc demonstration grid in the north-sea: A cost-effective option, in: 2021 International Conference on Smart Energy Systems and Technologies (SEST), IEEE, 2021, pp. 1–6.
2. C. K. Jat, Stephen Hardy, J. Dave, H. Ergun, D. Van Hertem, Powering Europe's Energy Transition: Financial Viability of a Full-Scale Meshed HVDC Grid and Hybrid Offshore Assets in the North Sea, in IEEE PES ISGT Europe 2023 [accepted].

KU LEUVEN vito imec UHASSELT economie

With the support of the Energy Transition Fund

A Planning Methodology for HVDC Interconnectors and Grids Considering Security Related Costs

Hakan Ergun, Jay Dave, Dirk Van Hertem

INTRODUCTION

- This work introduces a transmission expansion optimisation (TNEP) tool to determine the optimal size and location of HVDC lines and converters.
- During the optimisation, power system security related costs are taken into account.
- The tool is implemented in Julia/JuMP as an extension of *PowerModelsACDC.jl* and is applicable to large networks

HVDC GRID MODEL

- Point to point and meshed configurations
- Possibility to introduce intermediate DC buses
- Full converter station representation with transformer and filter
- Separate decision variable for lines and converters

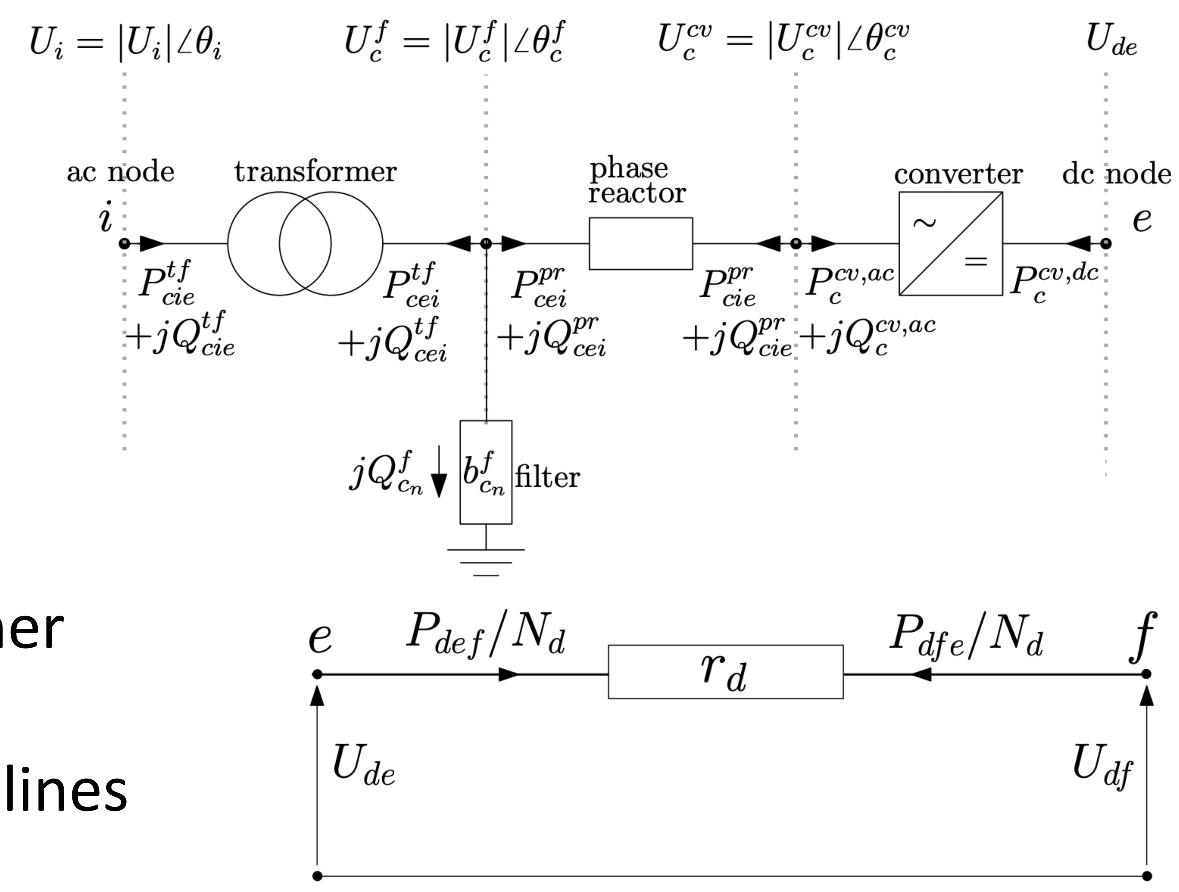

METHODOLOGY

- Iterative solution of mixed-integer transmission expansion optimisation, and optimal power flow to determine minimum redispatch cost of contingencies
- TNEP objective: Minimise generation operational cost and transmission investment cost for all considered time samples

$$minC = \sum_{t=1}^{T_s}\left(\sum_{i=1}^{C_n} C_c(i)\ ' \cdot \xi_{c,t} + \sum_{i=1}^{D_n} D_c\ '(i) \cdot \xi_{d,t} + \sum_{g=1}^{\mathcal{G}} \cdot C_g\ ' P_{gi,t}\right)$$

- Optimal redispatch objective: Minimise weighted redispatch and possible load shedding cost for all contingencies of newly built lines/converters for all time samples

$$minC_{s,c,d} = \pi_c \sum_{t \in T_s}\left(\sum_{g \in \mathcal{G}} \Delta P_{g,t} \cdot C_g^{rd} + \sum_{m \in \mathcal{M}} \Delta P_{m,t} \cdot C_m^{voll}\right) \forall c \in \mathcal{C}, \forall d \in \mathcal{D}$$

- TNEP and optimal redispatch optimisation constraints: AC & DC power flow constraints for new and existing lines, time linking constraints for candidate DC lines and converters, power, current, voltage limits of AC and DC equipment

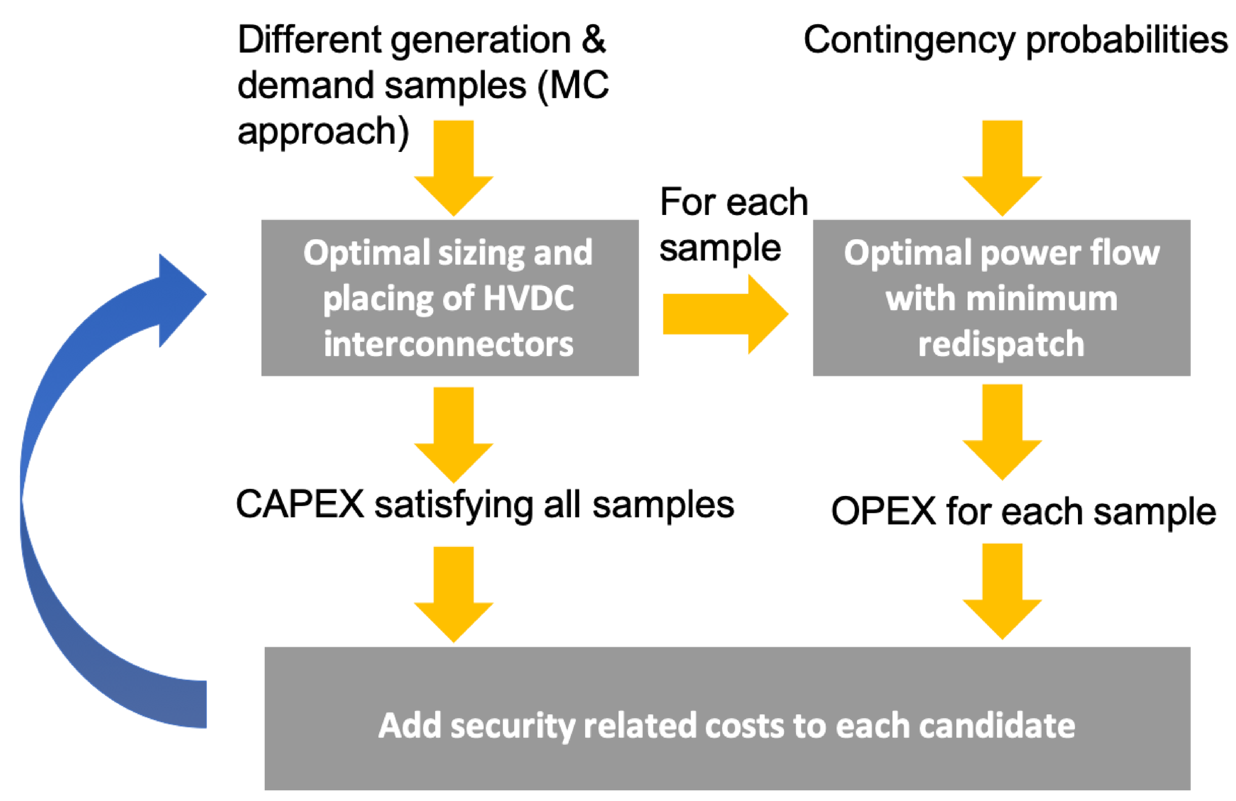

IMPLEMENTATION AND APPLICATION

- Model implemented as an extension of *PowerModelsACDC.jl* for different (non)linear power flow formulations (MINLP, MISOCP, MILP) to achieve best trade-off between accuracy and speed
- Illustrative test case consisting of DE, NL and BE transmission grids (based on publicly obtained data)
  - 608 buses, 1202 AC branches, 4 DC branches, 8 HVDC converters, 1795 generators
  - 27 HVDC overhead lines and 33 HVDC converter stations defined as candidates with ratings of 2 and 4 GW
  - 100 different time samples for high wind and high demand considered
  - Additional wind power injection in the northern part of the system to strengthen the need for expansion
- Solution time for the optimisation problem is 4 hours in total for 3 iterations (3 x MILP - TNEP, ~2000 x LP - OPF)

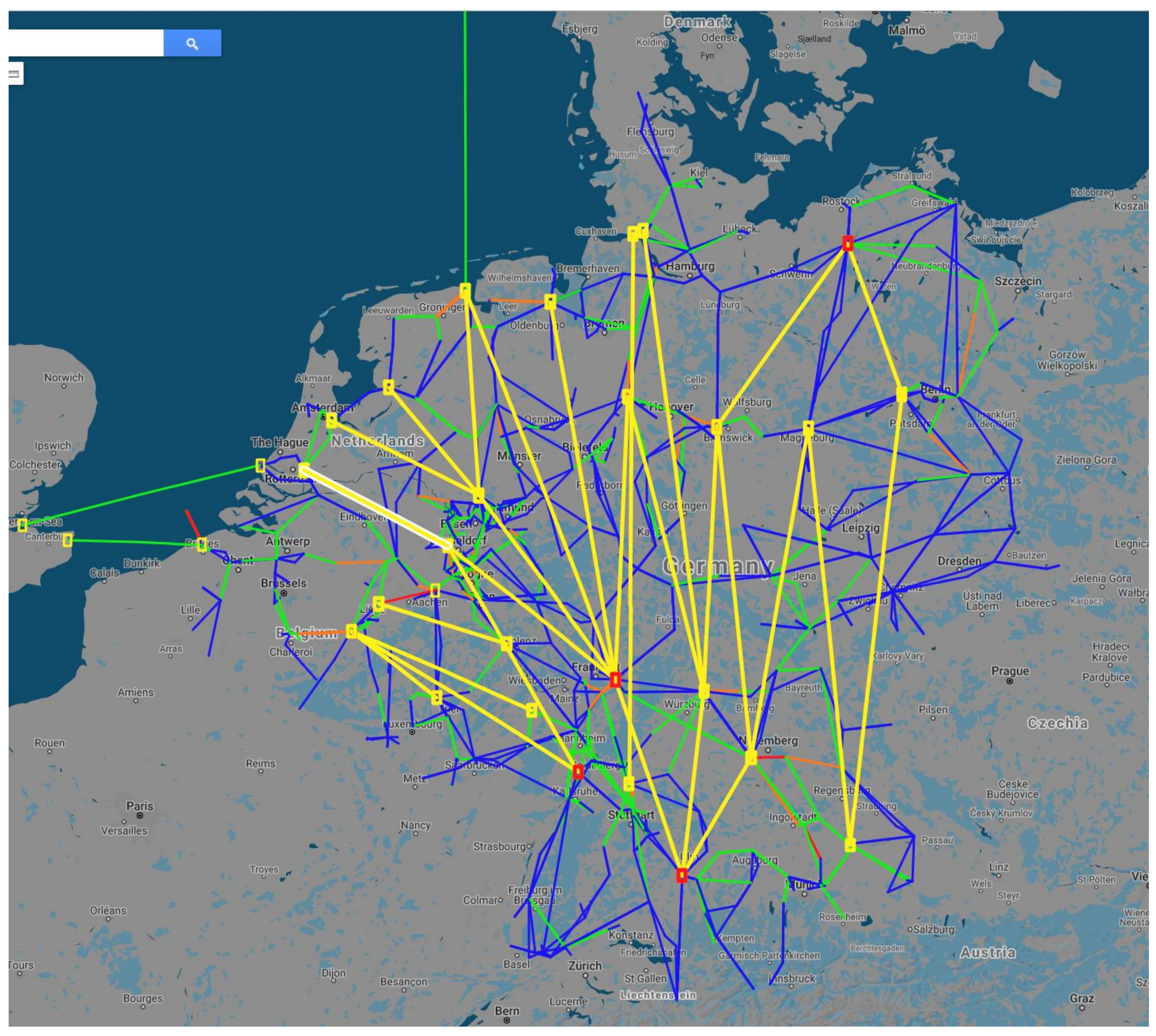

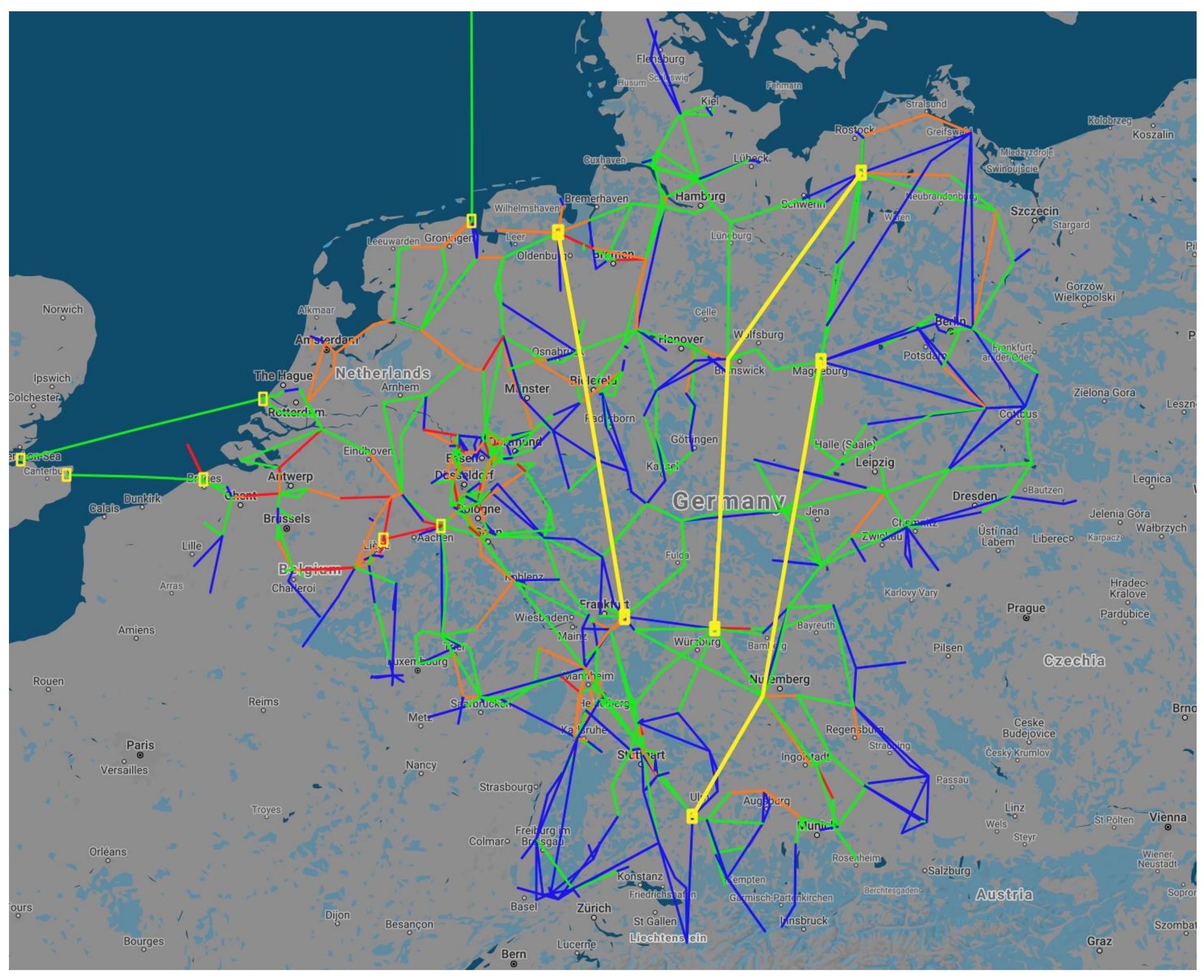

With the support of the Energy Transition Fund

HVDCstability.jl – An Impedance-Based Stability Analysis Toolbox

Thomas Roose, Özgür Can Sakinci, Aleksandra Lekić, and Jef Beerten
ELECTA, KU Leuven, Belgium and EnergyVille, Genk, Belgium

INTRODUCTION

- A Julia package for impedance-based stability analysis is presented.
- Accurate stability analyses can be carried out over a wide frequency range.
- Nyquist plots and stability margins are obtained for assessing the system stability.
- Julia implementation ensures a high computational efficiency.

MODEL DEVELOPMENT

- Passive power system components are represented in terms of their ABCD parameters.
- Modular multilevel converters (MMCs) and synchronous generators are modeled by their state-space and equivalent admittance matrix representation.

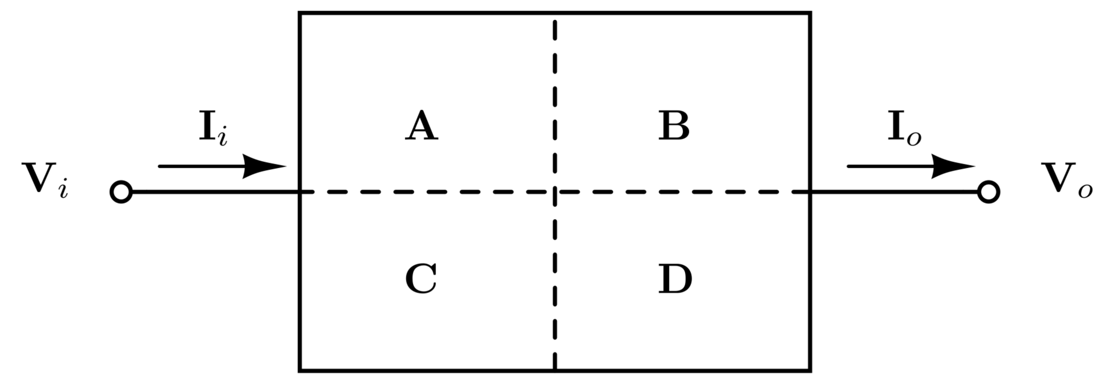

$$\mathbf{Y}_{MMC}(s) = \begin{bmatrix} Y_{dc} & Y_{dc,d} & Y_{dc,q} \\ Y_{d,dc} & Y_{d,d} & Y_{d,q} \\ Y_{q,dc} & Y_{q,d} & Y_{q,q} \end{bmatrix}$$

METHODOLOGY

- Automated formulation of the network impedance between given input and output pins.
- A power flow model is developed to obtain the operating points around which nonlinear components are linearized.
- Multi-terminal stability analysis using node and edge admittance matrix representation of the system.
- System oscillation mode and bus participation factor (PF) analysis based on eigenvalue decomposition.

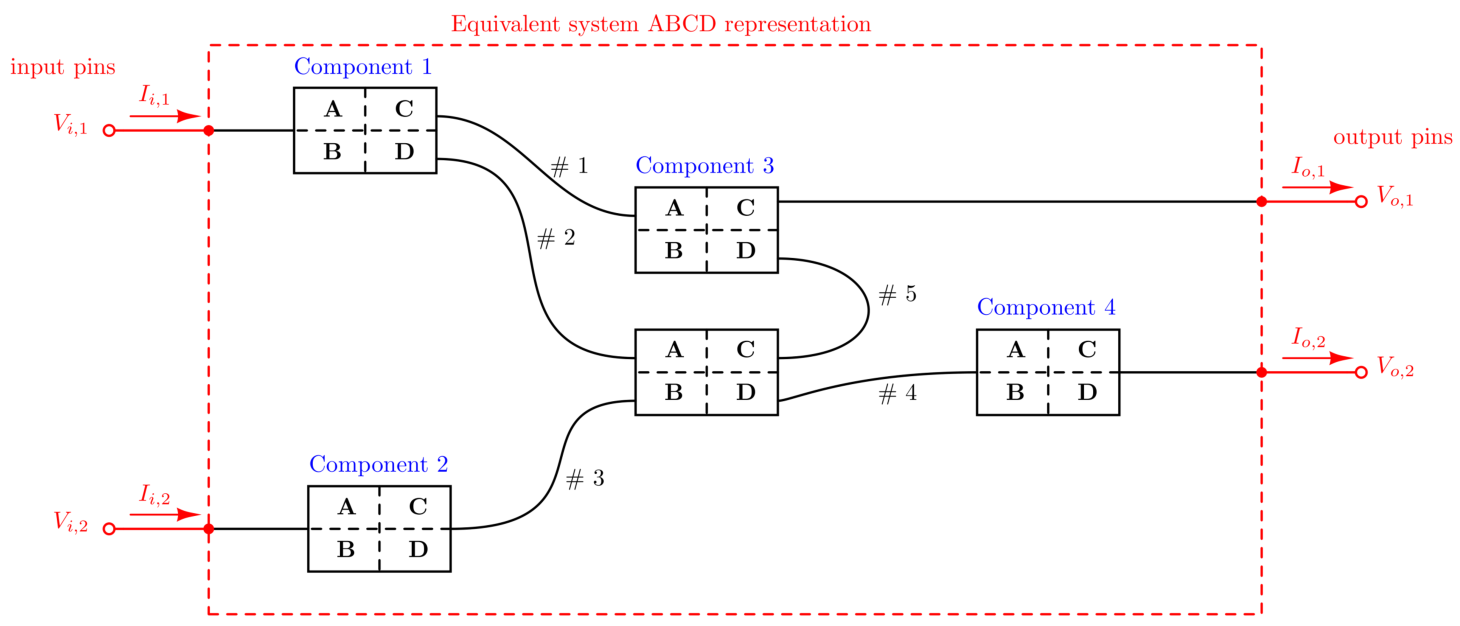

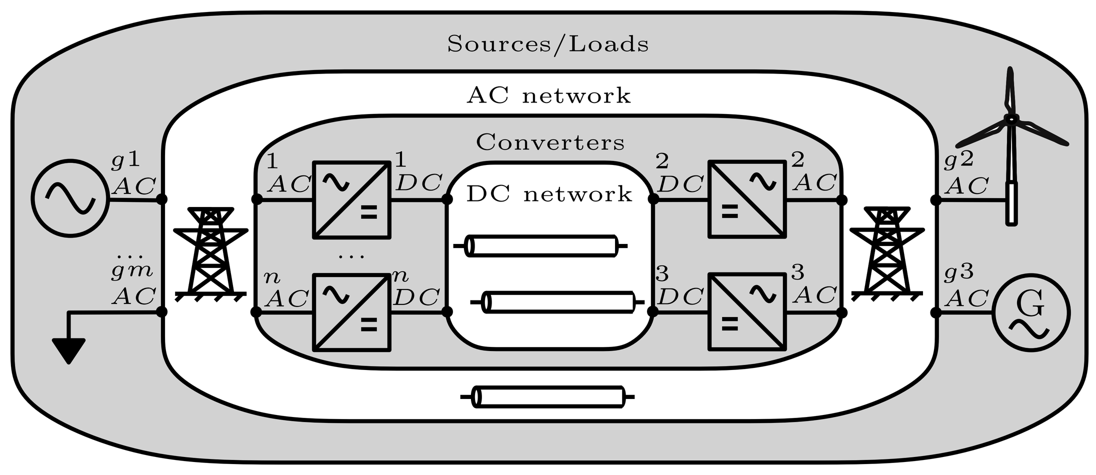

$$\Delta V = (I + Z_{edge}(s)Y_{node}(s))^{-1} Z_{edge}(s)\Delta I_N$$

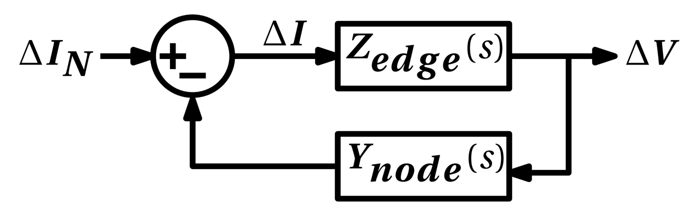

$$L(s) = Z_{edge}(s)Y_{node}(s)$$

$$\Delta V = Z^{cl}_{bus}(s)\Delta I_N$$

$$Z^{cl}_{bus}(j\omega) = \Phi(j\omega)\Lambda(j\omega)\Psi(j\omega)$$

RESULTS

- The dq-frame network admittance obtained from the Julia implementation shows a good match with the corresponding nonlinear model implemented in the EMT software PSCAD.
- Impedance-based stability analysis for a modified IEEE 9 bus model including two HVDC links takes less than a minute in a Windows PC with an i7-1185G7 processor and 32 GB RAM.
- A multi-terminal impedance-based representation enables the stability assessment based on black-box models.
- Critical oscillation modes are identified and terminals contributing to these modes are indicated by the bus PFs.

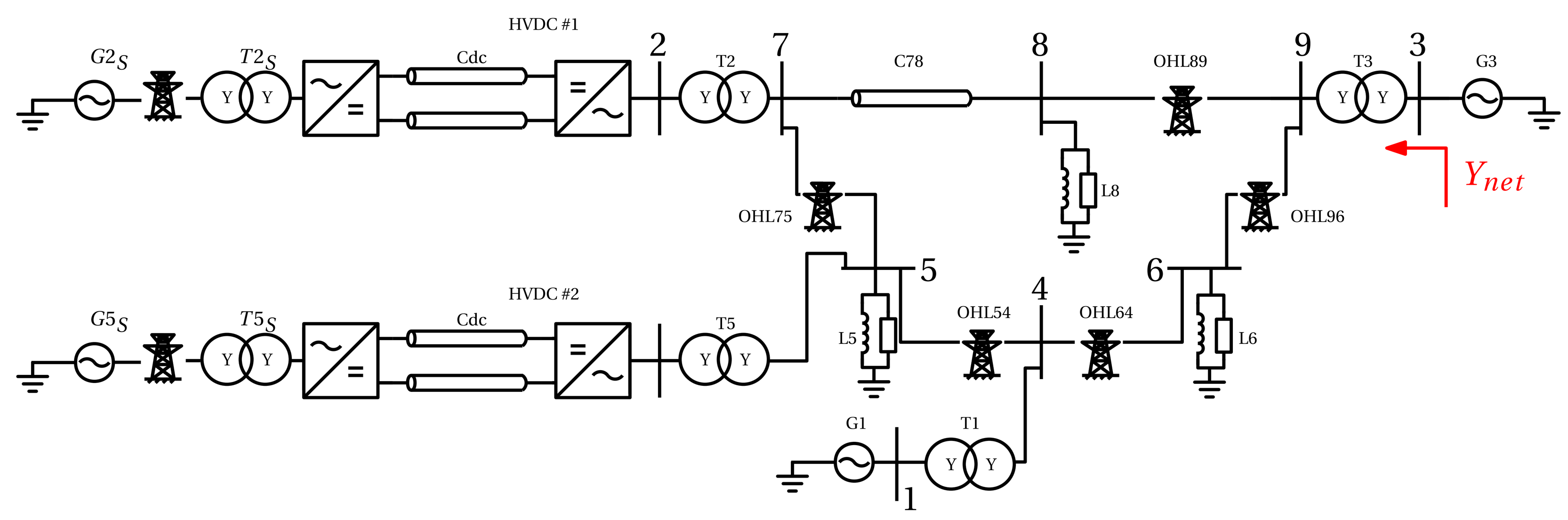

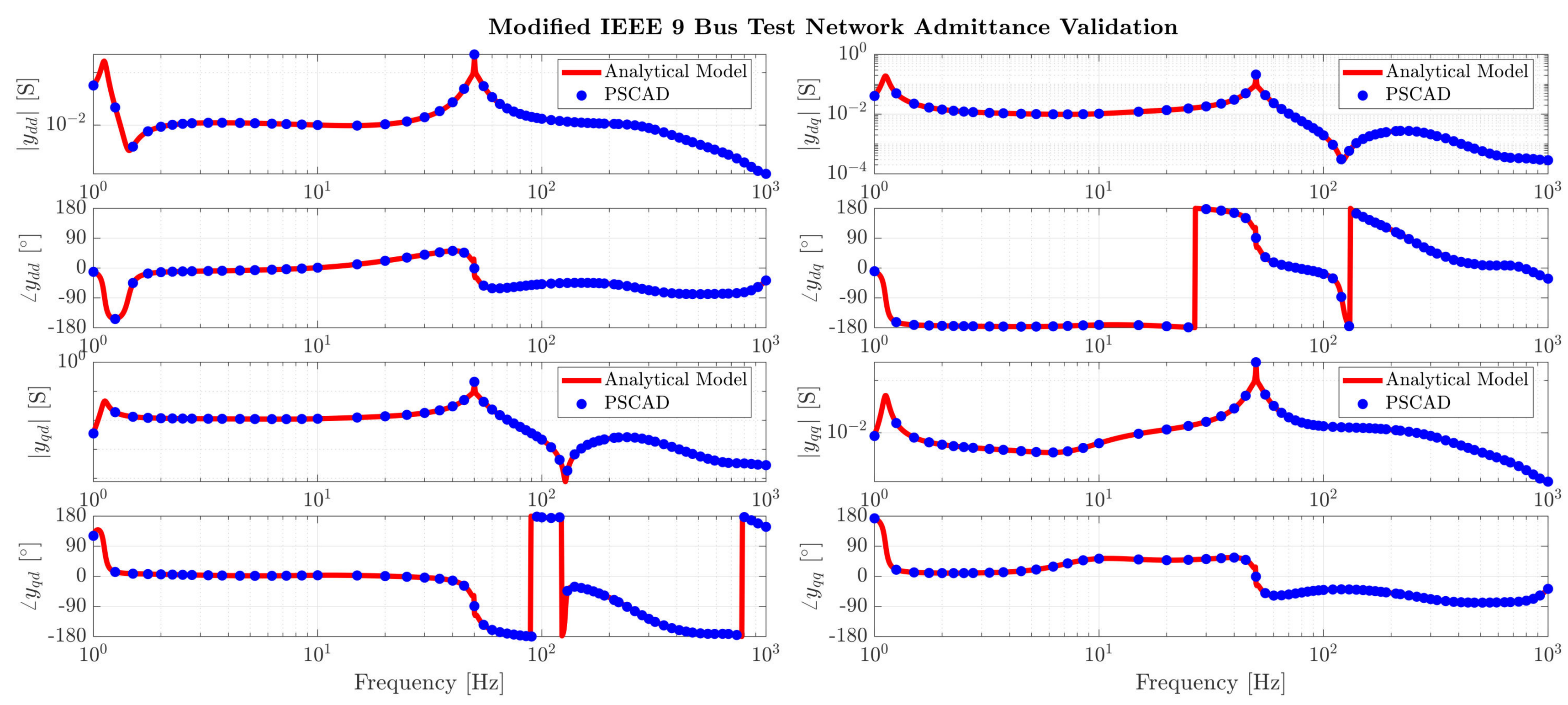

Eigenvalue decomposition

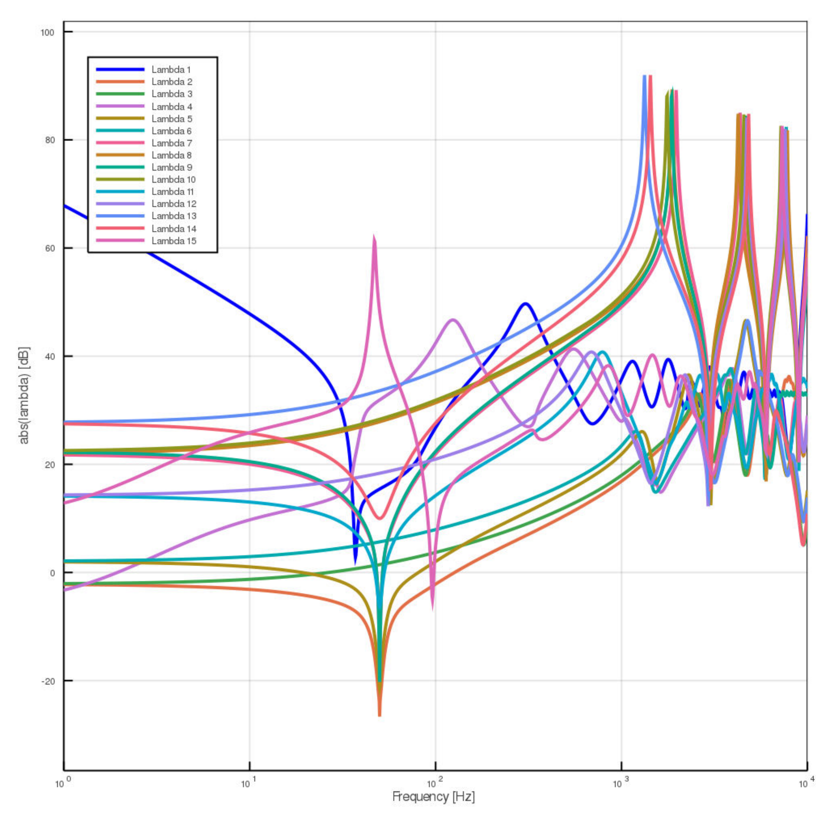

For f_{osc} = 1456 Hz	
PF_1^d	0.38
PF_1^q	0.44
PF_{g1}^d	0.08
PF_{g1}^q	0.10

Single-terminal stability assessment

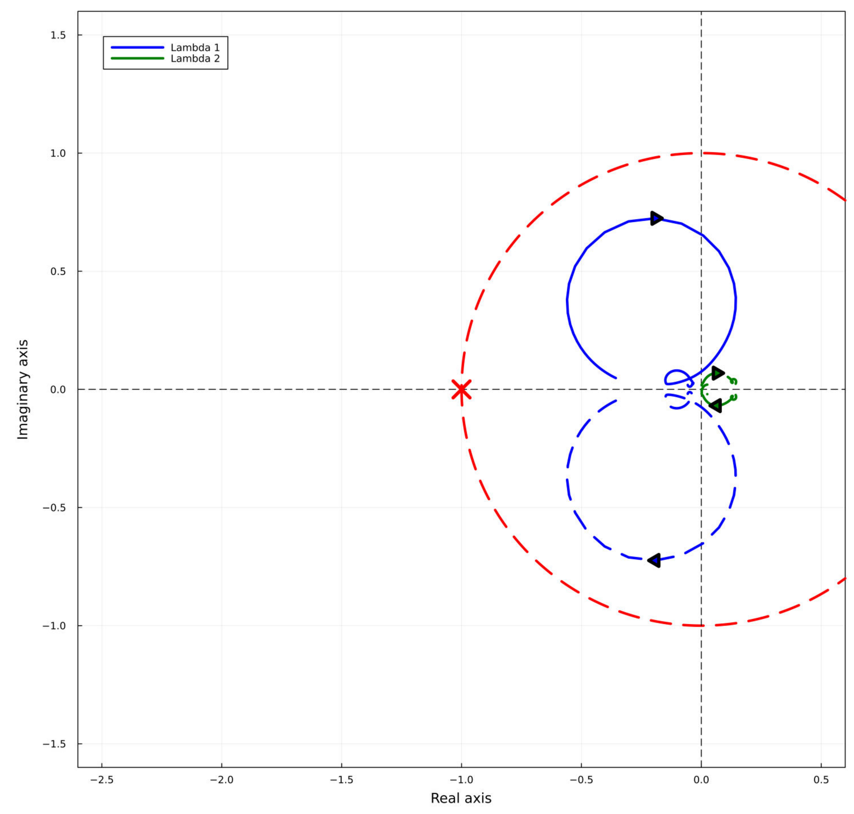

Multi-terminal stability assessment

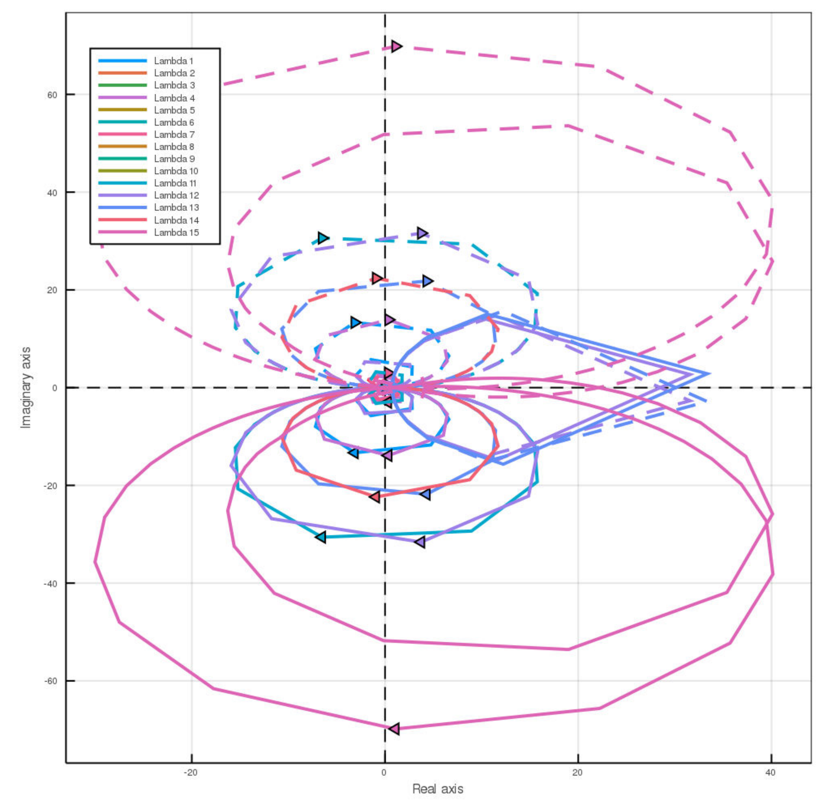

With the support of the Energy Transition Fund

Incorporating HVDC grid protection, frequency stability and reliability into offshore dc grid planning

C.K. Jat, J. Dave, H. Ergun, D. Van Hertem

Background:

- The protection system design for HVDC grids affects observed power deviations in case of faults
- This has an effect on the observed frequency stability, and the amount of frequency reserves to be committed

Contributions:

- Determining FFR requirement through temporary loss of supply offered by dc grid protection.
- Using a dynamic dimensioning incident considering wind generation, and the changing hourly inertia of the ac grid and HVDC grid protection selectivity.
- A probabilistic method to find a trade- off between yearly under frequency load shedding (UFLS) duration and the needed FFR capacity.

Methodology:

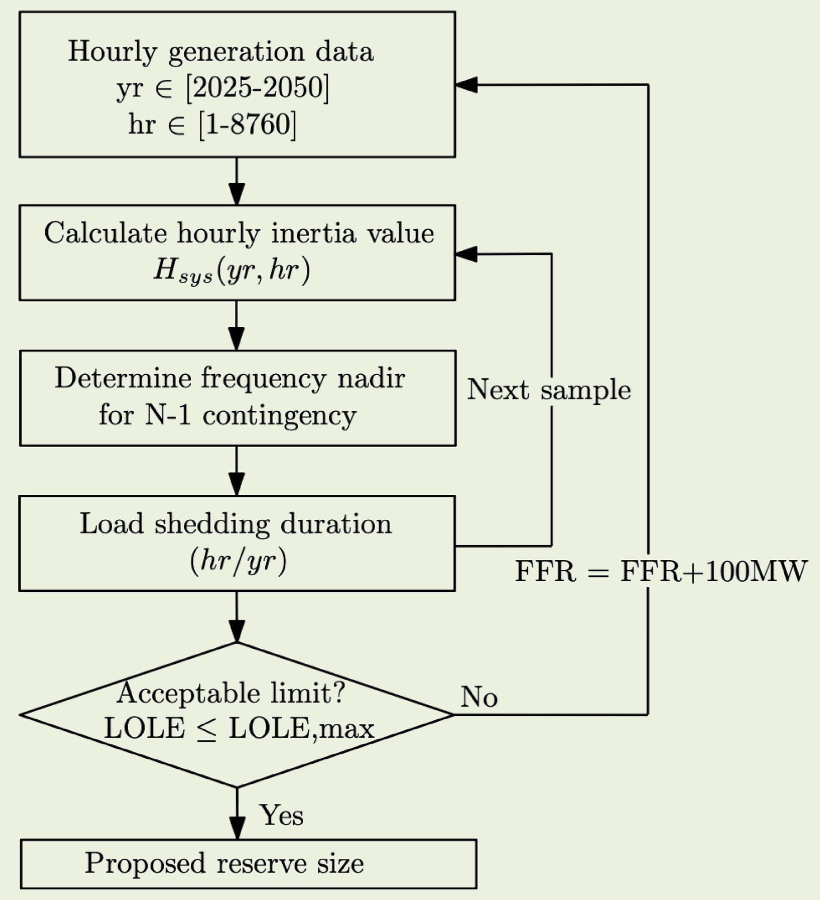

Protection and test system designs:

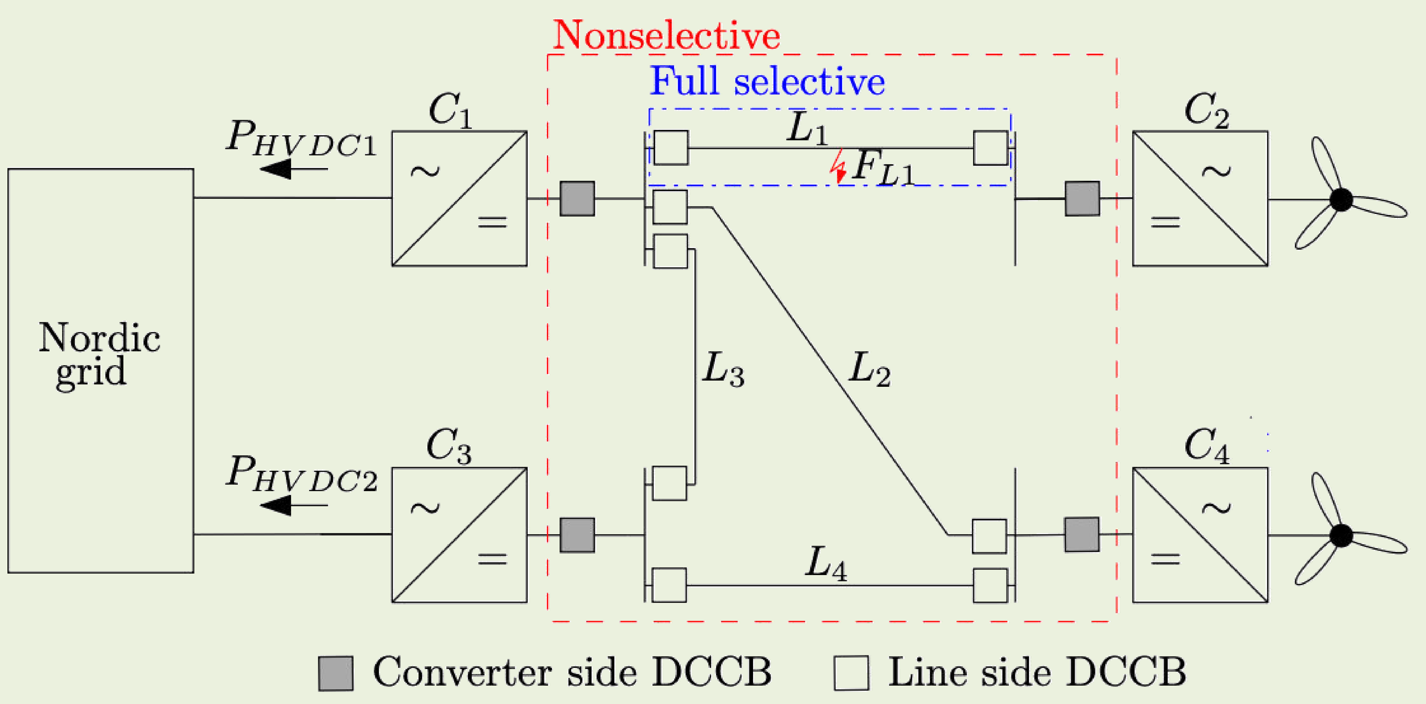

- Meshed HVDC grid connected to Nordic grid
- Fully selective and nonselective HVDC grid protection

Protection characteristics and frequency response model:

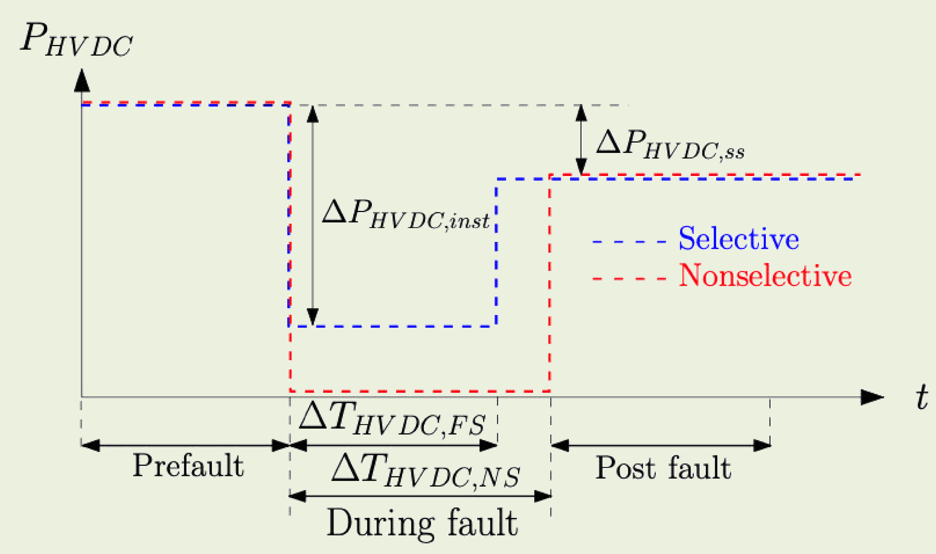

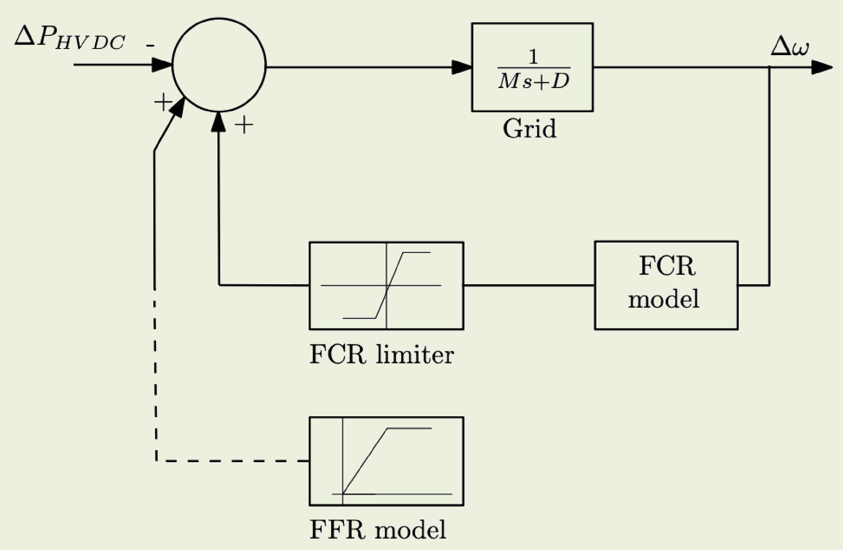

- Selectivity dependent power deviation
- Two stage open loop representation of FCR and FFR

Conclusions:

- Use of frequency stability constraints in the planning process are crucial to determine the required reserve volumes, properly design the protection system, and identify redundancy requirements
- Using a fixed dimensioning incident can be too optimistic or too conservative depending on the amount of RES generation in the system, and such should be determined dynamically
- Furthermore, the dimensioning incident puts restrictions on the OWF and HVDC connection sizes. As such, by jointly optimizing grid design and dimensioning incident, the least cost solution can be identified.

Load shedding vs FFR requirement

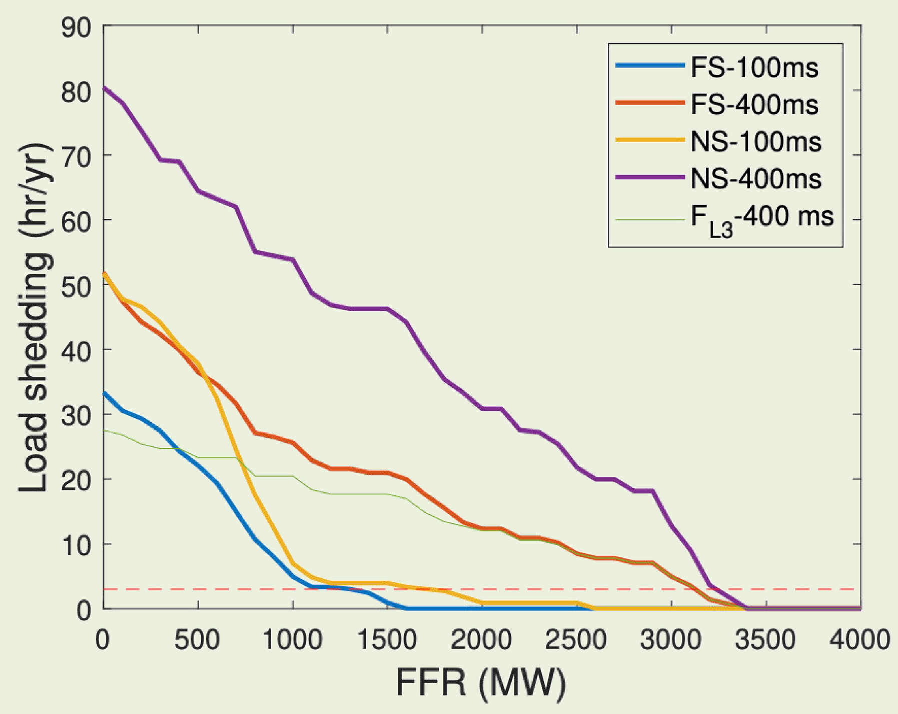

Protection dependent FFR cost

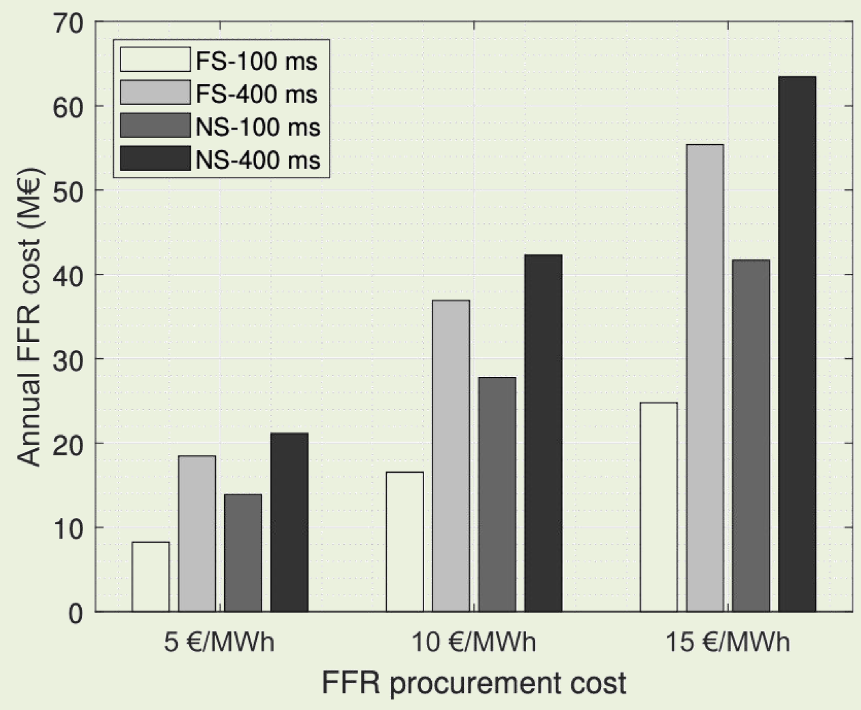

FFR volume based on 3h LOLE requirement

Prot. strategies		FS	NS	NS
ΔT_{HVdc}		100 ms/400 ms	100 ms	400 ms
Injection	2 GW	1400 MW	2500 MW	2800 MW
	4 GW	3300 MW	5300 MW	6800 MW
	6 GW	5200 MW		
	8 GW	7200 MW		
Connections	1	1100 MW	1100 MW	1100 MW
	2	1700 MW	2600 MW	2800 MW
	3	1700 MW	2800 MW	4900 MW
	4	1800 MW	5800 MW	7200 MW

Protection dependent FFR activation instances

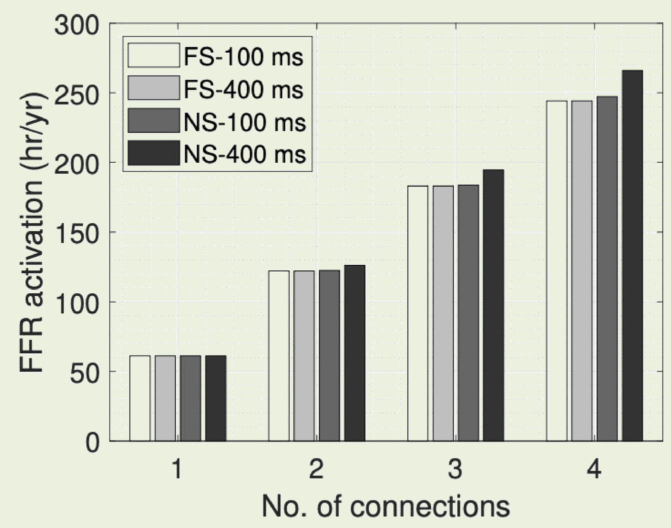

References:

[1] Dave, J., Ergun, H., Van Hertem, D. (2020). Incorporating dc grid protection, frequency stability and reliability into offshore dc grid planning. IEEE Transactions On Power Delivery, 35 (6), 2772-2781. doi: 10.1109/TPWRD.2020.3011897

[2] Dave, J., Ergun, H., Van Hertem, D. (2021). Reducing the cost of maintaining the frequency stability using dc grid protection. In: 2021 International Conference on Smart Energy Systems and Technologies (SEST), (1-6). Vaasa, Finland. ISBN: 978-1-7281-7660-4. doi: 10.1109/SEST50973.2021.9543118

With the support of the Energy Transition Fund

Empowered by KU Leuven, VITO, imec & UHasselt

Novel sensor types for AC and DC grid protection

Mohammad Heidari, Dr. Willem Leterme, Prof. Dirk Van Hertem
Dept. Electrical Engineering, KU Leuven/EnergyVille, Leuven/Genk, Belgium

A. Context

HVDC sensors are currently under development for long HVDC cables and are required for protection, monitoring, and fault localisation. Possible sensor solutions have been developed for land applications; however, they are not yet fully applicable offshore. A few of these sensor arrangements take advantage of fiber optic cables embedded within or close to HVDC cables. We aim to design and implement semi-distributed sensors for HVDC offshore cables, with direct insight into voltage levels and transients. The sensor arrangement combines concepts used before in the literature.

Spatial distribution of sensors

- Localised → at cable ends
- Semi-distributed → at cable joints or close to them
- Distributed → All along the cable (DAS, DTS, DVS)

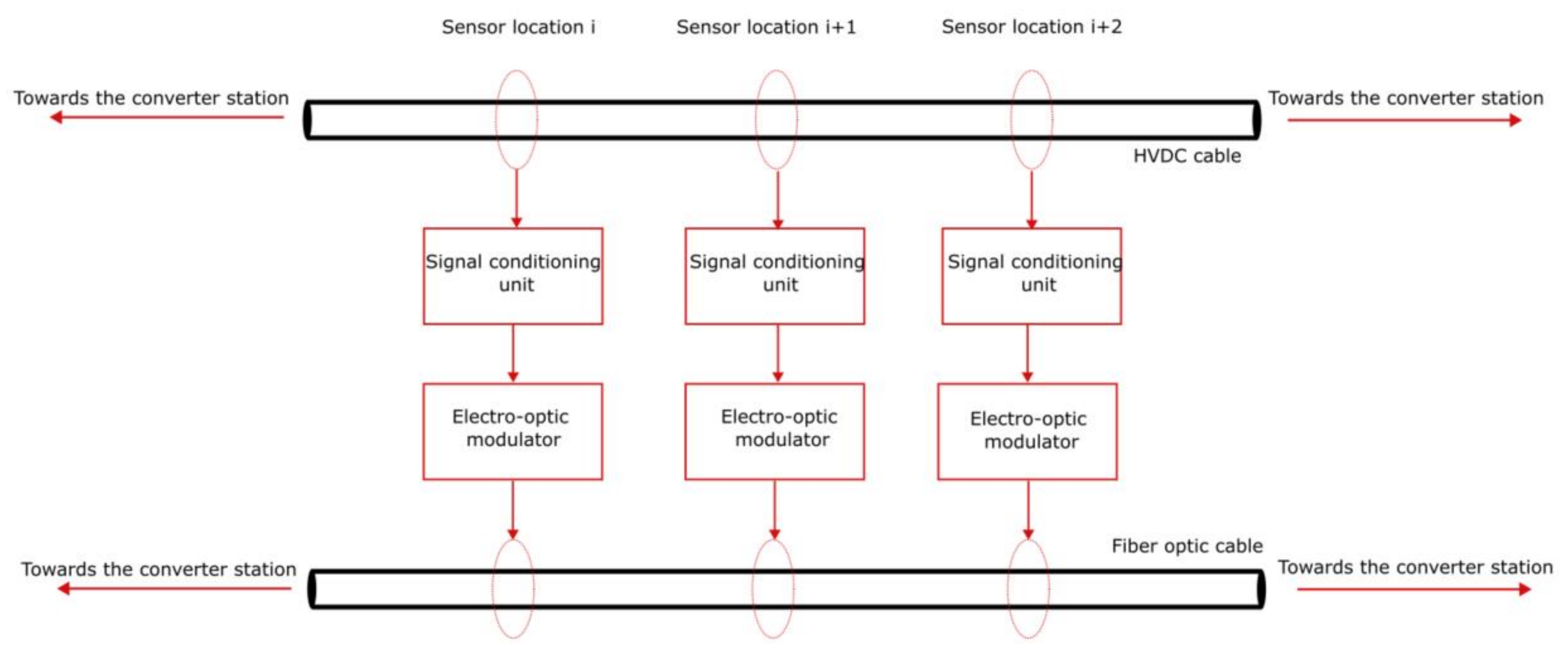

B. Characterisation of localized and semi-distributed sensors

Sensor types	Measured parameter	Bandwidth	Application
Conventional VT/CT	Voltage or current	Few kHz	AC
Rogowski coil	Current	Few MHz	AC and DC
Shunt capacitive divider	Voltage or current (electric fields)	Few MHz	AC and DC
Hall effect	Voltage or current (magnetic fields)	Few hundred kHz	AC and DC
Fluxgate	Current (magnetic fields)	Few hundred kHz	AC and DC
Magnetorestrictive	Current (magnetic fields)	Few hundred kHz up to a few MHz	AC and DC
Pockels effect optical	Voltage (electric fields)	Few GHz	AC and DC
Faraday effect optical	Current (magnetic fields)	Few MHz	AC and DC
Hybrid Fiber Bragg Grating optical with piezoelectric sensor	Voltage (electric fields)	Not specified	AC and DC
Hybrid magnetorestrictive optical	Current (magnetic fields)	Not specified	AC and DC

Semi-distributed and applicable for HVDC cable transients

C. Hardware implementation of LVAC voltage sensor-Key learnings

o Interfacing analog circuits and sensors with a loaded cable
o Proof of concept o Sensor arrangement limitations

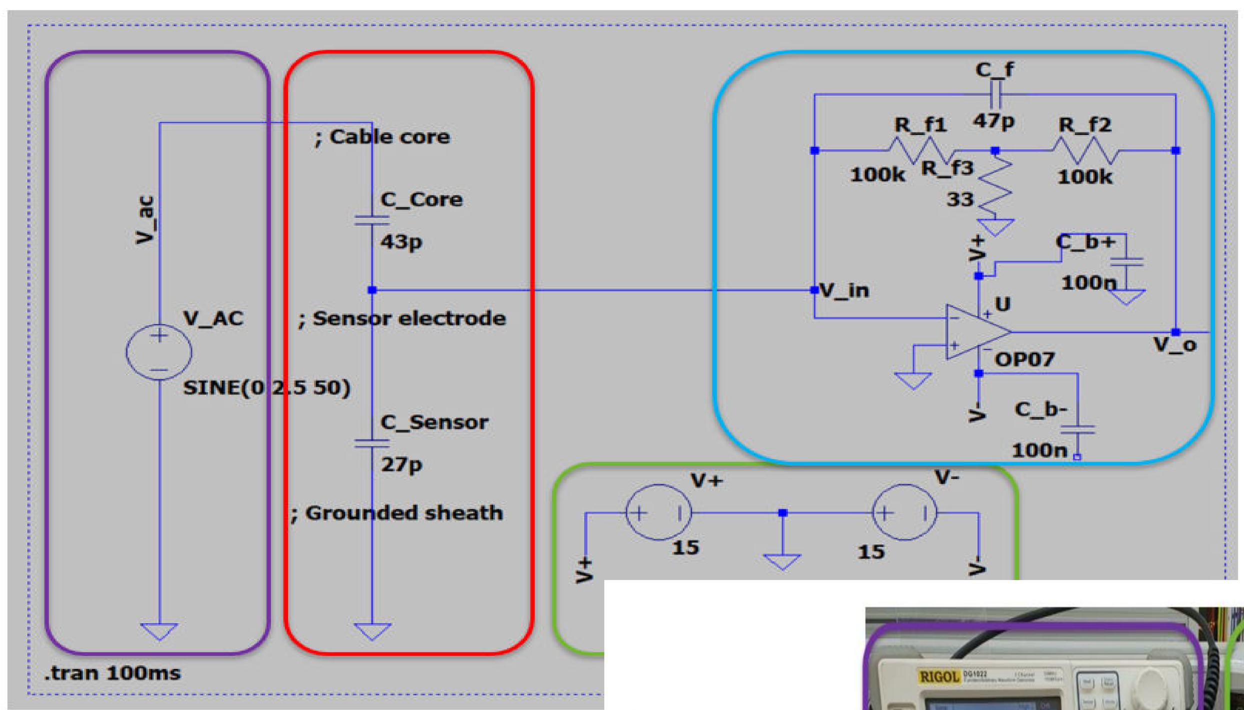

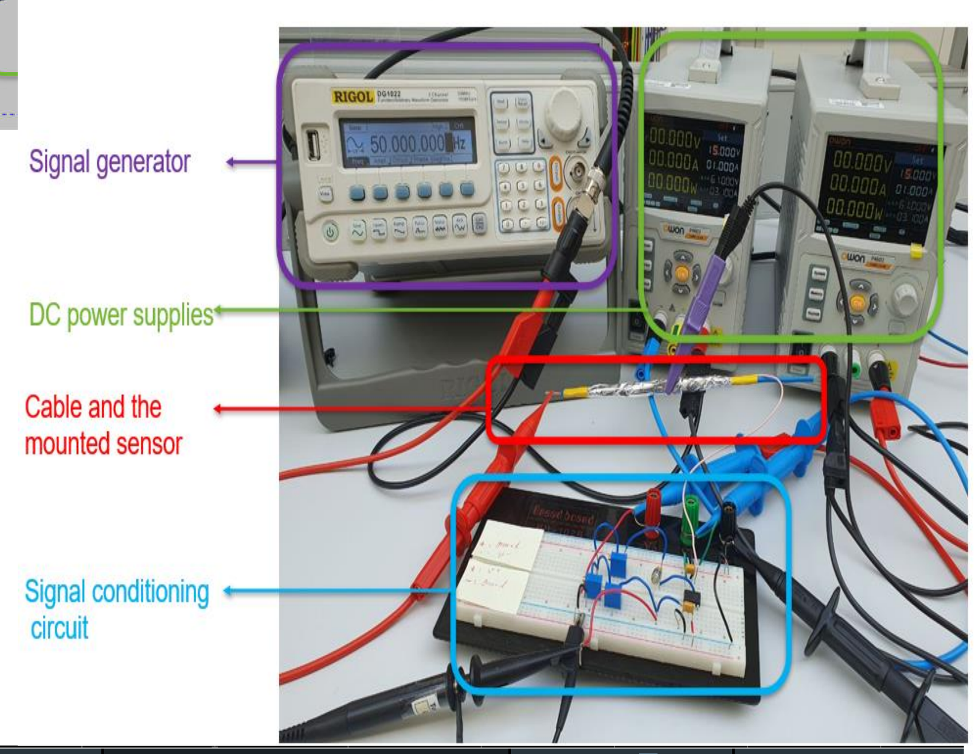

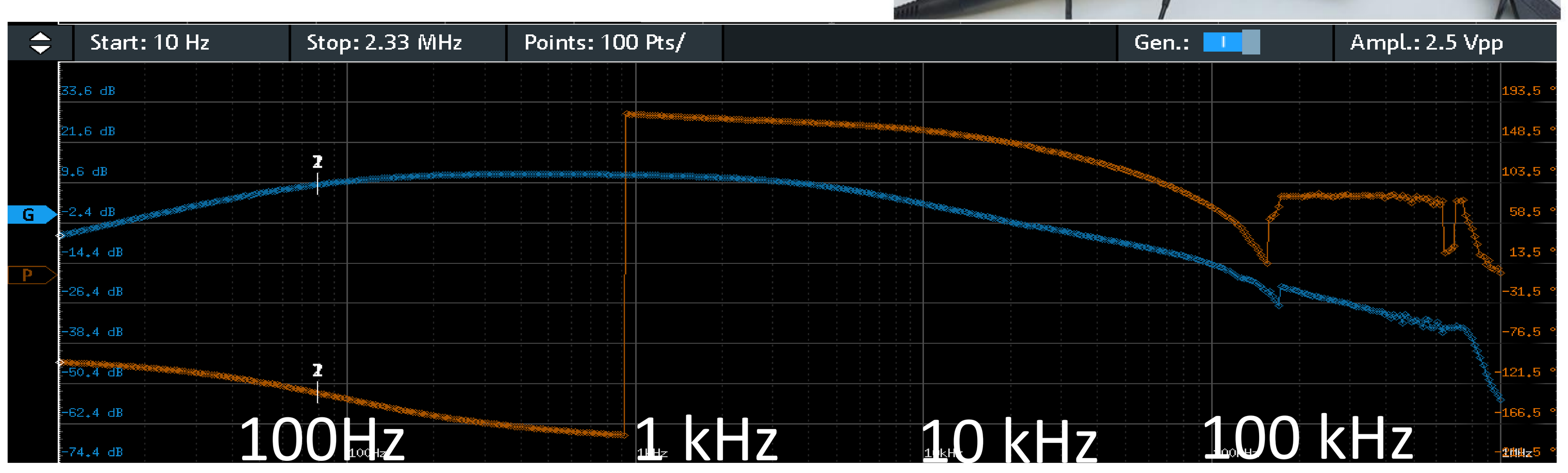

D. Concept design of HVDC voltage sensor

Measurement steps:

1. Coupling capacitor as the sensor electrode (voltage)
2. Signal conditioning by the analog circuit on flex PCB (voltage to current to voltage)
3. Piezoelectric stack (voltage to strain)
4. FBG inscribed fiber optic cable (strain to light refraction)
5. Optical demodulation (light refraction to strain and voltage)
6. Additional signal processing for condition monitoring

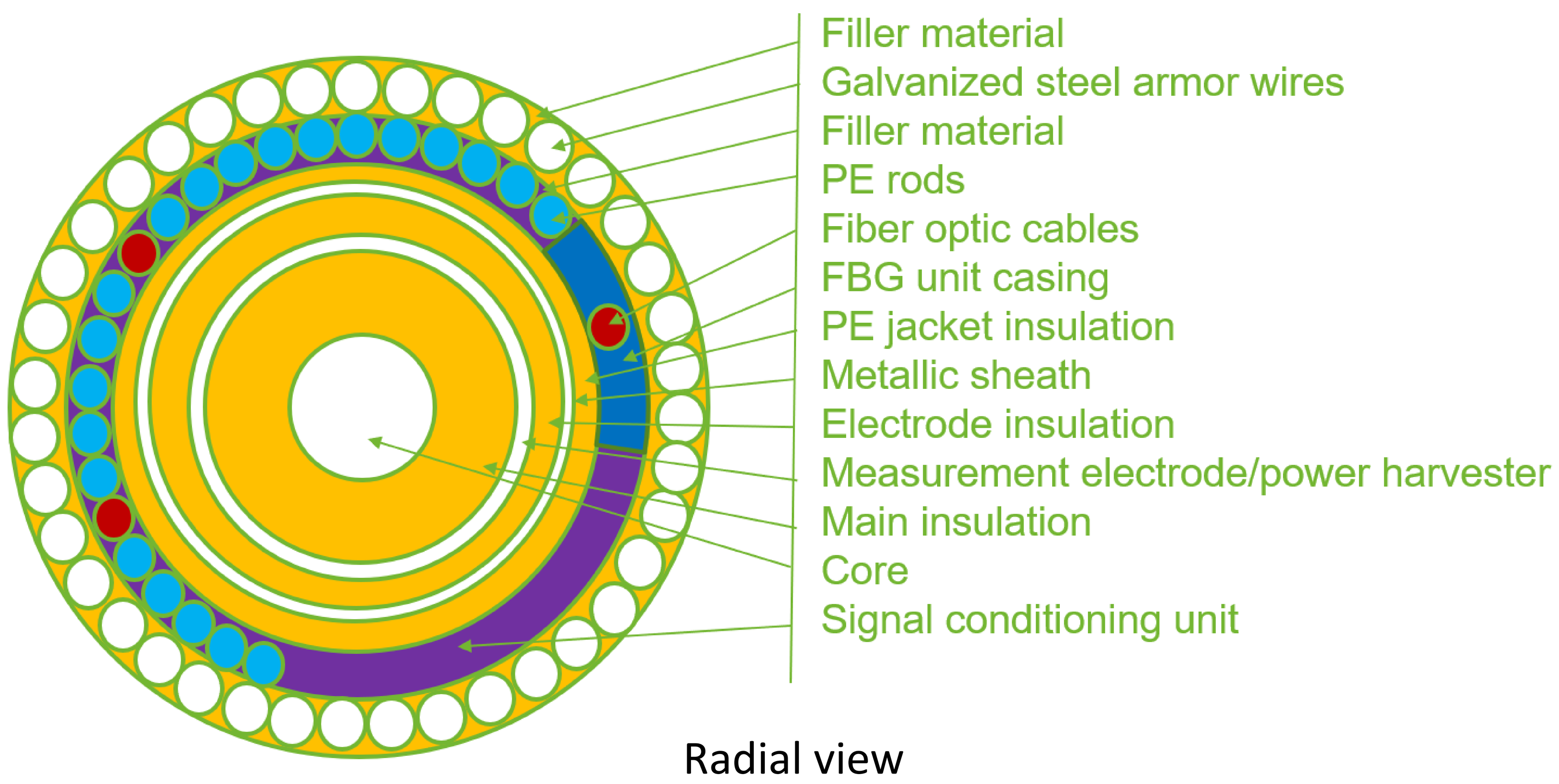

Radial view

Main challenges

- Accuracy in measurement
- Reference for measurements and sensor calibration
- Stability of the sensor arrangement
- Noisy environment (thermal, acoustic, and electrical noises)
- Increased risk of electrical and mechanical stress in the cable
- Power supply for the sensor arrangement
- Data transmission, integrity, and analysis

KU LEUVEN vito imec UHASSELT Neptune economie
With the support of the Energy Transition Fund

Active Harmonic Filtering as an Interaction Mitigation Measure and its Impact on Small-Signal Stability

Özgür Can Sakinci and Jef Beerten
ELECTA, KU Leuven, Belgium and EnergyVille, Genk, Belgium

INTRODUCTION

- The small-signal stability of an MMC-HVDC station acting as an active filter is studied.
- Using novel dynamic phasor models of the converter enables using eigenvalues for stability assessment.
- The impact of active filtering and computational time delays on small-signal stability are evaluated.

MODEL DEVELOPMENT

- Active filtering is implemented as an additional controller to suppress output current harmonics.
- Dynamic phasor model of a half-bridge MMC representing harmonics up to 650 Hz is used.

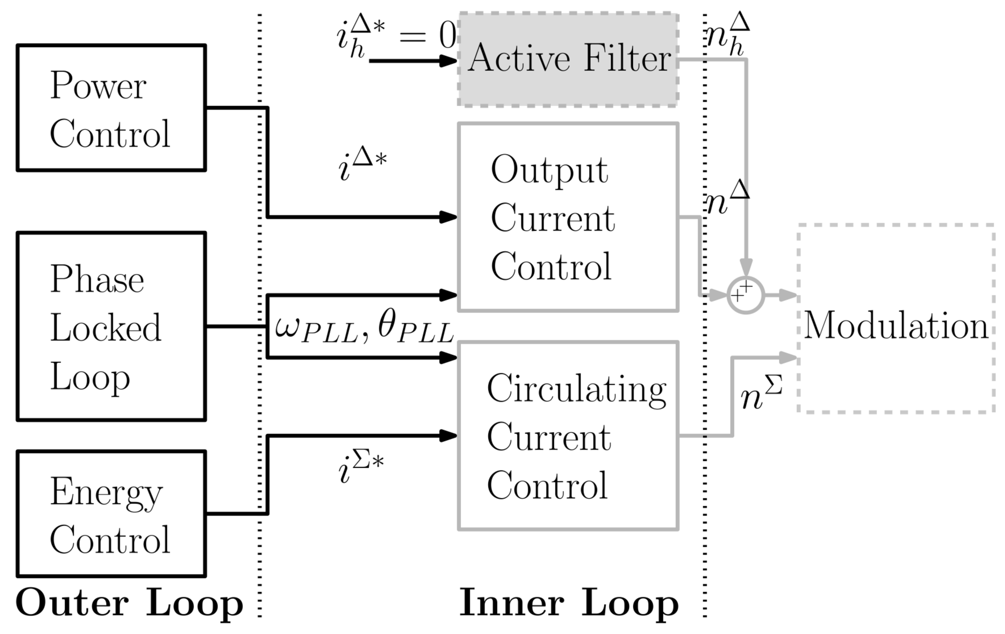

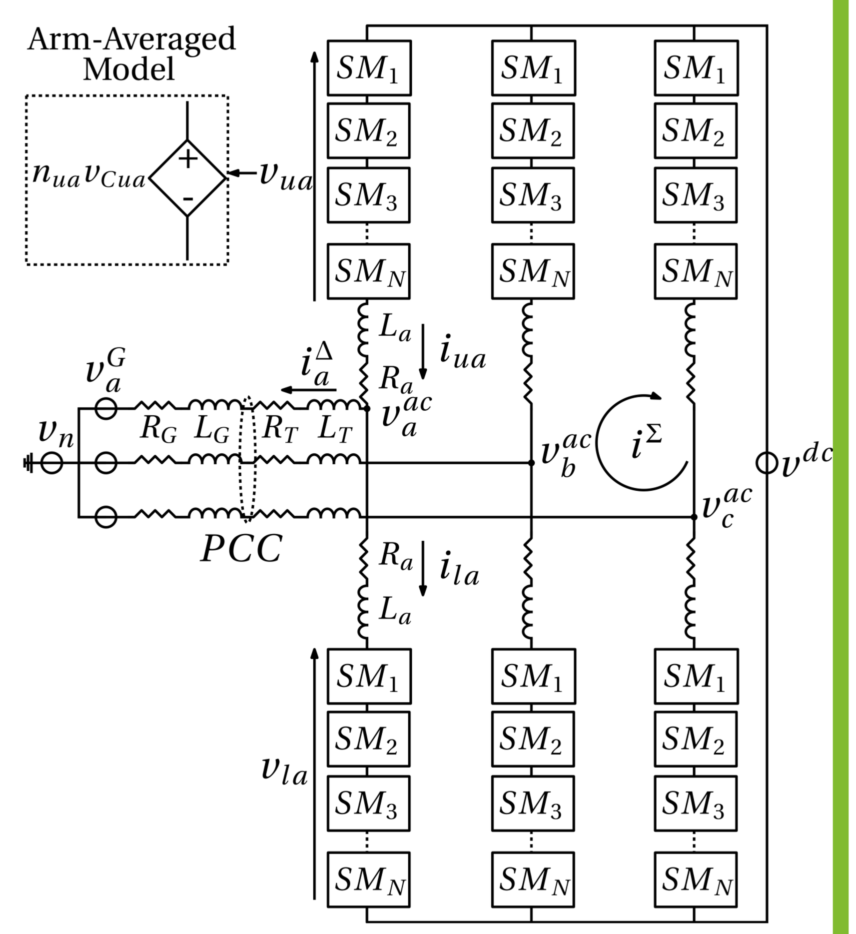

METHODOLOGY

- Harmonics detected by means of low-pass filters.

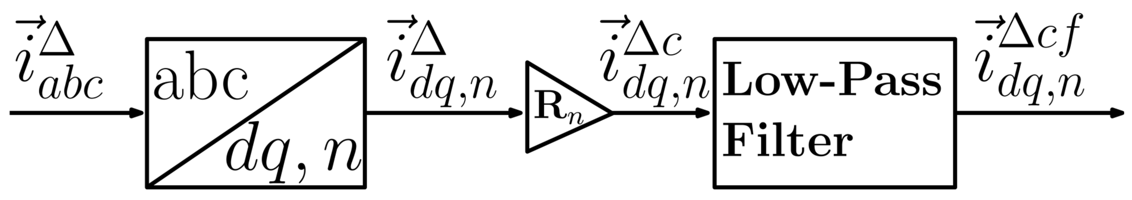

- 5[th] and 7[th] harmonics suppressed using dq-frame PI controllers.

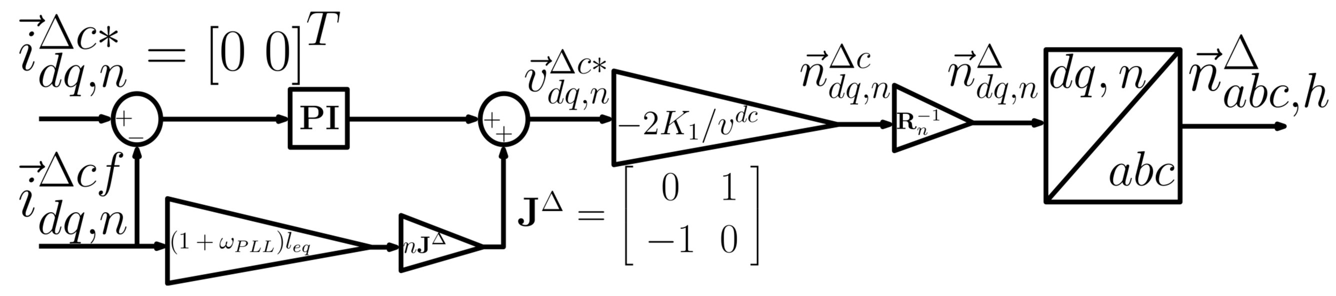

- Two different PI controller tunings:
  - ➢ Fast tuning: Specify a closed-loop bandwidth and apply pole placement (e.g., 150 Hz, same as the output current controller).
  - ➢ Slow tuning: Low integral gain and a slightly higher proportional gain (e.g., $k_P = 10$ and $k_I = 0.1$).

RESULTS

- In the absence of time delays, converter eigenvalues shift considerably when fast tuning is used (top plot, shifts from blue asterisks to purple dots).
- With slow tuning the changes (and the risk of interactions) are reduced (bottom plot, blue asterisks and yellow plus signs largely coincide).
- Slow tuning shows good performance in time domain when current harmonics are generated by adding harmonics in the PCC voltage.

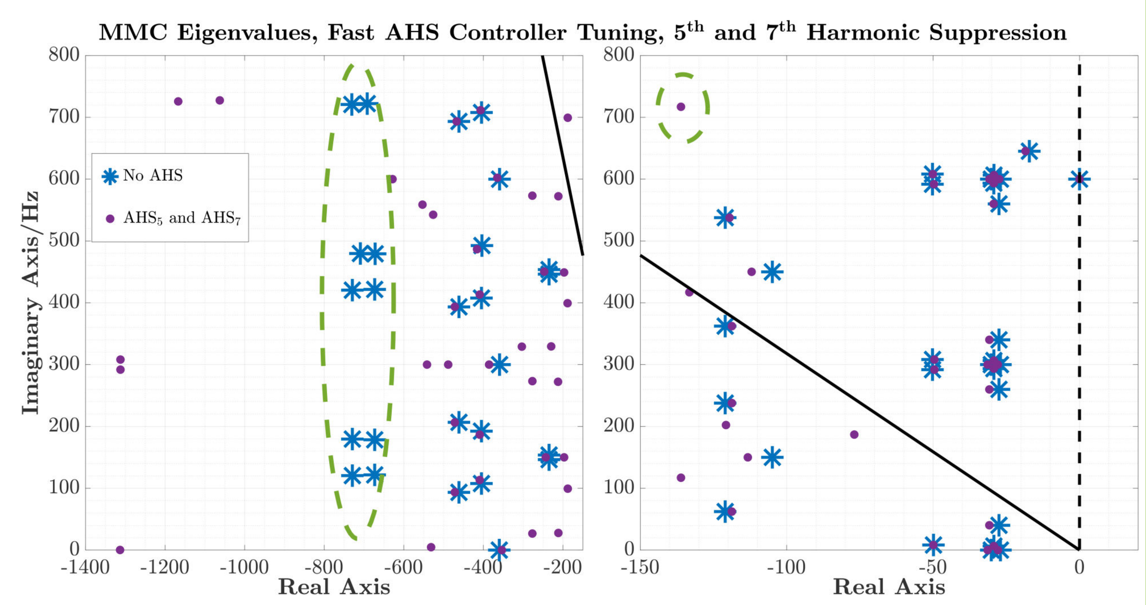

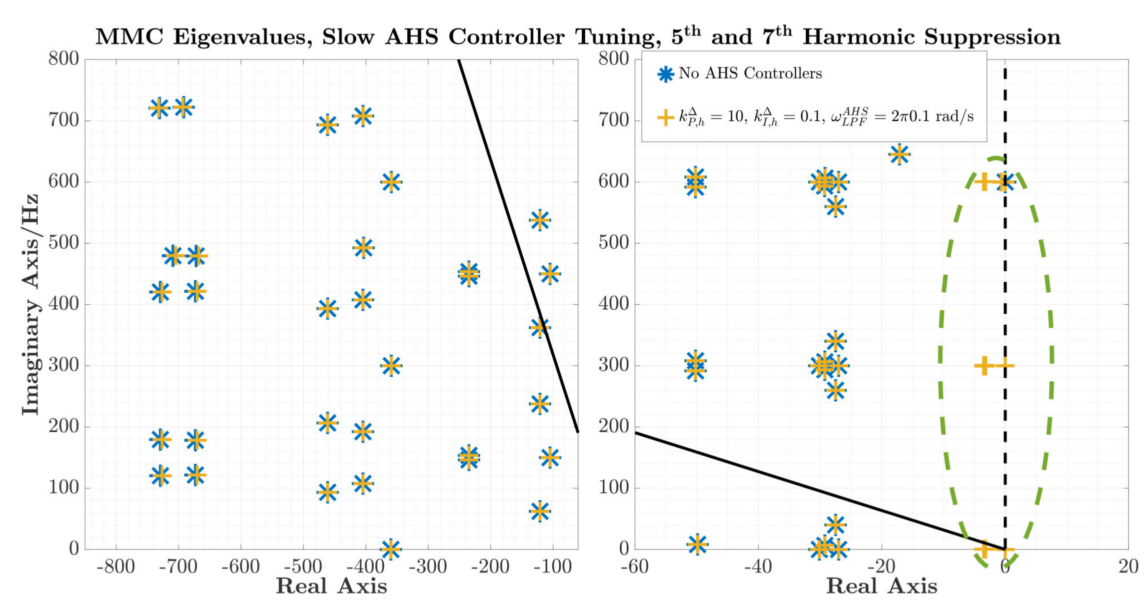

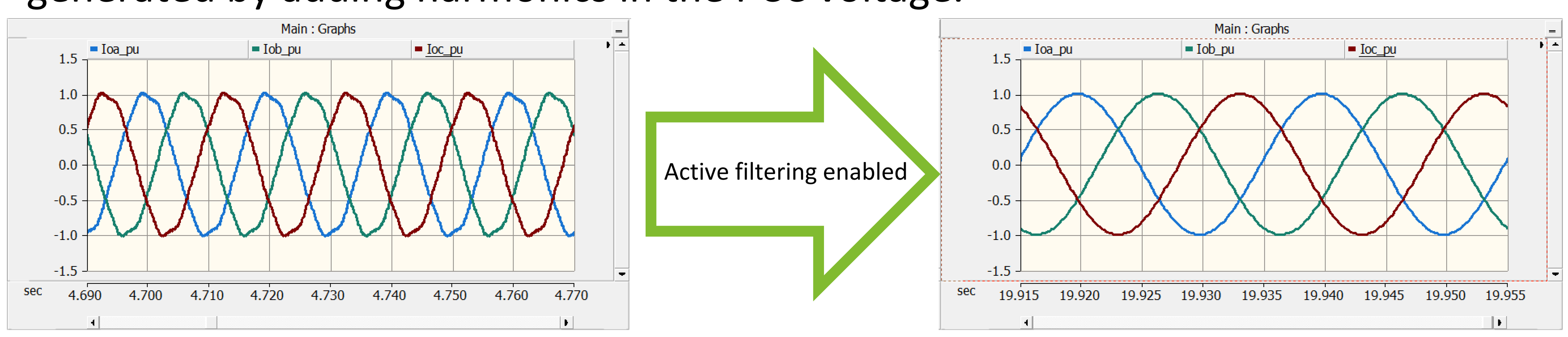

- Instabilities are observed when time delays are modeled.
- ❖ Stability margins are higher when slow tuning is used (i.e., lower time delays combined with fast tuning gives instability).

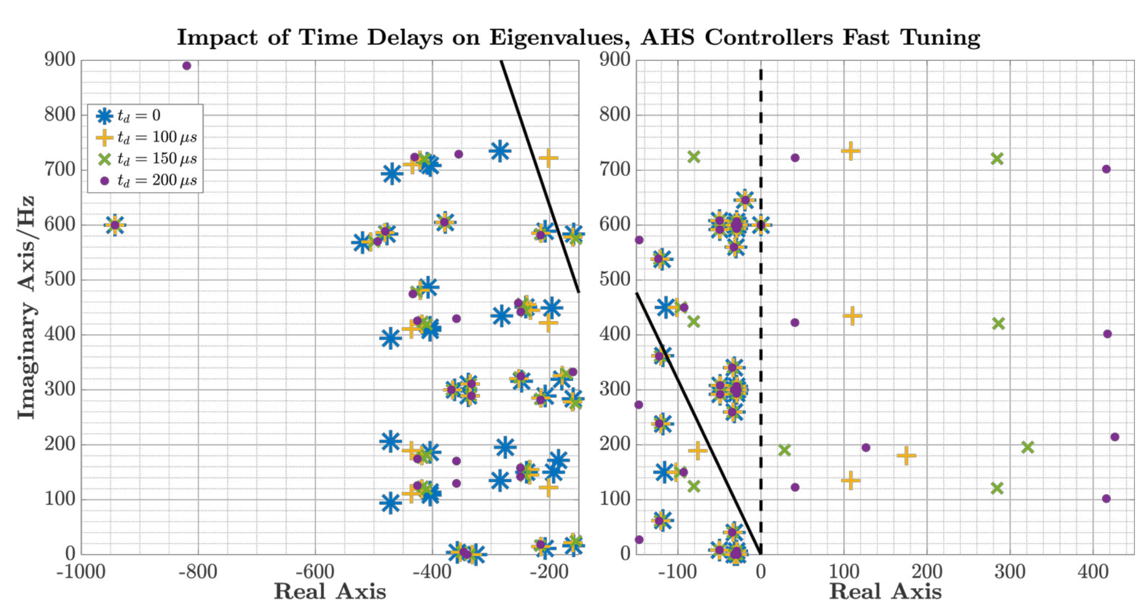

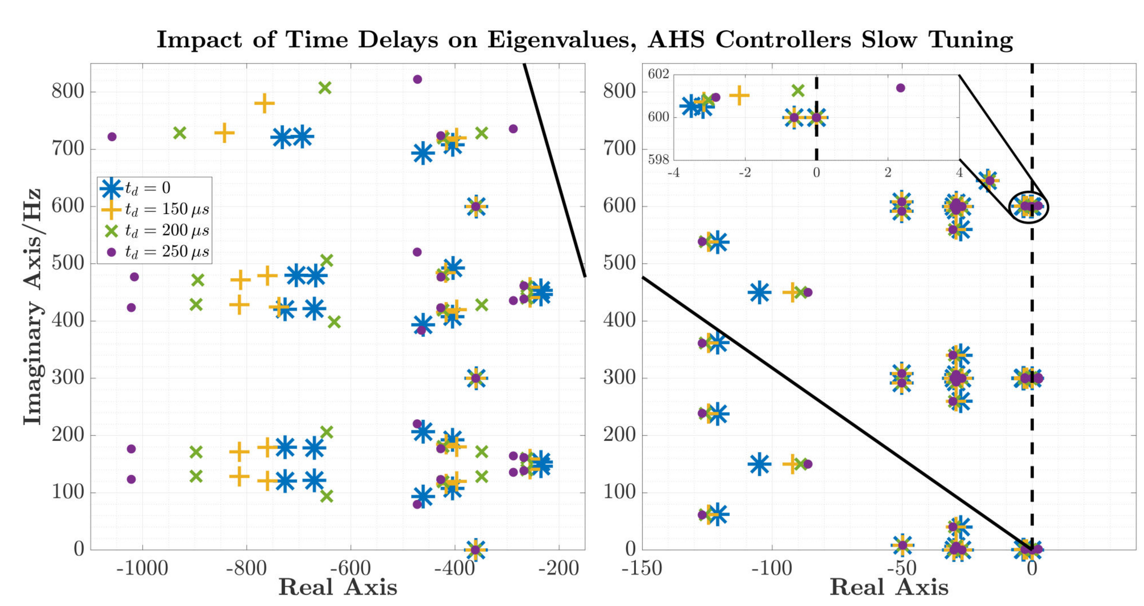

With the support of the Energy Transition Fund

Power Flow and Optimal Power Flow Models for Asymmetric HVDC Grids: A Julia-Based Open-Source Implementation

Empowered by KU Leuven, VITO, imec & UHasselt

C. K. Jat, J. Dave, H. Ergun, D. Van Hertem

Point to point HVDC configurations

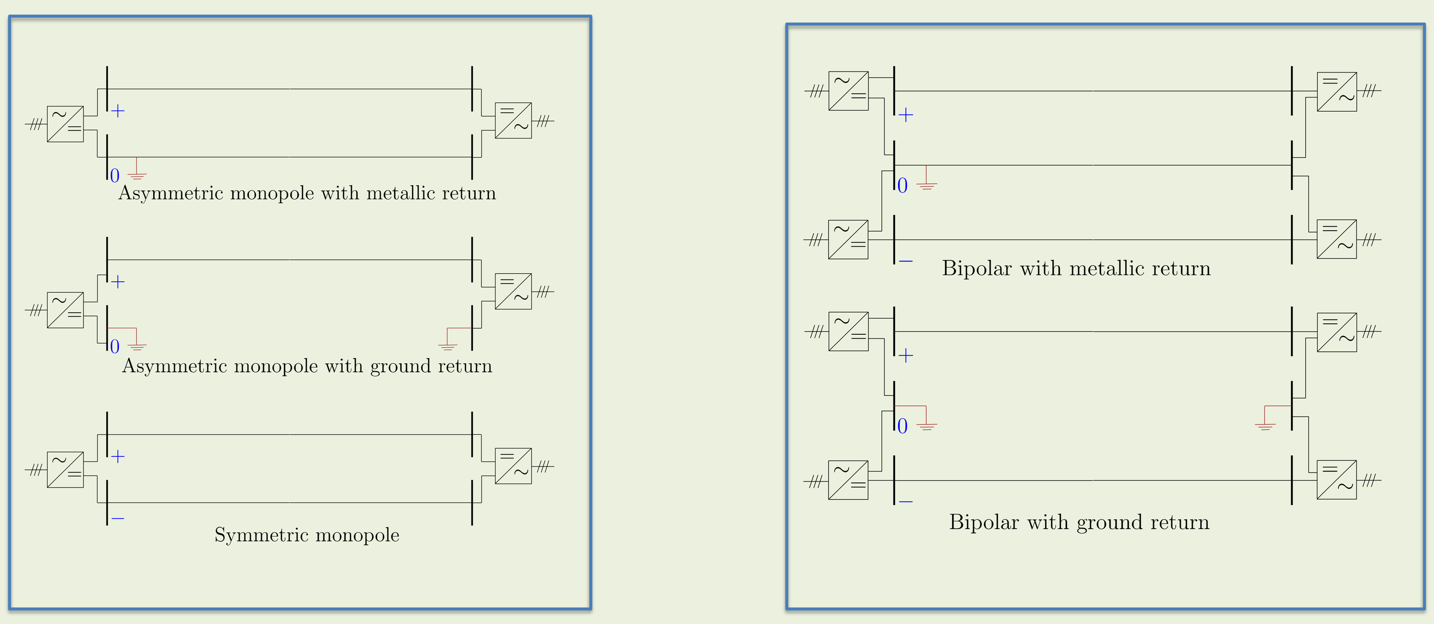

Operation of the system with mixed configurations would create unbalance in the DC grid. The mixed configurations can occur either by grid design or in case of contingencies.

HVDC grid configurations

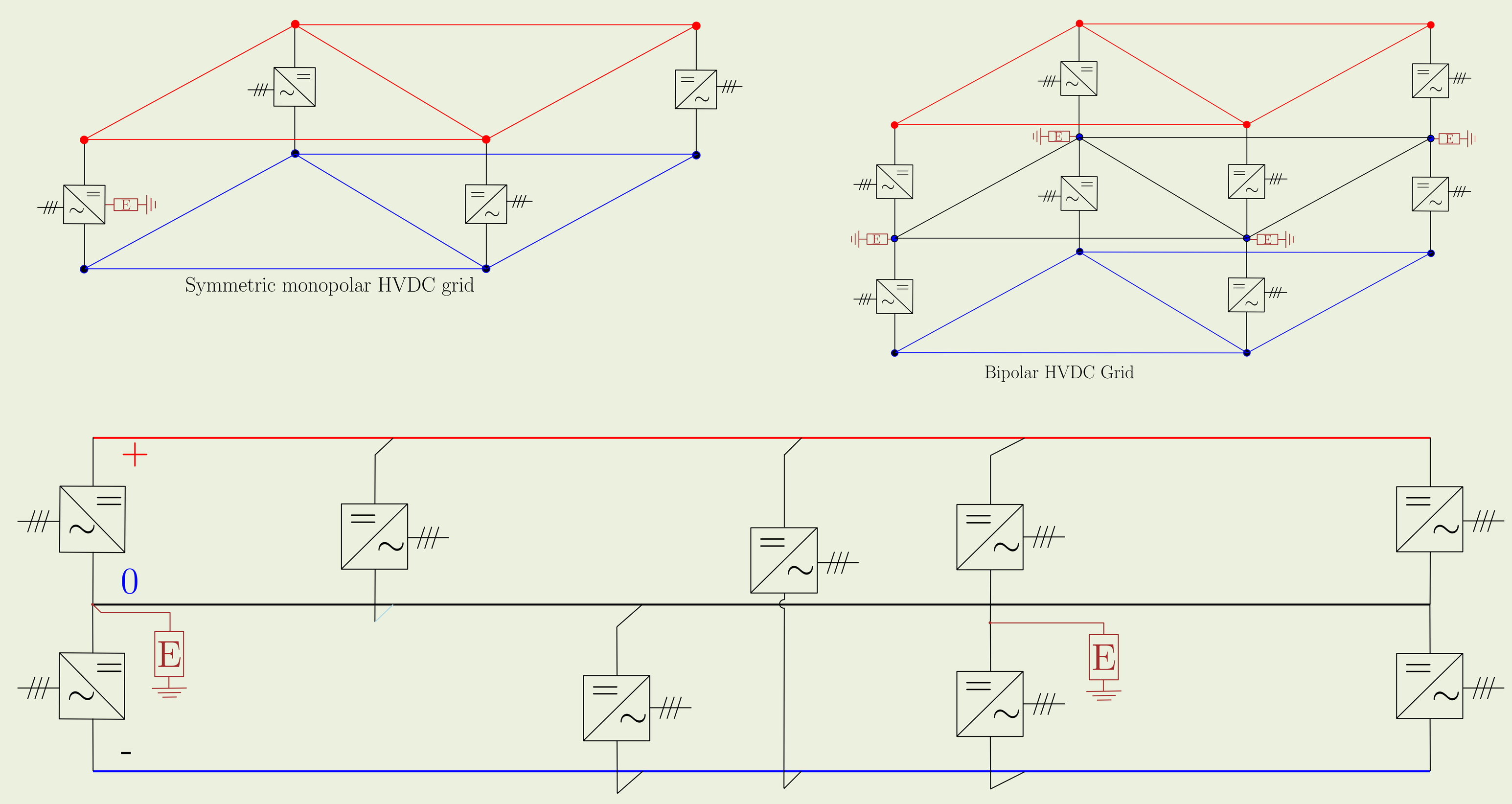

Generic HVDC grid

Multiconductor HVDC model:

In case of the unbalanced operation, the single-conductor representations of AC/DC converter stations and DC lines would not be valid. Therefore, a multi-conductor model is proposed with

- Separate modeling of each converter pole
- Explicit modeling of the metallic or ground return

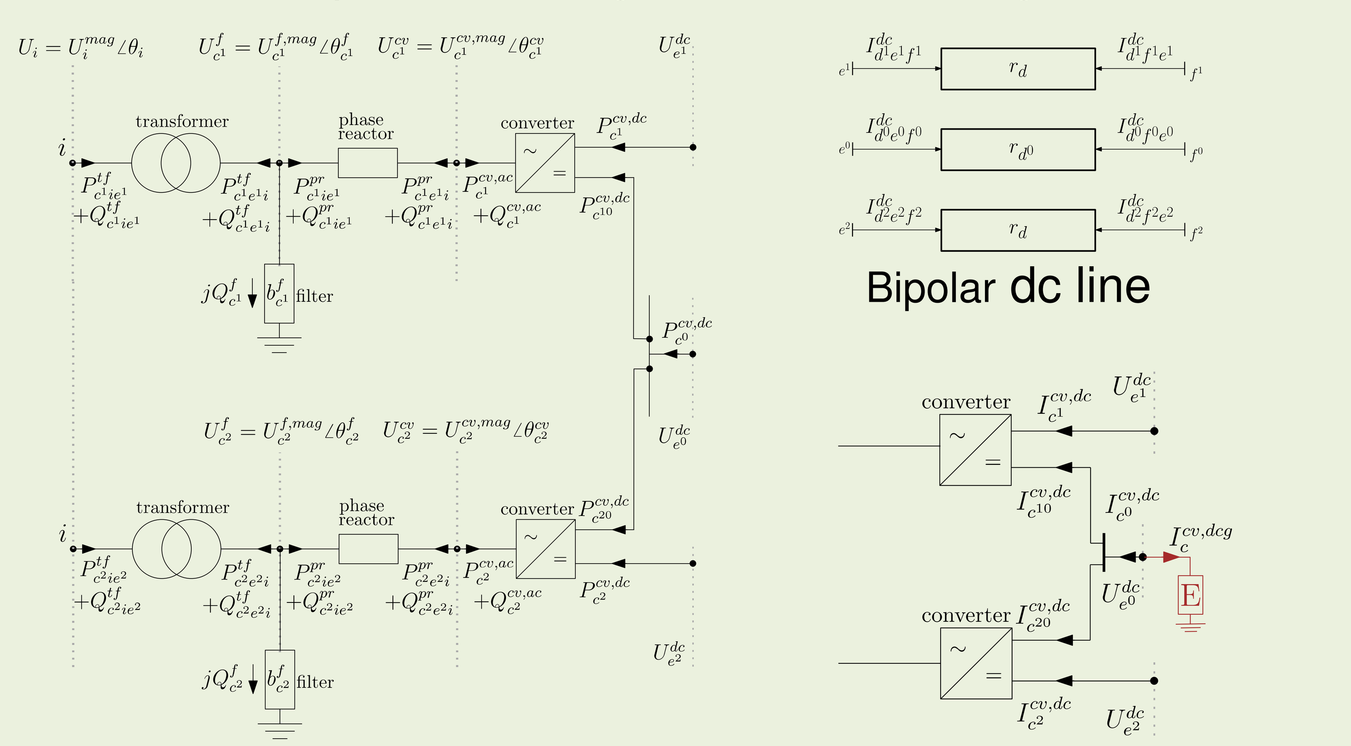

Bipolar dc line

Bipolar converter station

Converter grounding

Optimal Power Flow:

$$Min \sum_{g \in G} a_g + bgPg + cg * (Pg)^2$$

Subject to:

- AC and DC side voltage constraints
- Generator power constraints
- AC branch flow constraints
- DC branch flow constraints
- AC bus KCL constraints
- DC bus KCL constraints
- AC/DC converter constraints

Modified equations

Power Flow:

- More constrained problem
- Some of the variables have predetermined (defined/ measured) values
- For a converter station it depends on the choice of control modes
- Each converter of a bipolar converter station can have various control modes such as *DC slack, active power control, DC-droop* etc.
- Both the poles of a bipolar converter station can have different AC buses

Applications and Results:

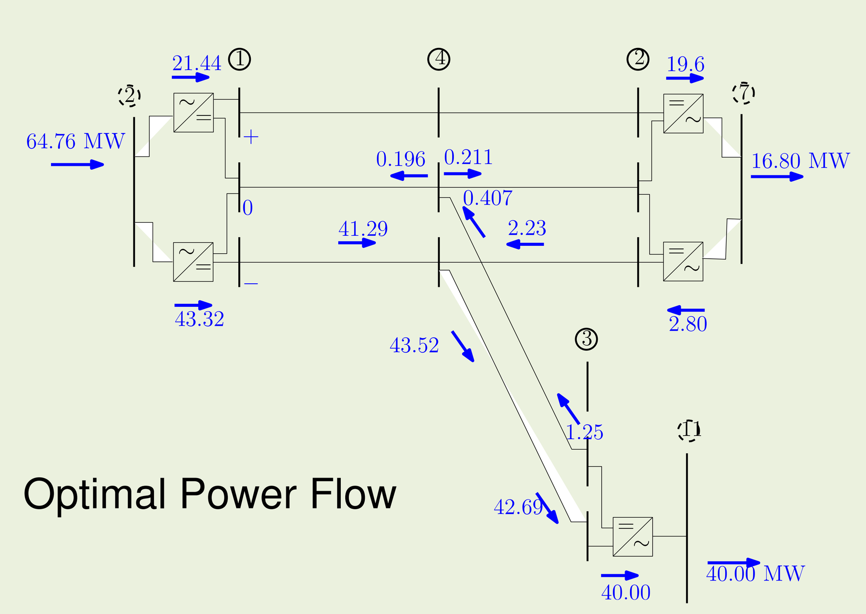

Optimal Power Flow

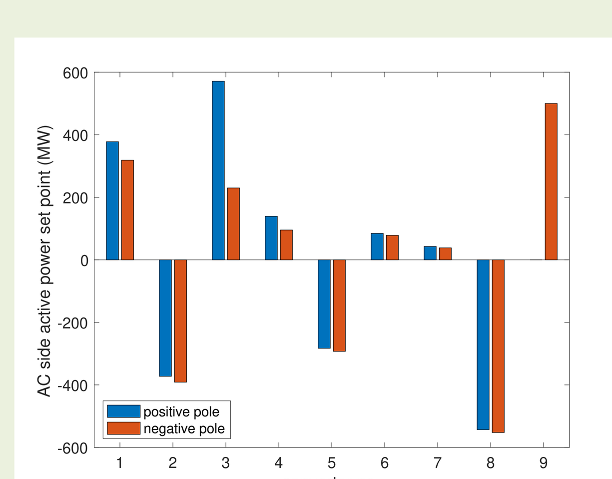

Security constrained OPF

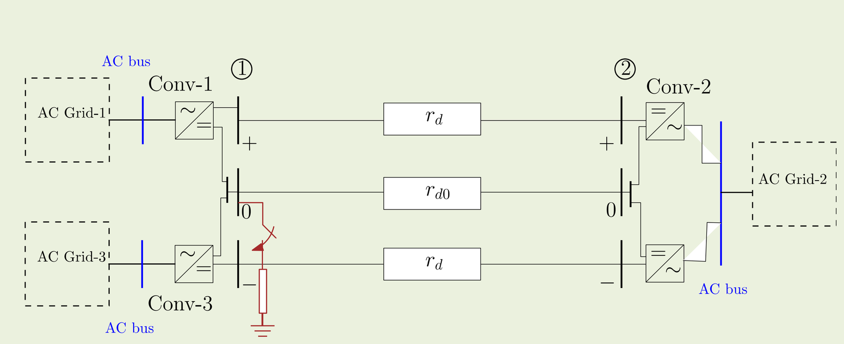

Power flow and control modes

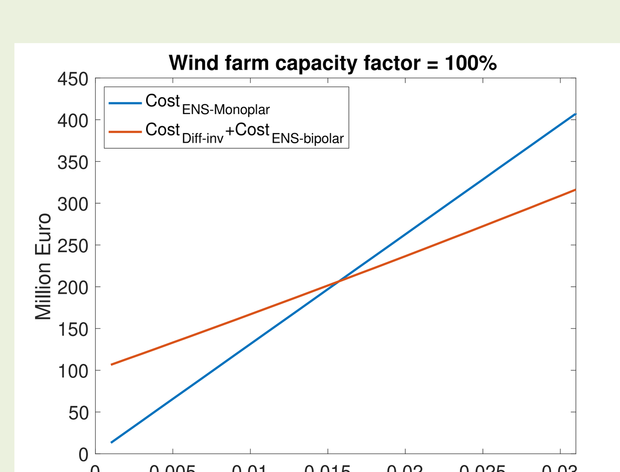

Investment planning

Key Takeaways:

- Loop flow through converter poles could help in achieving system level optimality
- Neutral point voltage can also be a limiting factor and therefore, can not be neglected
- Increased number of control options and therefore, a higher degree of freedom for an economic, and secure operation of the system
- *S*ecurity constrained operation with the unbalanced operation ➔ significant cost savings.
- Flexibility provided by the HVDC system is better harnessed with unbalanced operation
- Trade off between investment cost and operational benefits of a new DC link configuration

References

[1] C. K. Jat, J. Dave, H. Ergun, and D. Van Hertem, "Unbalanced OPF Modelling for Mixed Monopolar and Bipolar HVDC Grid Configurations," [Uploaded on "arxiv.org"].
[2] C. K. Jat, V. Bhardwaj, H. Ergun, and D. Van Hertem, "Security Constrained OPF Model for AC/DC Grids with Unbalanced DC Systems," [ACDC 2023]

Open-source implementation:

https://github.com/Electa-Git/PowerModelsMCDC.jl

With the support of the Energy Transition Fund

Inertial Support by Virtual Synchronous Machine Control of an MMC-based VSC HVDC link

Francesco G. Puricelli, Adedotun J. Agbemuko, Jef Beerten

KU Leuven-ELECTA & EnergyVille, Leuven & Genk, Belgium

INTRODUCTION

- This work evaluates the inertia support provided by an HVDC link with one converter in GFM control.
- The assessment of the HVDC inertial response considers the influence of grid inertia, GFM converter control parameters and converter limitation.
- The time-domain analysis is carried out in PSCAD.

HVDC AND AC GRID MODEL

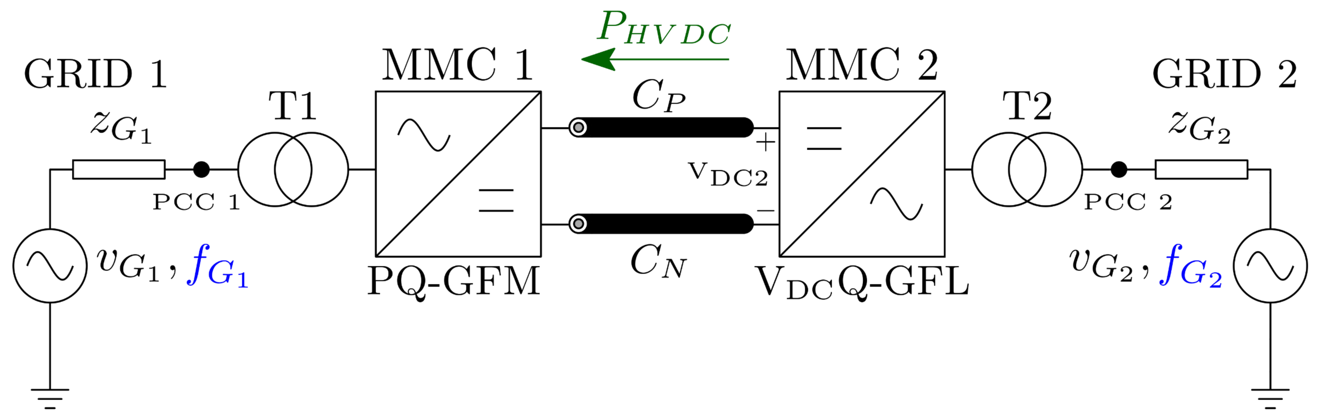

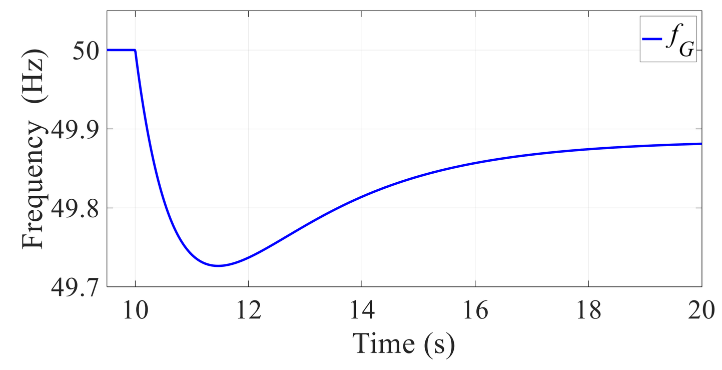

- 1 GW Monopolar HVDC link transferring 600 MW and with a maximum allowed power flow of 1.1 GW.
- The AC grids are represented with a Thevenin equivalent, and their frequency is modeled considering a single machine equivalent response.

METHODOLOGY

- Time-domain assessment of MMC 1 inertial response when this converter is in GFM-VSM mode, and a sudden 1.5 GW generation loss occurs in grid 1.
- Virtual swing equation in GFM-VSM MMC 1:

$$\frac{d\omega_{VSM}}{dt} = \frac{1}{2H_{VSM}}[P_m^* - P_{el} - K_d(\omega_{VSM} - \omega_{PLL}) - K_\omega(\omega_{VSM} - \omega_{VSM}^*)]$$

- $\Delta P_{pk,HVDC}$, $RoCoF$, and f_{nadir} are used as metrics to evaluate the inertial support from the HVDC connection.

$$\Delta P_{pk,HVDC} = P_{pk,HVDC} - P_{HVDC|t=t_{in}^-}\,;\; RoCoF(t_{in}+\Delta t) = \frac{f(t_{in}+\Delta t) - f(t_{in})}{\Delta t};\; f_{nadir} = min(f_G)_{|t>t_{in}^-}$$

- Parametric analysis of H_{G_1}, H_{VSM}, and K_ω.

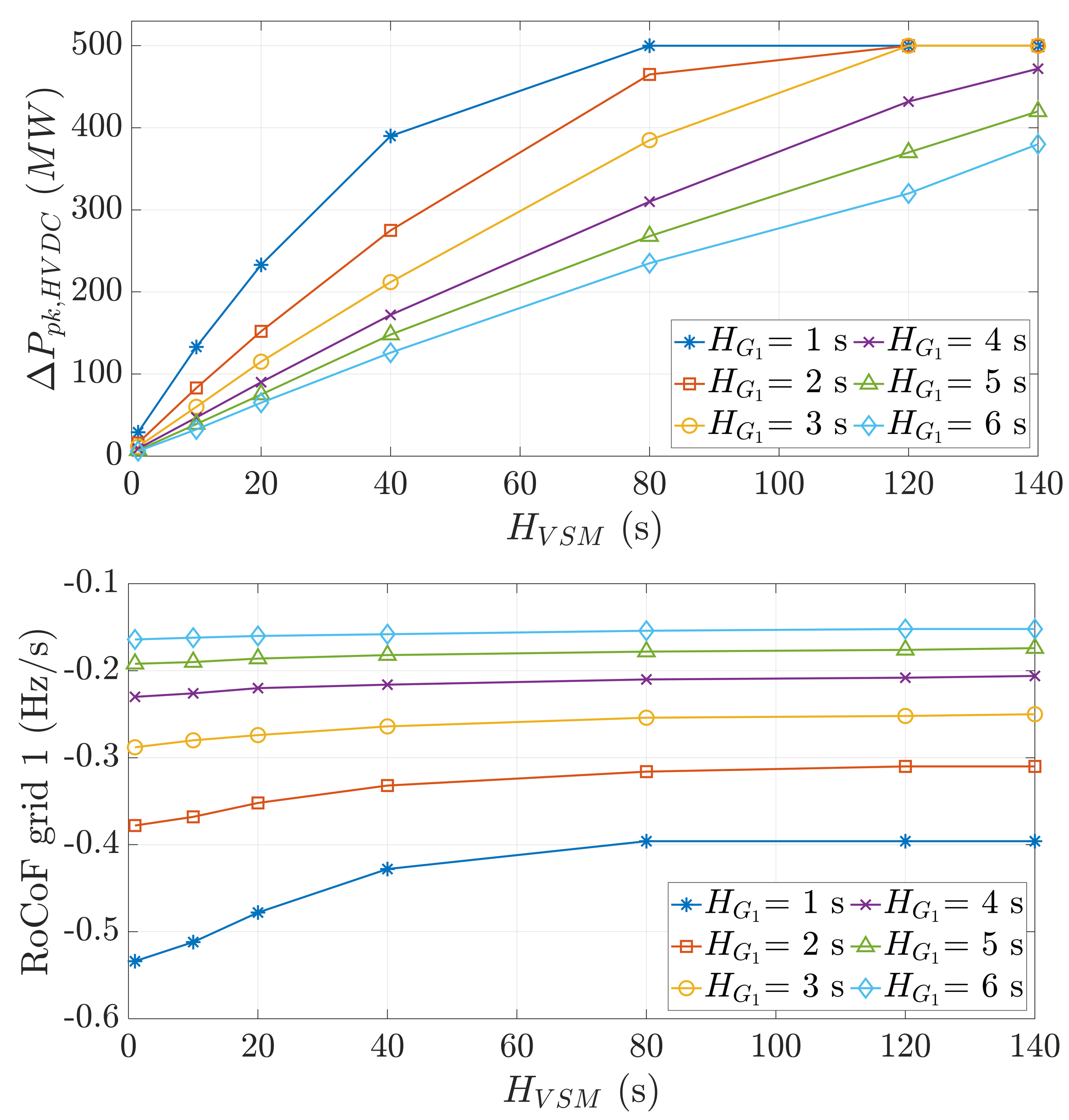

RESULTS

- The peak value of power injected by the HVDC connection $\Delta P_{pk,HVDC}$ also depends on the inertia of the grid connected to the GFM-VSM.
- A large value of H_{VSM} can worsen the AC grid frequency nadir in case of low damping of the GFM-VSM inertial response.
- The limit in maximum power transferable by an HVDC connection clearly shows the existing relationship between inertial support from HVDC links and their operating point.

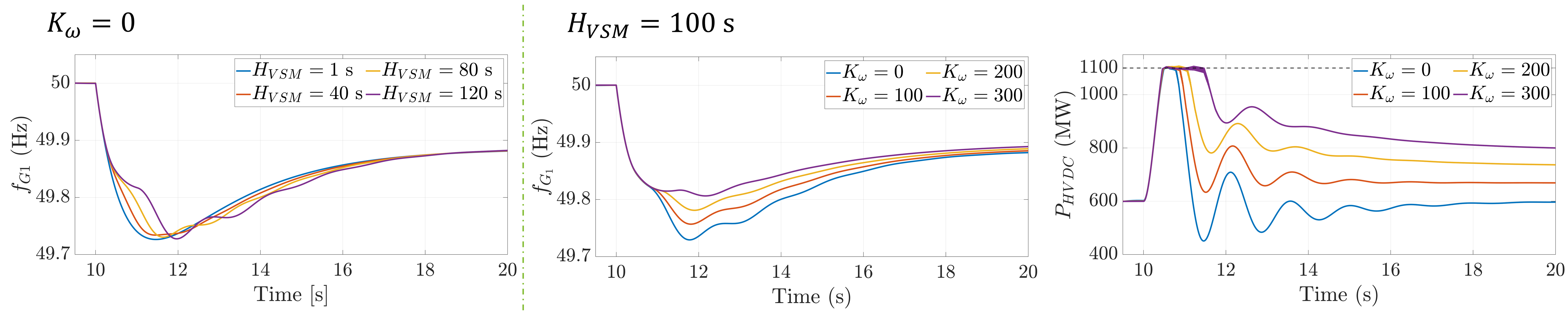

KEY OUTCOMES

- The inertial response from VSM-MMC in an HVDC link can contribute to improving the $RoCoF$ and f_{nadir} of AC grids, especially in systems with low inertia, characteristic of future electric grid scenarios.
- The coefficient K_ω has a positive effect both on the $RoCoF$ and f_{nadir}. Furthermore, K_ω increases the damping of the oscillations introduced by large values of H_{VSM}.
- The introduction of converter saturations highlights the importance of carefully choosing the VSM coefficients to avoid interactions between the converter inertial response and saturations.

With the support of the Energy Transition Fund

Black Box-Based Incremental Reduced-Order Modeling Framework of Inverter-Based Power Systems

Weihua Zhou, Jef Beerten

ELECTA, KU Leuven, Belgium and EnergyVille, Genk, Belgium

INTRODUCTION

- This work introduces a black box-based incremental reduced-order modeling framework of the VSC-and transmission cable-based power systems.
- Black box-based frequency range-oriented reduced-order models of VSCs and transmission cables are presented.
- Participation factors of the black-boxed VSCs are identified.

SYSTEM DESCRIPTION

- Four VSCs
- Five cables
- Five transformers
- These components are assumed to be black boxes.

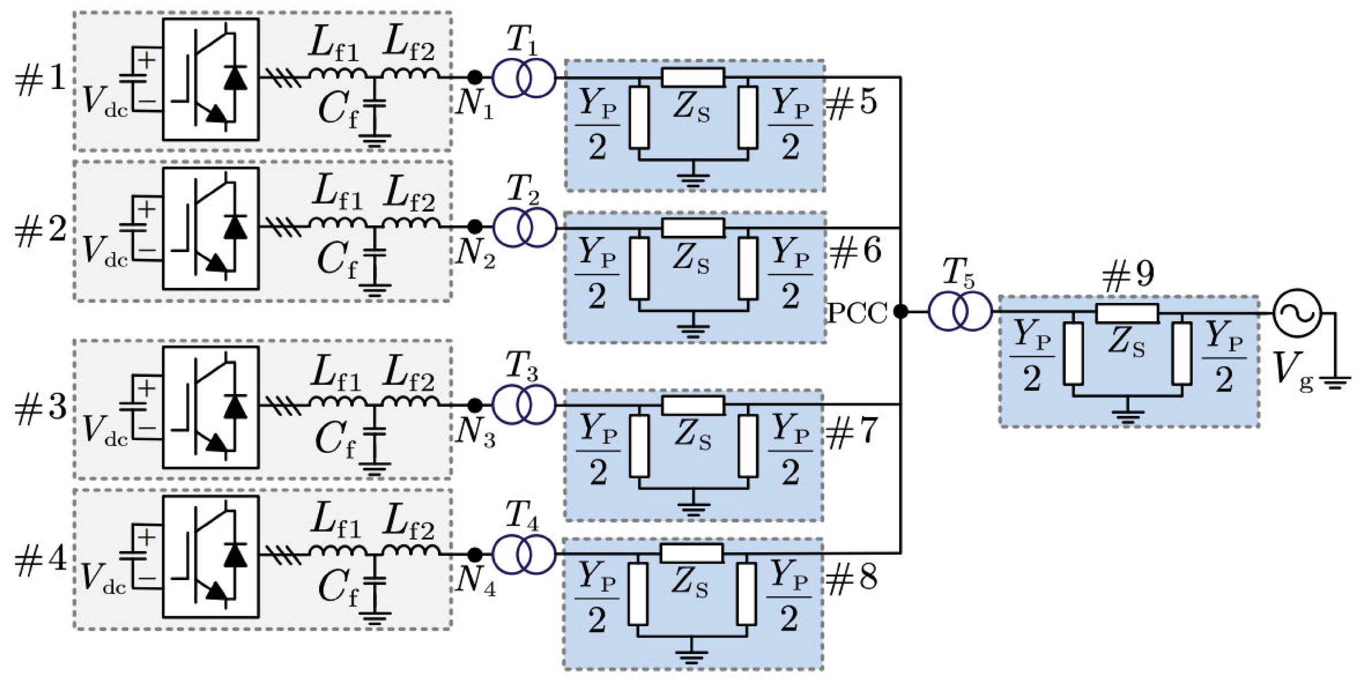

METHODOLOGY

- The roadmap A shows that the proposed method needs only the measured admittance frequency responses for components' reduced-order state-space modeling at component level, can assemble these components' SSMs at subsystem level in a way similar with impedance aggregation, and can perform global PF analysis at system level.

- The roadmap B shows that the impedance-based Nyquist criterion can only obtain local stability feature at system level, which cannot identify the problematic subsystems/components and cannot further implement the stability enhancement strategies, e.g., controller parameters re-tuning.

- The roadmap C shows that the component connection method needs to theoretically derive the components' SSMs at component level and the interconnection matrices at subsystem level, which cannot cope with the black-box issue and can bring in heavy computational burden.

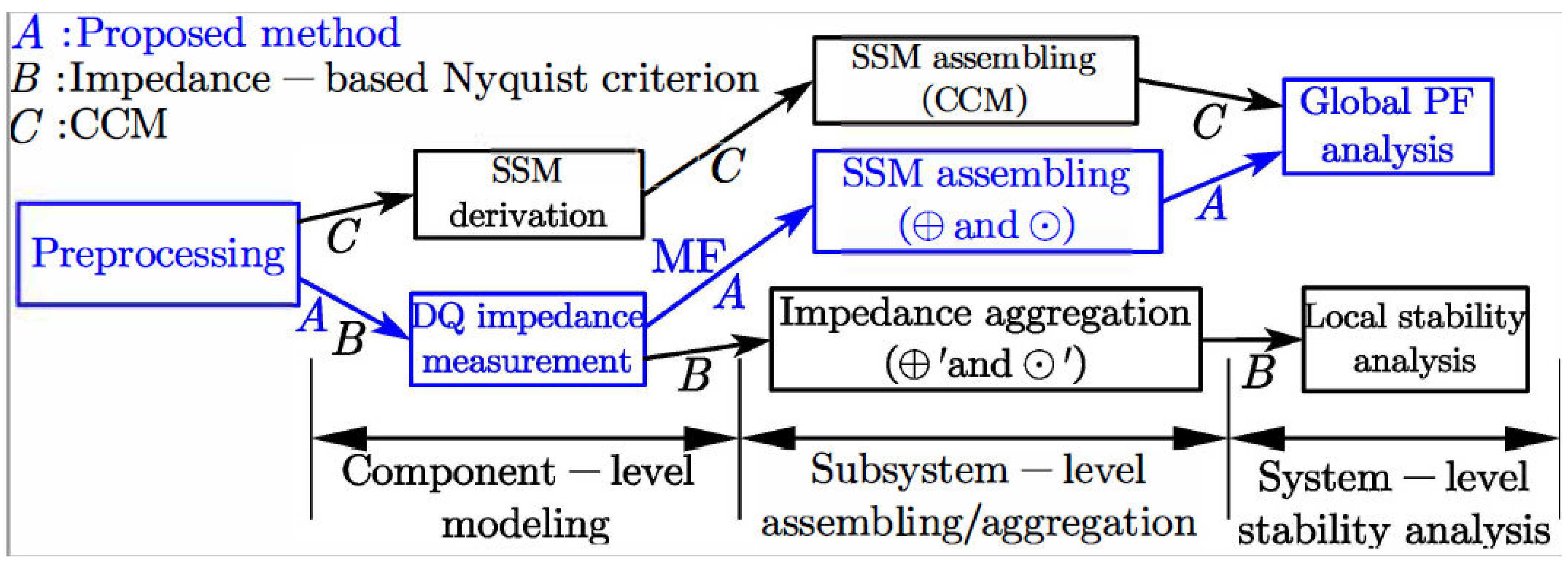

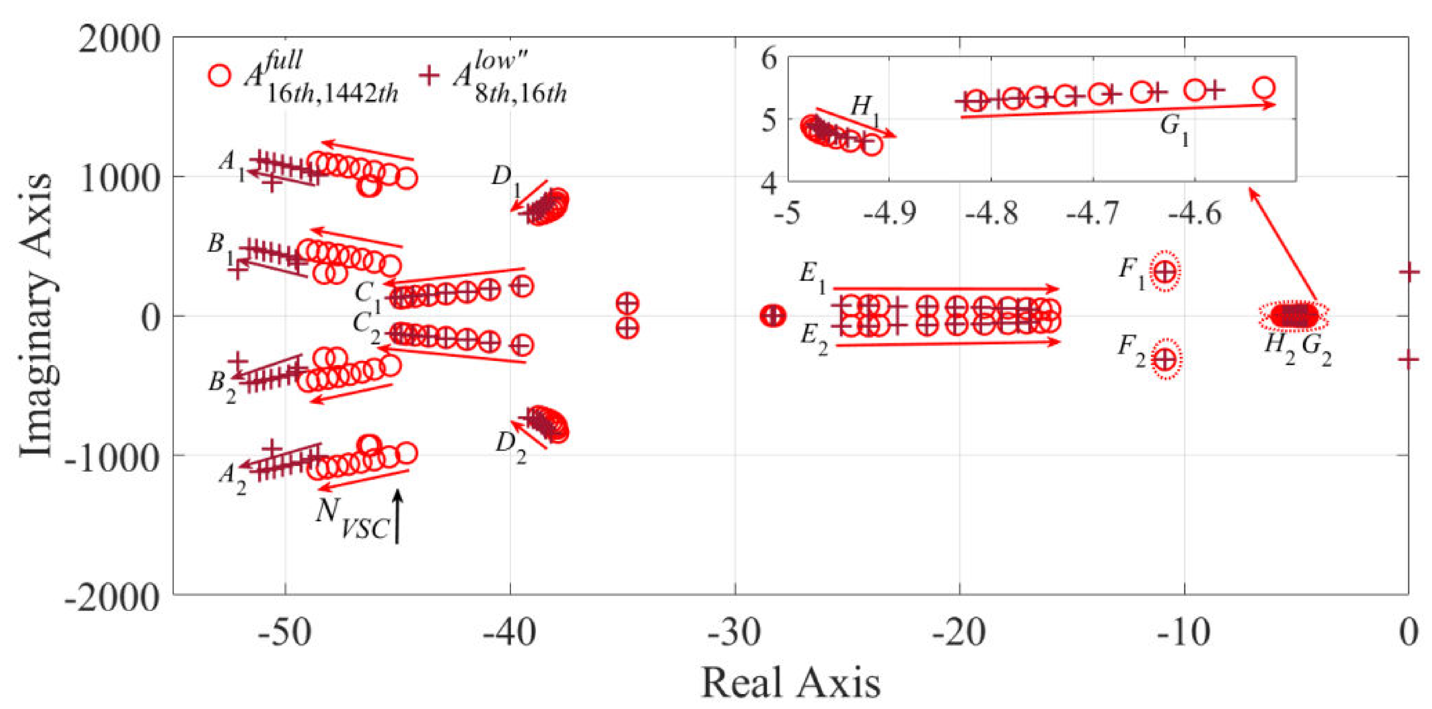

Eigenvalues loci of the full-order (symbol O) and reduced-order (symbol +) SSMs when paralleled branches increases from 4 to 32 with step size 4.

IMPLEMENTATION AND VERIFICATION

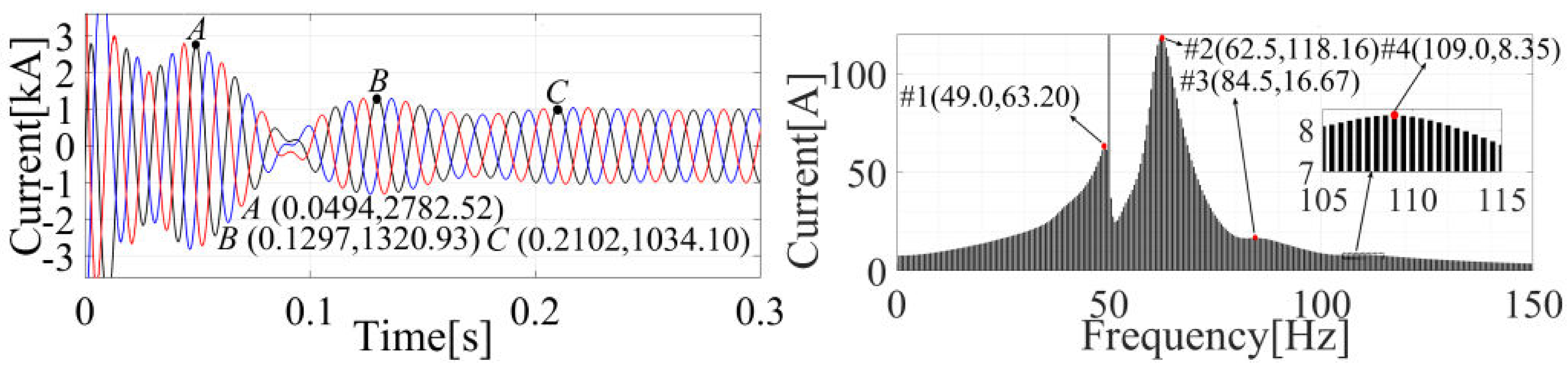

Time-domain simulation results of three-phase output currents of VSC #1. (a) Waveform and (b) FFT. (#1, #2, #3, #4 correspond to $G_{1,2}$, $E_{1,2}$, $C_{1,2}$, and $B_{1,2}$, respectively.)

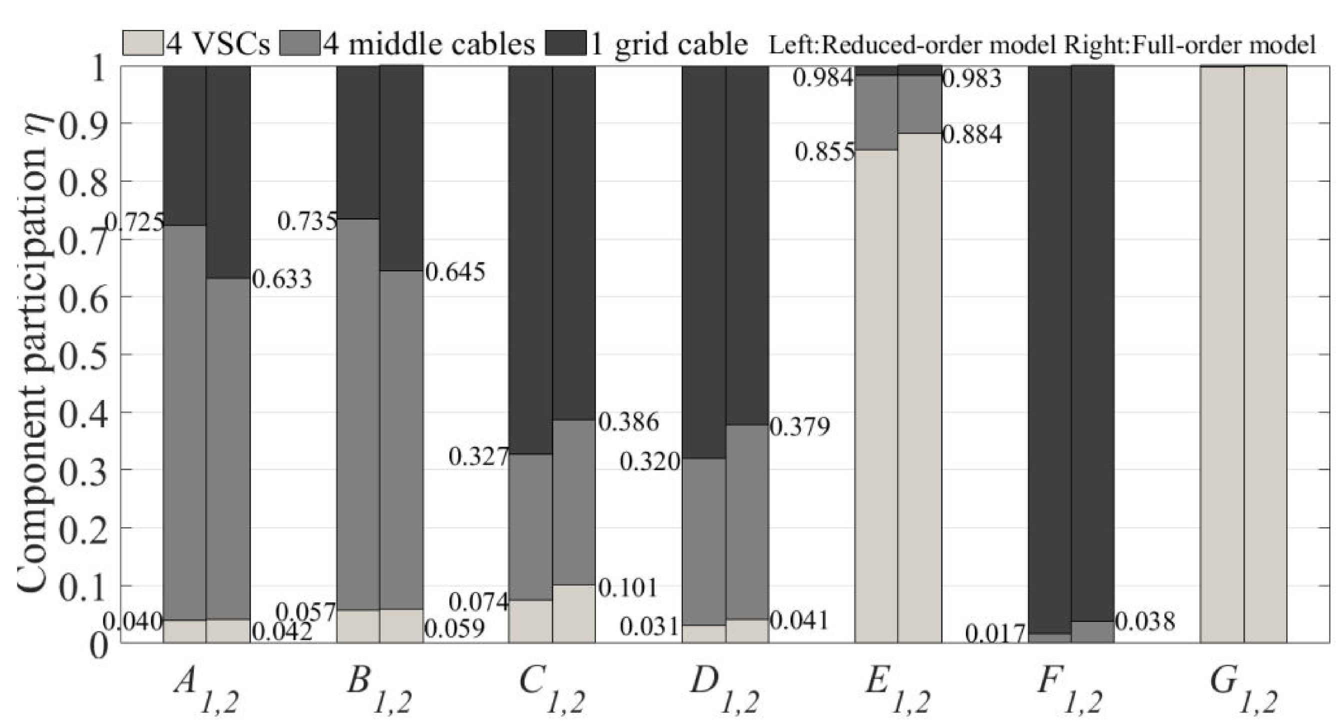

PF results of the reduced- and full-order models when the number of the paralleled branches is 4.

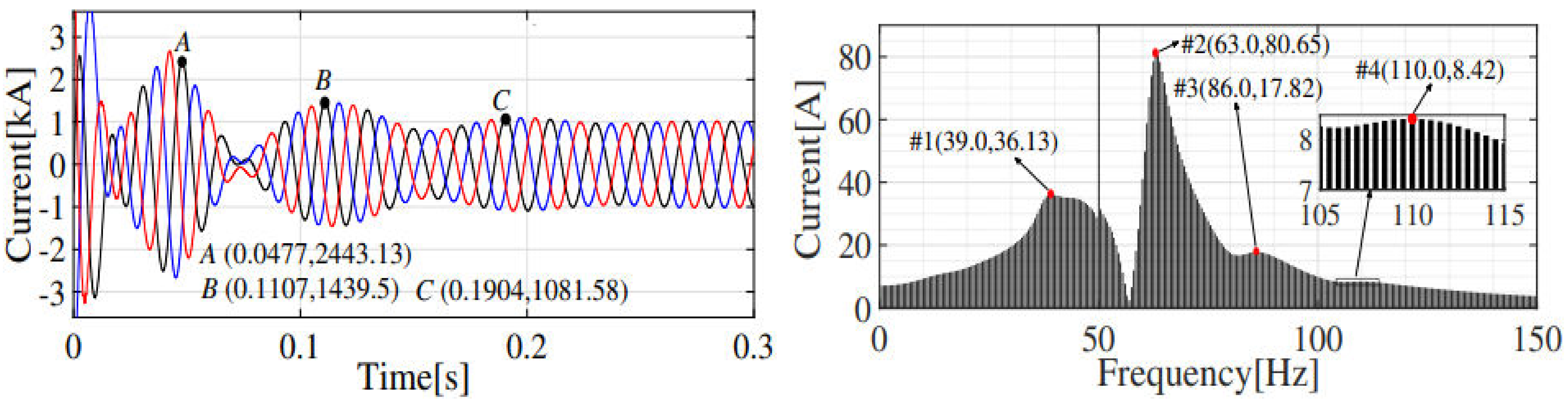

Time-domain simulation results of three-phase output currents of VSC #1. (a) Waveform and (b) FFT as the PLL parameters of the four VSCs are increased.

By increasing the PLL parameters, the peak #1 experiences the largest variation from 49.0 to 39.0 Hz. It indicates that the four VSCs significantly affect the modes $G_{1,2}$, which agrees with the PF analysis result.

With the support of the Energy Transition Fund